Dissertations   Theses and Dissertations

2015

The Role of Alveolar Macrophages in Pulmonary Inflammation After Intoxication and Burn Injury

Jill Ann Shults
Loyola University Chicago

Follow this and additional works at: https://ecommons.luc.edu/luc_diss

Part of the Cell Biology Commons

LOYOLA UNIVERSITY CHICAGO

THE ROLE OF ALVEOLAR MACROPHAGES IN PULMONARY INFLAMMATION

AFTER INTOXICATION AND BURN INJURY

A DISSERTATION SUBMITTED TO

THE FACULTY OF THE GRADUATE SCHOOL

IN CANDIDACY FOR THE DEGREE OF

DOCTOR OF PHILOSOPHY

PROGRAM IN INTEGRATIVE CELL BIOLOGY

BY

JILL ANN SHULTS

CHICAGO, ILLINOIS

DECEMBER 2015

ACKNOWLEDGEMENTS

I would like to thank my entire family for all their love and encouragement. Mom and Dad, I love you and I appreciate all your support. Joy, you have shown me that nothing is impossible. Thank you for being a wonderful friend, sister and mentor. Megan and Kara, thank you for all of your love and helping me take a break when I needed it.

Thank you to my mentor, Liz, for all of your guidance and wealth of knowledge. You helped me conquer my fear of public speaking and kept believing, even when I did not, that I would eventually get significant data. Thank you to Dr. Witte, for all of your patience and wisdom. Working in your laboratory led me to fall in love with research and believe in myself as a scientist. "You are only as good as your controls" will always be my mantra in science. Thank you to my committee for all of your support and helpful suggestions. And thank you to everyone I worked with in both the Kovacs's Empire and Witte laboratory. All the laughter, tears and life talks made this journey an amazing experience.

Most importantly, thank you to my amazing husband, Cody Shults, Ph.D. I could not have done this without you. You are my rock. I love you.

TABLE OF CONTENTS

LIST OF TABLES

LIST OF FIGURES

LIST OF ABBREVIATIONS

ALT   alanine aminotransferase

ANOVA   one-way analysis of variance

AM   alveolar macrophage

ARDS   acute respiratory distress syndrome

ARG1   arginase 1

AST   aspartate aminotransferase

BAC   blood alcohol content

BAL   bronchoalveolar lavage

DC   dendritic cell

ELISA   enzyme-linked immunosorbent assay

ERK 1/2   extracellular-regulated kinase 1 and 2

FasL   fas ligand

FIZZ1   resistin-like α (Retnla)

GM-CSF   granulocyte monocyte- colony stimulating factor

H&E   hematoxylin and eosin

HGF   hepatocyte growth factor

INF   interferon gamma

IL   interleukin

IM   interstitial macrophage

iNOS	inducible nitric oxide synthase
KC	cxcl1 (homologous to human IL-8)
LPS	lipopolysaccharide
MARCO	macrophage receptor with collagenous structure
MAPK	mitogen-activated protein kinase
MFI	mean fluorescence intensity
MIP-2	macrophage inflammatory protein 2
MSC	mesenchymal stem cell
MHC II	major histocompatibility complex II
NADPH	nicotinamide adenine dinucleotide phosphate
NO	nitric oxide
OCT	optimal cutting temperature
PDGF	platelet derived growth factor
PFA	paraformaldehyde
PMN	neutrophil
PSG	penicillin-streptomycin-glutamine
ROS	reactive oxygen species
SEM	standard error of the mean
Siglec-F	sialic acid-binding immunoglobulin-like lectin F
SIRPα	signal-regulatory protein α
SP	surfactant protein
STAT	signal transducer and activator of transcription

TBSA   total body surface area

TGFβ   transforming growth factor β

TLR   Toll-like receptor

TNFα   tumor necrosis factor alpha

TUNEL   terminal deoxynucleotidyl transferase-dUTP nick end labeling

VEGF   vascular endothelial growth factor

YM1   chitinase 3-like 3 (Chi3l3)

CHAPTER 1

INTRODUCTION

A positive blood alcohol concentration is detected in nearly half of burn patients admitted to the emergency room. The combined insult of being intoxicated at the time of burn injury results in more clinical complications, in comparison to non-intoxicated burn patients. Severe burn, with or without inhalation injury, is a common predisposing factor for the development of acute respiratory distress syndrome (ARDS). Exacerbated pulmonary inflammation and a net result of insufficient gas exchange underlie the large percentage of burn fatalities due to pulmonary complications. Previous studies in our laboratory indicate a drastic elevation in pulmonary inflammation in a mouse model of intoxication and burn injury. This was characterized by heightened levels of alveolar wall thickening, neutrophil accumulation, neutrophil chemokines KC and macrophage inflammatory protein 2 (MIP-2), and pro-inflammatory IL-6. Reducing levels of pulmonary inflammation and restoring the lungs to homeostasis is essential to prevent lung complications and failure.

Alveolar macrophages (AMs) are the lungs first line of defense against inhaled particles or pathogens and elegantly coordinate the on-set and resolution of inflammation. The transition from steady-state healthy conditions to a pro-inflammatory state is a result of macrophage plasticity to readily activate into a reversible pro- or anti-inflammatory profile, depending on mediators present within the microenvironment. Importantly, AM

efferocytosis of apoptotic cells stimulates anti-inflammatory mediator release and promotes the resolution of inflammatory responses, while a disruption in this function can result in drastically increased levels of inflammation.

A common feature of both ARDS and burn injury is an increase in apoptosis in lung tissue. Specifically, ARDS has been associated with the apoptosis of lung epithelial cells. Since the removal of apoptotic cells by AMs is important for the termination of inflammation, a dysregulation in the activation state or survival of AMs can result in prolonged pulmonary inflammation. Thus, the role of AMs in pulmonary inflammation after intoxication and injury is extremely important. With this knowledge, <u>we hypothesize that intoxication at the time of burn injury leads to an increase in AM apoptosis, resulting in exacerbated pulmonary inflammation and impaired lung function.</u> To test this hypothesis, three aims are proposed: 1) to determine if pulmonary inflammation after intoxication and burn injury affects physiological parameters of lung function, 2) identify the role of alveolar macrophages in post-burn pulmonary inflammation, and 3) to determine if exogenous mesenchymal stem cell treatment will attenuate pulmonary inflammation after intoxication and burn injury.

Lung function will be measured using non-restrained whole body plethysmography. AMs will be isolated and their activation profiles will be assessed using flow cytometry, immunofluorescent staining, and cytokine assays. Multiple apoptosis identification methods, including TUNEL, Annexin V/PI, and caspase-3/7 staining, will be used to evaluate apoptosis in lung tissue and alveolar macrophages. The role of alveolar macrophages in pulmonary inflammation after intoxication and injury

will be determined by selectively depleting alveolar macrophages from the lungs with clodronate liposomes. Finally, the ability of mesenchymal stem cells to attenuate pulmonary inflammation will be assessed.

CHAPTER 2

REVIEW OF RELATED LITERATURE

Alveolar macrophages: key regulators of pulmonary inflammation

Lung anatomy

The respiratory system is an essential organ system that influences whole body homeostasis; the import of oxygen and export of carbon dioxide is crucial to maintaining the function of other vital organs. The respiratory system is comprised of the upper respiratory tract (mouth, nose, pharynx, and larynx) and the lower respiratory tract (trachea and within the lungs, the bronchi, bronchioles and alveoli). The lungs are specifically essential to transporting oxygen to the capillaries and rest of the body. This major organ system is organized into 2 lungs that are divided into a total of 5 lobes, a likely evolutionary advantage in the event one lung or lobe is damaged. In humans, the right lung is divided into 3 lobes while the left lung is divided into 2 lobes. In mice, however, the lungs have a different anatomical makeup where the right lung is comprised of 4 lobes and the left lung is smaller and comprised of a single lobe [1]. Other anatomical differences in mice include the close positioning of the epiglottis to the soft plate, which restricts breathing solely to the nasal passageways and makes oral breathing nearly impossible.

The lung is intricately organized into a vast tree-like structure subdivided into large and small airways. The larger airways include the trachea, bronchi and bronchioles, while the smaller airways include the terminal bronchioles, alveoli ducts and the alveoli.

4

As air is breathed in through the nose or mouth it passes through the trachea into the bronchi and bronchioles until it reaches the alveoli, the minuscule bulb-shaped ends of the airways that are the main functional components of gas exchange. Ninety-five percent of the alveolar surface area is covered by large, flat type I epithelial cells, with an occasional type II, surfactant-producing epithelial cell. Other cells found within the alveolar wall include interstitial cells, as well as endothelial cells that comprise the capillaries that are distributed throughout the walls [1]. The fusion of basement membranes between the thin, type I epithelial cells and capillary endothelial cells creates the alveolar septum where gas exchange occurs.

<div align="center">Alveolar macrophages (AMs)</div>

In humans, the average size of an alveolus is about 0.25mm in diameter, while in mice this is much smaller but exact measurements have not been determined. There is an estimated 300 million alveoli within human adult lungs, calculating to an overall surface area over 90 m^2 [2, 3], while in mice, there is an estimated 2.3 million alveoli, resulting in an area of 82.2 cm^2 [4]. With its large surface area and direct connection to the outside air, the lungs are continuously exposed to inhaled pathogens and particles and are at risk for infection. Innate immune cells, alveolar macrophages (AMs), are strategically located with in the alveolar space and are the most abundant antigen presenting cell in the lung [5]. AMs monitor the airways for infectious agents, preventing excessive lung inflammation, as well as stop pathogens from crossing the alveolar-capillary interface into the bloodstream [6]. Under healthy conditions, AMs are 90-95% of airway cells (the remaining fraction belonging to lymphocytes) [7-9], and in mice, it is estimated there are

a total of 1-2 million AMs distributed within the airspace in the ratio of 1 AM to 3 alveoli [10]. During fetal development, AMs originate from monocytes [11], but adult AMs are thought to be long-lived cells with a half-life of 30 days and minimal self-renewal in naïve mice [12]. Other studies suggest lung-injury induced loss of AMs stimulates local proliferation of AMs and is the main mechanism of repopulation [13-15]. It is also estimated that in steady-state conditions only 40% of AMs are replaced by infiltrating monocytes within 1 year [16]. These long-lived AMs may comprise only 10% of the total cells found in the alveoli, yet their function in maintaining a pathogen-free environment is critical for lung homeostasis.

Lung environment determines AM phenotype

Macrophages were first described in 1892 by Russian scientist Ilya Metchnikoff [17], but the isolation of AMs using bronchoalveolar lavage (BAL) was not described until 1961 [18]. The alveoli are home to both AMs and interstitial macrophages (IMs), but the ease of isolating a pure population of AMs through BAL has directed lung immune research toward AM-focused studies [7]. Of note, there is also a population of macrophages found in large airways, but at this time it is not known if this population differs from AMs. Additionally, it is unclear whether the various methods of AM isolation also include interstitial macrophages [19]. For the purpose of these studies, our results indicate we have isolated a population of only AMs.

In mice, it has been shown AMs have a unique phenotype in comparison to IMs, as well as other tissue-resident macrophages. Unlike macrophage populations found in other organs, AMs express low to negative levels of classic macrophage marker CD11b,

high levels classic dendritic cell (DC) marker CD11c, and eosinophil marker sialic

acid-binding immunoglobulin-like lectin F (Siglec-F), as well as low to negative

expression of major histocompatibility complex class II (MHC II) and high expression of

mannose receptor CD206 (Table 1) [20-22]. AM steady-state phenotype can be

classified as CD11c$^+$CD11b$^-$Siglec-F$^+$F4/80$^+$CD206$^+$. Guth et al. demonstrated that the

lung environment rich in granulocyte/macrophage colony-stimulating factor (GM-CSF),

and to a lesser extent, surfactant protein (SP)-D, both produced by alveolar

epithelial cells, facilitates the uniqueness of the AM, specifically the expression of

CD11c [11, 20]. It is important to note that due to this environment, CD11c has also

been described on IMs, but in contrast to AMs, IMs are CD11b$^+$Siglec-F$^-$CD206$^{low/-}$

(Table 1) [21]. Guth et al. also demonstrated that AMs cultured with medium for 24-48 h

before activation were able to present antigen *in vitro* and speculated that freshly isolated

AMs are not able to present antigen, presumably because of the immunosuppressive

properties of lingering surfactant proteins [23]. Both SP-A and SP-D have also been

shown to bind AMs through signal-regulatory protein α (SIRPα) and suppress AM

phagocytosis. Therefore, in addition to their ability to suppress antigen presentation, it is

likely these proteins have a significant role in suppressing AM pro-inflammatory

activation, overall preventing excessive inflammation in the lungs [24, 25].

Interestingly, Guth et al. also speculates this unique phenotype parallels that of an

immature DC cell. Development of macrophages is typically facilitated by CSF-1 and

DCs by GM-CSF [26], and, similar to immature DCs, but unlike other macrophage

Table 1: Comparison of tissue-resident macrophage cell surface markers

	CD45 Leukocyte	F4/80 Mac/Mono	CD11b Mac/Mono/ Granulocyte	CD11c Dendritic Cell	Ly-6G Neutrophil	Siglec-F Eosinophil	MHC II	CD206
Alveolar Macrophage	+	+	Low/−	+	−	+	Low/−	High
Interstitial Macrophage	+	+	+	+	−	−	+	Low/−
Peritoneal/ Splenic Macrophage	+	+	+	−	−	−	+	Low

Red font indicates unique phenotype markers on both AMs and IMs in the lung, in comparison to other tissue-specific macrophage populations.

populations, AMs are constantly cleaning up the lung environment through

macropinocytosis [27]. Other research shows that SP-D binds to immature DCs, but not

mature DCs, further supporting why this phenotype may be advantageous to managing

lung inflammation [28]. This combination of a macrophage-dendritic cell phenotype that

is generated by the lung environment is advantageous for both steady-state and

inflammatory conditions. The ability of AMs to recognize and respond to non-infectious

agents and debris without initiating inflammation, but also have the ability to mount a

pro-inflammatory response to infectious agents, is an efficient function that keeps

inflammation under control.

<center>Inhibitory receptors</center>

In addition to surfactant protein binding to SIRPα, inhibitory receptors, such as

mannose receptor CD206, macrophage receptor with collagenous structure (MARCO),

and interleukin (IL)-10 receptor (IL-10R) on AMs are important in regulating

inflammation. CD206 on AMs is acquired during lung development [29] and selectively

binds bacterial glycoproteins and glycolipids. The interaction of CD206 with

unopsonized (not targeted for destruction) bacteria suppresses an inflammatory response,

highlighting a role for this receptor in maintaining tolerance against small amounts of

infectious agents or commensal bacteria located in the distal airways [30, 31]. In

humans, scavenger receptor, MARCO, is also important in binding unopsonized inhaled

particles and bacteria in the lung and aids in the clearance of apoptotic cells [32].

Moreover, ligation of IL-10R inhibits pro-inflammatory cytokine release and has been

shown to indirectly inhibit the toll-like receptor (TLR)-4 signaling pathway [33]. Recent

studies by Westphalen et al. also demonstrated the interaction of AMs with the alveolar

epithelium and the use connexin 43 gap junctions allow AMs to communicate between

alveoli and suppress lipopolysaccharide (LPS)-induced inflammation [10]. Together,

these factors manage tolerance in the steady-state lung.

<div align="center">Activation profiles of AMs</div>

Preventing excessive inflammation in the lungs is a tightly controlled process and

is facilitated by many different factors. The transition from the steady-state to a

necessary inflammatory state is made possible by the plasticity of macrophages to readily

activate into a reversible inflammatory profile, depending on factors present within the

microenvironment. Classification of macrophage activation profiles has varied since the

early 1990's. It was not until recently that the major macrophage research investigators

collaborated and addressed the confounding classification terminology [34]. This group

of investigators determined 3 guidelines to use when describing the activation state of

macrophages. First, identify the model (*in vitro* versus *in vivo)* and method of isolation.

Second, identify the mediators that were used to stimulate macrophage activation. Lastly,

describe the upregulation or downregulation of cell surface or intracellular markers that

are associated with specific-mediator induced activation.

Prior to these guidelines, our laboratory generalized macrophages into either a

classical, pro-inflammatory M1 activated macrophage or an alternative, anti-

inflammatory M2 activated macrophage (this included all postulated subsets of M2: M2a,

M2b and M2c). Figure 1 outlines our generalized classification of M1 and M2

macrophages. M1 macrophages were characterized by mediators of activation, such as

interferon gamma (IFNγ), tumor necrosis factor α (TNFα), and lipopolysaccharide (LPS) that activate signal transducer and activator of transcription (STAT) 1 signaling and upregulate MARCO, inducible nitric oxide (iNOS, Nos2), IL-6 and TNFα gene expression. In contrast, M2 macrophages were summarized as activated by IL-4, IL-10, IL-13 and transforming growth factor β (TGFβ) stimulating the STAT3 or STAT6 signaling cascade, and upregulating gene expression of CD206, IL-4R, IL-10, TGFβ, arginase 1 (ARG1), resistin-like α (Retnla, Fizz1), and chitinase 3-like 3 (Chi3l3, Ym1) [35]. Thus, the studies herein used these markers for the general classification of AMs in our model (Figure 1).

<center>Initiation and resolution of inflammation</center>

AMs produce various pro-inflammatory cytokines in response to inflammatory stimuli, including IL-6, TNFα, IL-1β, nitric oxide (NO), reactive oxygen species (ROS), and neutrophil chemokine MIP- 2 [36-39]. AM release of IL-1β also stimulates epithelial cells to produce large amounts of neutrophil chemokine CXCL8 (homologous to mouse KC) that recruits neutrophils into the lung to aid in bacterial clearance [40]. Prolonged pro-inflammatory activation of macrophages has been shown to result in tissue damage if not regulated [41]. Therefore, lung inflammation needs to be a highly monitored process.

Resolution of inflammation is achieved through the removal of pathogens by neutrophils and AMs, as well as the downregulation of neutrophil chemokines and the removal of apoptotic neutrophils, both functions AMs [42]. Specifically, phagocytosis of apoptotic cells (termed efferocytosis), such as neutrophils, by macrophages can

Tissue Resident Macrophage Polarization

Senescent Macrophage
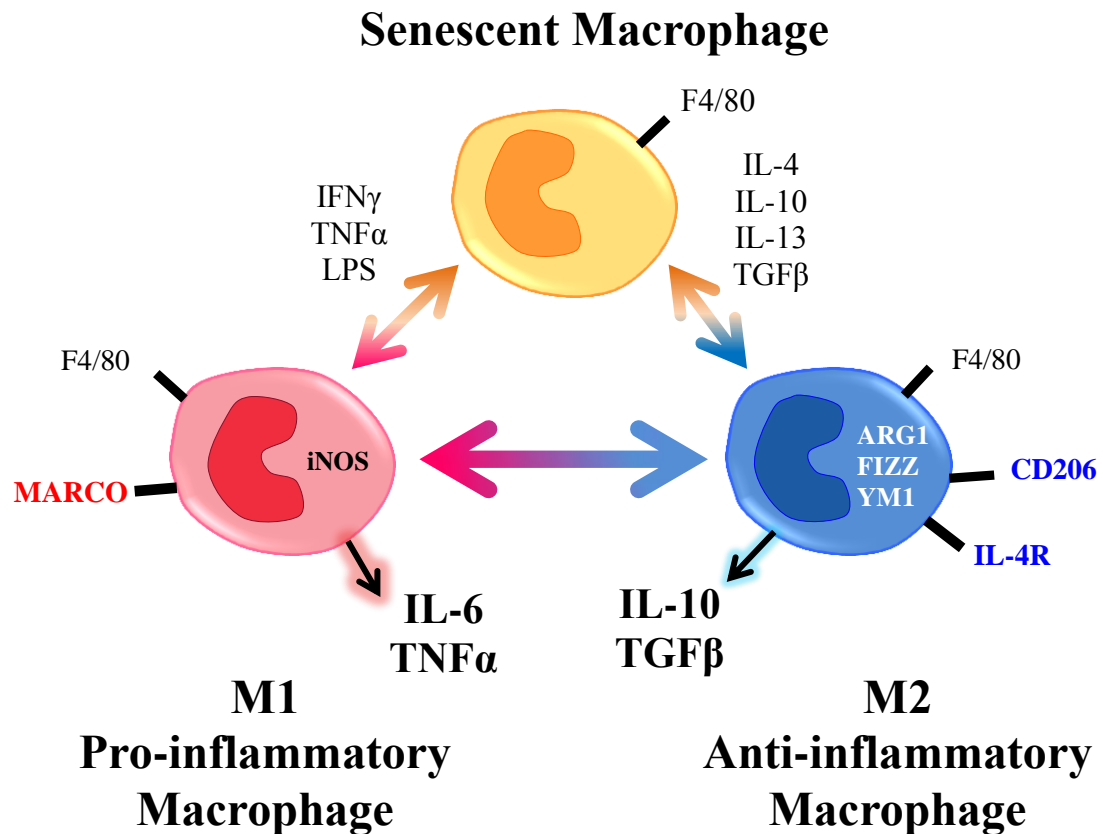
Figure 1 : Macrophage activation profiles. Tissue resident macrophages express pan macrophage cell surface marker F4/80 and retain this marker during their reversible activation states. M1 macrophages can be polarized by pro-inflammatory mediators, such as IFNγ, TNFα and LPS, subsequently releasing pro-inflammatory cytokines, such as IL-6 and TNFα. M1 macrophages also upregulate intracellular iNOS gene expression and can be characterized by upregulated levels of MACRO. M2 macrophages are polarized by anti-inflammatory mediators IL-4, IL-10, IL-13, and TGFβ to secrete anti-inflammatory cytokines, such as IL-10 and TGFβ. M2 macrophages can also upregulate intracellular ARG1, Fizz, and YM1 gene expression, as well as cell surface markers CD206 and IL-4R.

Modified from Clària et al., *Front. In Immuno* 2011

downregulate TNFα, NO release and upregulate IL-10 and TGFβ [43-46]. Efferocytosis by macrophages also helps facilitate restoration of lung tissue integrity through macrophage release of epithelial growth factors platelet derived growth factor (PDGF), vascular endothelial growth factor (VEGF), and hepatocyte growth factor (HGF) [47, 48] and through their release of prostaglandin E(2), which stimulates endothelial cell migration and promotes neoangiogenesis [49]. Additionally, migration of AMs to the lung draining lymph nodes or the apoptosis of AMs themselves can promote the resolution of inflammation [50, 51]. Overall, AM efferocytosis and apoptosis are both important in the restoration and remodeling of injured lung tissue, but they are not without consequence. Other studies have also shown that the increase in anti-inflammatory mediators and a decrease in the number of neutrophils infiltrating into the tissue, as a result of efferocytosis by AMs, can lead to an increased risk of secondary infection if the lungs are not able to mount a pro-inflammatory response [52]. Taken together, the initiation and resolution of inflammation is a closely synchronized process that is dependent on AMs and their elegant role in coordinating both pro- and anti-inflammatory responses.

Binge alcohol consumption paradigm

Alcohol drinking patterns

Historically, alcohol has been a common factor in various cultures for thousands of years [53, 54]. Fermented beverages have been found as far back 6000 and 7000 BC in Iran and China, respectively, and 3000 BC in Egypt [55-57]. The advancement of

technology has led to the increased production, variety and wide distribution of alcohol, ultimately resulting in the evolution of modern-day drinking patterns [58]. Only 7.4% alcohol users are considered alcohol-dependent, revealing that the majority of alcohol intake in the United States is through non-dependent patterns of occasional, moderate or binge drinking [59]. Moderate drinking is defined as 2 drinks a day for men and 1 drink a day for women and has been postulated to have positive health benefits, including decreased risk of heart disease, stroke, and diabetes [60]. Interestingly, the consumption of alcohol in a binge-like pattern is the most common form of drinking among young adults, with half the alcohol consumed by adults being in the form of binge drinks and 69% of binge drinkers falling into a category of adults 26 years and older [61]. The National Institute on Alcohol Abuse and Alcoholism (NIAAA) defines binge drinking either as either a blood alcohol concentration (BAC) level greater than or equal to 0.08% (80 mg/dL) or by the number of drinks consumed within a 2 hour window, 5 drinks for men and 4 drinks for women [62]. One drink is defined by the type of alcohol and percentage of alcohol content within each beverage and is equivalent to either 12 oz. of.beer (5% alcohol), 8 oz. of malt liquor (7% alcohol) 5 oz. of wine (12% alcohol) or 1.5 oz of 80-proof liquor (40% alcohol).

Binge drinking can be correlated with adverse health outcomes, especially unintentional injuries, such as vehicle accidents, falls, and burn injury, making alcohol the 3rd leading cause of preventable death [63]. Annually, there are about 88,000 alcohol related deaths in the United States, two-thirds of which are men [64], while globally, in 2012, alcohol-related deaths reached 3.3 million a year, representing 6% of all global

fatalities [65]. With over 50% of trauma patients presenting a positive BAC at the time of hospital admission [66], it is important we understand how alcohol can modulate the post-injury cellular and systemic response.

Alcohol mediates cellular responses

The immunosuppressive effects of alcohol consumption have been well documented to correlate with increased incidences of infection [67]. Regardless of the type of alcohol ingested, in mouse studies, a single exposure of alcohol (acute) alcohol consumption can result in the suppression of cellular immune responses [68, 69]. The function of various adaptive and innate immune cells, including T cells, DCs, monocytes, and macrophages, are affected by alcohol exposure [67].   Ethanol is a small compound with a hydrophobic carbon tail that allows itself to easily pass through phospholipid bilayers in cell membranes [70]. It can modify lipid membrane properties and well as directly interact with transmembrane proteins [71]. Specifically, acute alcohol has been shown to increase membrane fluidity and decreased TLR4 migration to the cell surface, overall downregulating TLR4-CD14 signaling pathways after LPS stimulation, and highlighting a mechanism behind increased susceptibility to infection [72].

Human DC and monocyte studies have demonstrated acute alcohol can inhibit DC and monocyte antigen presentation, as well as T cell proliferation [73, 74]. In murine macrophages, acute alcohol exposure *in vitro* reduces TLR4 signaling and IL-6 production via the suppression of extracellular-regulated kinase 1 and 2 (ERK1/2) and p38 mitogen-activated protein kinase (MAPK) [75]. Additionally, our laboratory has shown that *in vivo* ethanol exposure suppresses both the production of IL-6, TNFα, and

IL-12 after *in vitro* LPS stimulation of alveolar macrophages, as well as suppresses the *in vitro* phagocytosis of *Pseudomonas aeruginosa* (*P. aeruginosa*) [8, 76]. Overall, these data emphasize the profound affects a single exposure to alcohol can have on the immune system.

<center>Alcohol and the lung</center>

Chronic alcohol consumption leads to an increased risk lung infections and a decreased ability to clear the infection [77]. Acute ethanol exposure has also been described to inhibit inflammatory responses in the lung in response to bacterial infection [67]. The literature suggests that one mechanism behind increased incidences of infection is the immunosuppression of alveolar macrophage function. Murine studies of chronic alcohol exposure and infection showed a decrease in alveolar macrophage phagocytosis, while rat studies with acute alcohol exposure revealed a decrease in the production of TNFα [78, 79]. Additionally, alcohol abuse has been linked to an increase incidence of acute respiratory distress syndrome (ARDS) [80]. ARDS is characterized by an increase in tissue edema and permeability to inflammatory cells that can lead to impaired gas exchange. In a murine model of LPS-induced lung injury, acute alcohol exposure *in vivo* increased neutrophil recruitment in to the alveolar space and decreased AM efferocytosis of apoptotic cells [81]. It has been postulated that resolution of inflammation in ARDS patients is in part impaired due to the effects of alcohol on AMs, once again emphasizing the importance of AMs in restoring normal lung function.

Burn injury, alcohol and systemic inflammation

Incidences of burn injury in the Unites States

In the United States, there are over 480,000 incidences of burn injures that require medical treatment [82]. The 2014 National Burn Repository Report revealed that within these incidences of burn injury, 40,000 patients are admitted to the hospital and over 3,200 patients per year succumb to either burn injury alone or burn injury and smoke inhalation injury. Additionally, fire/flame injuries and scald injuries are the two most frequent occurrences of injury, at 43% and 34% [82], respectively. Majority of patients had an average burn size under 10% total body surface area (TBSA) and 70% of burn patients are adult men. The cost of care for burn injury survivors is about $14,000 for every day spent in the hospital, with an average total bill of $86,000 [82].

Interestingly, pneumonia is the most common complication associated with burn injury and incidences of acquiring an infection correlated with an increased number of days spent in the hospital. Severe burn, with or without inhalation injury, is a common predisposing factor for the development ARDS [83, 84]. Clinical data show 42% of the mortality observed in burn patients is due to pulmonary complications [85, 86]. Respiratory dysfunction in burn patients can be characterized by shallow breathing and fluid accumulation in the lung interstitium, leading to heightened vascular resistance and an increased effort to breathe [84, 86]. A net result of insufficient gas exchange underlies the large percentage of burn fatalities due to pulmonary complications. Take together, these observations emphasize the importance of extreme care given to the lungs after burn injury.

Intoxication and burn injury

Of the burn patients hospitalized each year, it speculated that nearly half of this

population is under the influence of alcohol [87, 88]. Burn patients are already

immunosuppressed and susceptible to systemic complications, but the addition of alcohol

at the time of injury increases the chance of morbidity and mortality. Silver et al.

estimated that patients that present to the emergency room with a positive BAC spend

twice as many days in the intensive care unit, three times as many days on a ventilator,

require more fluid resuscitation and 60% more surgical procedures than burn patients that

were not intoxicated at the time of injury [89]. A longer hospital stay and more days

intubated on a ventilator leads to an increased risk of pulmonary complications that

predisposes burn patients to multiple organ failure, with the lungs preceding all other

organs, as well as a higher chance of mortality [90, 91]. Additionally, research at our

institution showed that intoxicated burn patients with inhalation injury had a smaller

percent burn area in comparison to non-intoxicated burn patients. Yet, these patients still

required the same amount of burn care treatment as patients that were not intoxicated and

had larger injuries, acquiring a hospital bill of over $200,000 even with a mild injury

[92]. Thus, the combined insult of being intoxicated at the time of burn injury is worse

than burn injury alone.

Gut-Liver-Lung Axis

Pulmonary complications are proposed to arise as a result of damage in other

organ systems after burn injury. Multiple organ failure after burn injury is associated with

overgrowth of gut-derived bacteria and its translocation out of the intestinal lumen and

into lymphatic and portal blood systems [93, 94]. In both mice and humans, the gastrointestinal system is the first system to interact with alcohol after it is consumed and it is the primary site of alcohol absorption. In animal models, the absorption of alcohol by the gut prior to burn injury has been shown to increase intestinal permeability and the translocation of bacteria and LPS out of the gut, in comparison to burn injury alone [95-98]. With the majority of the portal blood supply filtering through the liver, increased bacterial burden may result in a greater hepatic response [99, 100]. This, in turn, triggers the hepatic production of IL-6, a marker of inflammation that, when found in high concentrations in the plasma, has been correlated with increased chance of morbidity and mortality in burn patients [101]. The next extensive capillary bed the blood encounters is located within the lungs. Heightened IL-6 levels and bacterial byproducts that either directly enter the bloodstream or enter the lymph are postulated as a mechanism behind exacerbated pulmonary inflammation that is observed after a mouse model of intoxication and injury [99] and may highlight why the lungs are one of the first organs to fail [84].

Burn injury-induced lung apoptosis

Pulmonary inflammation after intoxication and injury associated with similar pulmonary characteristics to ARDS in humans, including increased neutrophil infiltration, capillary permeability and pulmonary edema [83, 102, 103]. Our laboratory and others have established the adverse effect intoxication and injury has on lung tissue [99, 104-107]. We have found elevated levels of alveolar wall thickening, neutrophil accumulation, neutrophil chemokines KC and MIP-2, and increased pro-inflammatory

cytokine IL-6 levels, relative to either ethanol exposure or burn injury alone [99, 104-107] (Figure 2). The increase in bacteria, LPS and IL-6 into the blood and lymph is likely a source of heightened pulmonary inflammation [108, 109]. As described above, AMs help coordinate inflammatory processes in the lungs, but their role and activation state in pulmonary inflammation after intoxication and injury is not known.

Another feature of ARDS is the increased apoptosis of epithelial cells in the lung tissue, described in both humans and in mouse models [110-112]. Not surprisingly, burn injury is associated with increased apoptosis in both lymphoid and parenchymal tissue, including the thymus, spleen, and lungs [113-115]. Mesenteric lymph nodes have also been highly postulated as likely source of gut-derived factors that initiate inflammation in the lungs after burn injury [115, 116]. In a rodent model of 40% TBSA scald injury, an increase in apoptotic cells in the lungs was found at 3 h, but a division of the mesenteric lymph prior to burn injury decreased lung apoptosis at this time point, in comparison to burn injured control counterparts [116]. This further supports the hypothesis that systemic inflammatory mediators are responsible for increased pulmonary inflammation after burn injury. In contrast, other studies have assessed apoptosis in the lungs at 3 and 8 h after a 20% scald injury in mice, but have found varying results on the presence of apoptotic cells in the lung tissue [113, 114, 117]. Fukuzuka et al. reported an increase in apoptosis in the thymus and spleen 3 and 24 h after burn injury, but not in the lungs and liver [113, 114]. Using various methods to detect apoptosis, including terminal deoxynucleotidyl transferase-dUTP nick end labeling (TUNEL) staining, caspase-3 activity and mRNA levels of TNFα and Fas ligand (FasL), their results suggested that the apoptosis observed
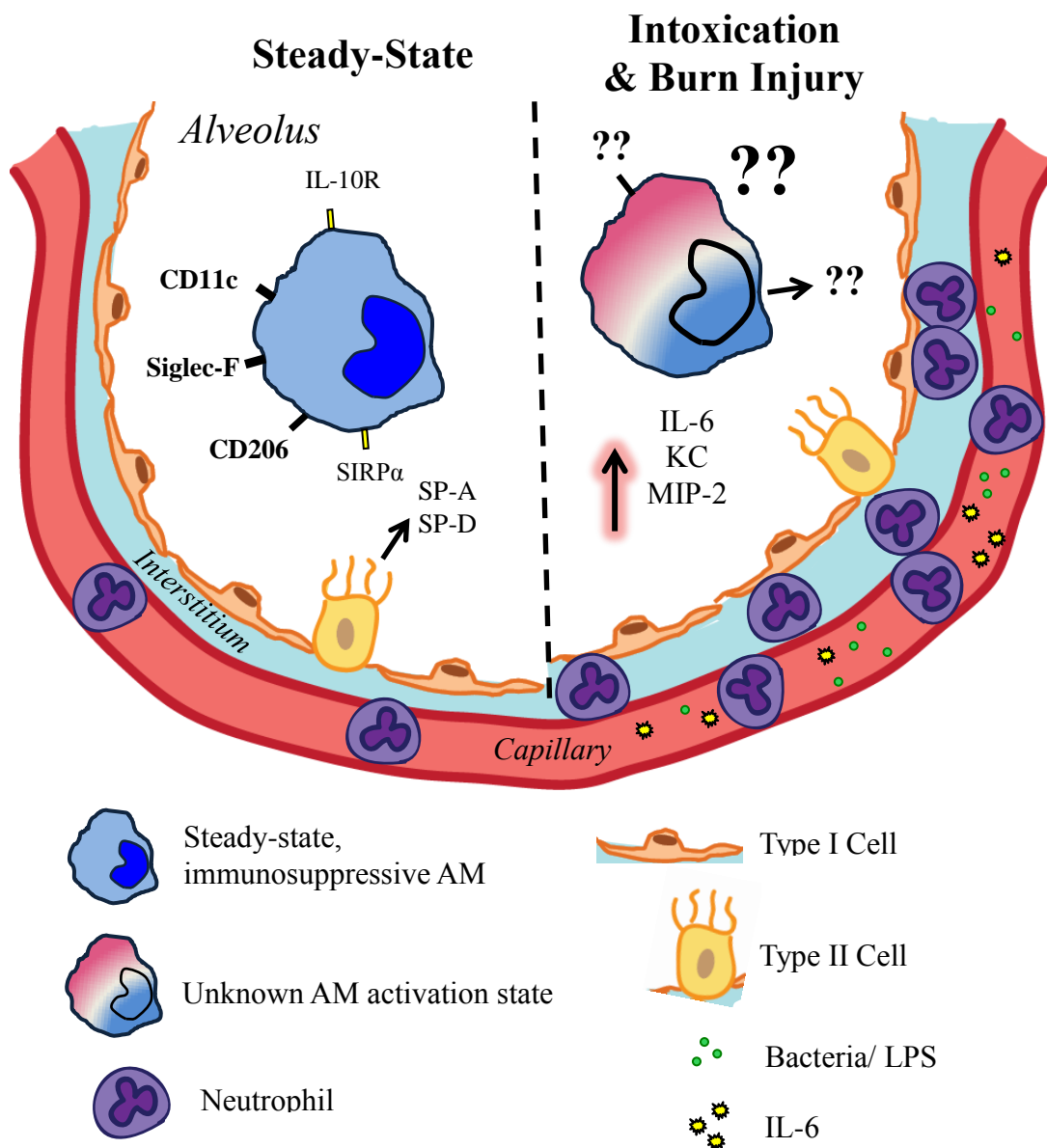
Figure 2: Pulmonary inflammation after intoxication and injury. In steady-state conditions, CD11c^{+}Siglec-F^{+}CD206[+](CD11b^{-}) AMs maintain tolerance and suppress inflammatory responses through inhibitory receptors SIRPα,that binds SP-A and SP-D, and mannose receptor CD206. As a result of heightened levels bacteria/LPS and IL-6 in the blood stream after intoxication and injury, there is increased alveolar wall thickening, neutrophil accumulation in the interstitium and an increase in neutrophil chemoattractants KC and MIP-2, and IL-6 in lung tissue. The activation state and mediators produced by AMs and their role in inflammation after intoxication and injury had not been determined. *Co-illustration credit to C.L. Shults*

in the lymphoid organs was a result of increased caspse-3 activity and was not

dependent on LPS or TNFα. Another study examined apoptosis in the lung at 8 h post-

burn injury and found at this time point there was an increase in caspase-3 activity, but

not in TUNEL^{+} cells in lung tissue [117]. The range of results of these studies are likely

due to differences in the model of burn injury, as well as the methods of apoptotic cell

detection. Of note, these studies failed to identity the cell type undergoing apoptosis in

any of the organs, including the lung. Since both AMs and epithelial cells are regulators

of neutrophil recruitment and AMs are also key organizers of resolving inflammation, the

fate of both of these cells after intoxication and injury is equally important.

Mesenchymal stem cells

Therapeutic agents in lung injury

Bone marrow-derived mesenchymal stem cells (MSCs) are a multipotent

population of stromal cells that are capable of differentiating into osteoblasts,

chondrocytes and adipocytes [118]. In addition to their differentiating properties, they

have been characterized as modulators of acute inflammation by virtue of their ability to

influence the phenotype of macrophages [119]. Exogenous MSC interaction with

macrophages and their release of paracrine soluble factors have been shown to suppress

inflammation and polarize macrophages into an M2, anti-inflammatory phenotype [119-

123]. Many studies suggest that the intravenous administration of MSCs results in the

entrapment of MSCs within the lungs [124-126]. Due to their large size, MSCs become

trapped within the pulmonary vasculature with only a fraction of these cells passing

through and migrating to other organs. Specifically, intravenous administered MSCs have been shown to localize in the lungs and interact with AMs, stimulating AM release of IL-10 [121]. This property characterizes MSCs as a useful therapeutic in acute lung injury.

Thus far, MSC therapy in burn injury has been focused on wound repair, where MSCs are administered near the site of injury [127-130]. Xue et al. demonstrated the plasticity of MSCs to differentiate into tissue-specific cells and to promote accelerated wound healing, while others have shown an increase in neoangeogenesis and a decrease in cellular infiltration at the wound site [130, 131]. Alternative routes of MSC administration and their therapeutic applications is an understudied field in burn research [129], but their anti-inflammatory properties and the ease of which they lodge in the lung after intravenous injections, suggests they would be beneficial to attenuating pulmonary inflammation after burn injury.

In summary, maintaining lung function after intoxication and burn injury is critical to promoting survival in burn patients. AMs are key orchestrators in both pro- and anti-inflammatory responses in the lung and their role in promoting the resolution of inflammation is necessary for the restoration of lung homeostasis. A disruption in the balance of this function can result in excessive inflammatory mediators and injury to the lung tissue, including damage to the alveolar-capillary interface and gas exchange. Therapeutic agents that specifically target AMs and their function in reducing inflammation would be beneficial to the indirect lung damage amassed after burn injury. Mesenchymal stem cell's ability to localize to the lungs and influence an anti-

inflammatory activation profile by AMs, underline MSCs as a promising therapeutic to

reduce inflammatory responses in the lung. Deciphering if MSCs can attenuate

pulmonary inflammation after intoxication and injury will highlight the potential benefits

of MSCs in other models of trauma injury and systemic inflammation.

CHAPTER 3

IMPAIRED RESPIRATORY FUNCTION PARALLELS HEIGHTENED
PULMONARY INFLAMMATION AFTER EPISODIC BINGE ETHANOL
INTOXICATION AND BURN INJURY

Abstract

Clinical data indicate that cutaneous burn injuries covering greater than ten

percent total body surface area are associated with significant morbidity and mortality,

where pulmonary complications, including ARDS, contribute to nearly half of all patient

deaths. Approximately 50% of burn patients are intoxicated at the time of hospital

admission, which increases days on ventilators by three-fold, and doubles length of

hospital admittance, compared to non-intoxicated burn patients. The most common

drinking pattern in the United States is binge drinking, where one rapidly consumes

alcoholic beverages (4 for women, 5 for men) in 2 hours and an estimated 38 million

Americans binge drink, often several times per month. Experimental data demonstrate a

single binge ethanol exposure prior to scald injury, impairs innate and adaptive immune

responses, thereby enhancing infection susceptibility and amplifying pulmonary

inflammation, neutrophil infiltration, and edema, and is associated with increased

mortality. Since these characteristics are similar to those observed in ARDS burn

patients, our study objective was to determine whether ethanol intoxication and burn

injury and the subsequent pulmonary congestion affects physiological parameters of lung

function using non-invasive and unrestrained plethysmography in a murine model system. Furthermore, to mirror young adult binge drinking patterns, and to determine the effect of multiple ethanol exposures on pulmonary inflammation, we utilized an episodic binge ethanol exposure regimen, where mice were exposed to ethanol for a total of 6 days (3 days ethanol, 4 days rest, 3 days ethanol) prior to burn injury. Our analyses demonstrate mice exposed to episodic binge ethanol and burn injury have higher mortality, increased pulmonary congestion and neutrophil infiltration, elevated neutrophil chemoattractants, and respiratory dysfunction, compared to burn or ethanol intoxication alone. Overall, our study identifies plethysmography as a useful tool for characterizing respiratory function in a murine burn model and for future identification of therapeutic compounds capable of restoring pulmonary functionality.

Introduction

Burn injury is associated with significant morbidity and mortality, with greater than 10% of patients succumbing to their injuries when the burn size exceeds 10% of their total body surface area [82]. Clinical data suggest that 42% of the mortality observed in burn patients is due to pulmonary complications [85, 86]. Severe burn, even in the absence of inhalation injury, is a common predisposing factor for the development of Acute Respiratory Distress Syndrome (ARDS) [83, 84]. ARDS is associated with rigid lungs, hypoxemia, and bi-lateral infiltrates in chest radiographs [132]. Overall, respiratory dysfunction in burn patients is characterized by shallow breathing and fluid accumulation in the lung interstitium, leading to heightened vascular resistance and an

increased effort to breathe [84, 86]. A net result of insufficient gas exchange underlies the large percentage of burn fatalities due to pulmonary complications.

Binge alcohol drinking is an increasingly prevalent activity, affecting an estimated 38 million adults in the United States [133]. It is characterized by either the number of alcoholic drinks one consumes in 2 hours (4 for women, 5 for men) or by a blood alcohol concentration of 0.08%. Interestingly, approximately 50% of burn patients are under the influence of alcohol at the time of hospital admission [88, 89]. Intoxicated burn patients have three times as many days on ventilators and an overall twice as long hospital stay compared to burn patients who were not intoxicated [89, 134]. This leads to an increased risk of pulmonary complications that predisposes burn patients to multiple organ failure, with the lungs preceding all other organs, as well as a higher chance of mortality [90, 91]. Notably, the vast majority of intoxicated burn patients are binge drinkers and not chronic dependent drinkers [59, 135, 136]. Experimental models of binge alcohol intoxication and burn injury have demonstrated alterations in innate and adaptive immunity that result in the marked immune dysfunction, greater susceptibility to infection, and amplified pulmonary inflammation [104-106, 137-143]. Previously, our laboratory established that in a mouse model of single-dose binge ethanol exposure and burn injury there is amplified neutrophil infiltration, alveolar wall thickening, and edema in the lungs when alcohol precedes burn injury [99, 104-107]. Since ARDS is associated with similar pulmonary characteristics in humans, including increased neutrophil infiltration, capillary permeability and pulmonary edema [83, 102, 103], the objective of our study was to determine whether intoxication and burn injury, and the resulting

histological pulmonary congestion, affects physiological parameters of lung function using a murine model system.

In these studies, we used non-invasive and unrestrained plethysmography to examine the impact of pulmonary congestion caused by burn injury on breathing patterns and respiratory function [144]. This system measures the box flow, or the airflow in and out of the plethysmography chamber as a result of respiration. Boyle's law states that there is an inverse relationship between the volume and pressure of a gas when the temperature remains constant. Therefore, using Boyle's Law and special algorithms, the box flow can then be translated to the respiratory flow of an individual animal.

The Center for Disease Control (CDC) has reported 1 in 6 adults binge drink at least 4 times a month. Additionally, weekend binge drinking is a pattern observed in many cultures [145]. To mirror this drinking pattern, our laboratory used a mouse model of episodic binge ethanol intoxication prior to burn injury (adapted from [146], [147-150]) to assess respiratory physiology and gain an understanding of the effect of intoxication on lung function after burn injury.

Overall, our analyses identify plethysmography as a useful tool for characterizing respiratory function in a murine model of ethanol intoxication and burn injury. Our studies demonstrate that episodic binge ethanol intoxication prior to burn causes increased pulmonary neutrophil infiltration. The timing of neutrophil accumulation in the lung parallels the heightened levels of lung neutrophil chemoattractants and is associated with respiratory dysfunction, which likely contributes to diminished survival rates.

Materials & Methods

Mice

Male (C57BL/6) mice were purchased from Jackson Laboratories (Bar Harbor, ME) and used at 8-10 weeks old. Mice were housed in sterile micro-isolator cages under specific pathogen-free conditions in the Loyola University Chicago Comparative Medicine facility. All experiments were conducted in accordance with the Institutional Animal Care and Use Committee. Mice weighing between 22 to 27 g were used in these studies.

Murine Model of Binge Ethanol and Burn Injury

A murine model of episodic binge ethanol intoxication and burn injury was employed using intraperitoneal injections as described previously [138, 150, 151]. Animals were given ethanol (1.2g/kg) or saline vehicle at a dose designed to elevate the blood alcohol concentration (BAC) to 150 mg/dL at 30 min after ethanol exposure [142]. This dose of 150 μl of 20% (v/v) ethanol solution or saline control was given daily for 3 days consecutively, mice were given 4 days without ethanol, and then given 3 additional daily ethanol doses. Thirty minutes following the final ethanol exposure, when the BAC was 150 mg/dl, the mice were anesthetized (100 mg/kg ketamine and 10 mg/kg xylazine) and their dorsums shaved. The mice were placed in a plastic template exposing 15% of the total body surface area and subjected to a scald injury in a 92-95°C water bath or a sham injury in room-temperature water [138]. The scald injury results in an insensate, full-thickness burn [152]. The mice were then resuscitated with 1.0 ml saline and allowed to recover on warming pads. All experiments were performed between 8 and 9

am to avoid confounding factors related to circadian rhythms. Animals were either euthanized at 24 hours or survival was measured out to 7 days post-injury.

<div align="center">Plethysmography</div>

Pulmonary function was assessed at 24 hours post-injury by using barometric plethysmography (Buxco Research Systems). BAC levels had returned to baseline undetectable levels at this time point [76]. Mice were placed in an unrestrained whole body barometric plethysmography chamber and allowed to acclimate to the environment before lung function parameters [99] were recorded for 10 minutes on a breath-by-breath basis. Enhanced pause (Penh), breath frequency (f), tidal volume (TVb) and minute volume (MVb) were analyzed.

<div align="center">Histopathologic Examination of the Lungs</div>

The upper right lobe of the lung was inflated with 10% formalin and fixed overnight as described previously [104], embedded in paraffin, sectioned at 5 μm, and stained with hematoxylin and eosin (H&E). Sections were evaluated using light microscopy (Zeiss AxioVert, Zeiss, Thorndale, CA) and histology photographs were taken at 1000x magnification. To measure pulmonary congestion, photographs were taken in a blinded fashion of 10 high power fields (400X) per animal and analyzed using the Java-based imaging program ImageJ (National Institutes of Health, Bethesda, MD). The images were converted to binary to differentiate lung tissue from air space and then analyzed for the percent area covered by lung tissue in each field of view as described previously [107]. Neutrophils were counted in a blinded fashion in 10 high power fields (400X).

Measuring Neutrophil Counts by Flow Cytometry

The upper left lung lobe was removed and cut into small pieces with a razor. The lung tissue was then transferred to a C-tube (Miltenyi Biotec, Auburn, CA) and processed using digestion buffer containing 1mg/ml of Collagenase D and 0.1 mg/ml DNase I (Roche, Indianapolis, IN) in HBSS and a GentleMACS dissociator (Miltenyi Biotec), according to manufacturer's instructions. The homogenates were then filtered through 70 um nylon cell strainers to obtain a single cell suspension. Red blood cells were lysed using ACK lysis buffer (Life Technologies, Grand Island, NY). Cells were counted using trypan blue to exclude dead cells. To assess neutrophil numbers, $1x10^6$ lung cells were first incubated with anti-CD16/32 (clone 93,eBioscience, San Diego, CA) to block unspecific binding to the Fcy II/III receptor. Cells were then immunostained with rat anti-mouse antibodies: CD45 e780 (clone30-F11, eBioscience), CD11b e450 (clone M1/70, eBioscience), and Ly6G (Gr-1) PE Cy7-conjugated (clone RB6-8C5, eBioscience). Antibody incubation was carried out for 30 minutes at 4°C. Cells were washed and fixed as described [143, 153]. Samples were run on a BD Fortessa cytometer (BD Biosciences, San Jose, CA). Data analysis was performed using Flow Jo FCS analysis software (Tree Star Inc., Ashland, OR).

Cytokine Analysis of Lung Homogenates

The right middle lung lobe was snap-frozen in liquid nitrogen and then homogenized in 1 ml of BioPlex cell lysis buffer according to manufacturer's protocol (BioRad, Hercules, CA). The homogenates were filtered and analyzed for cytokine

production using a BioPlex multiplex bead array. The results were normalized to total protein using the BioRad protein assay (BioRad) [106, 107].

Statistical Analysis

Statistical comparisons were made between the sham vehicle, sham ethanol, burn vehicle, and burn ethanol treatment groups. One-way analysis of variance (ANOVA) was used with Tukey's post-hoc test or Bonferroni Multiple Comparisons test and values were considered statistically significant when $p < 0.05$. Data is reported as mean values $\pm$ the standard error of the mean (SEM). The Gehan-Breslow-Wilcoxon test was used to generate comparisons between burn groups in the survival study and Pearson's correlation test was used to generate the correlation coefficient between neutrophil numbers and Penh, breath frequency, tidal volume, and minute volume.

Results

Binge Ethanol Intoxication Decreases Survival After Burn Injury

Mice exposed to episodic binge ethanol intoxication and burn injury were monitored for survival out to 7 days post-injury. Both sham groups had 100% survival regardless of ethanol intoxication (Figure 3). Survival of burn-injured mice exposed to ethanol was significantly lower (48% survival) ($p < 0.05$) when compared to burn-injured mice not exposed to ethanol (84% survival) ($p < 0.05$). Observed mortality in the combined injury group occurred within 72 hours of injury, with 5% succumbing by 24 hours, 16% mortality between 24 and 48 hours and the majority of death, 31%, occurring between 48 and 72 hours. This suggests there is a therapeutic window between time of injury and 24 hours to potentially prevent mortality when ethanol precedes burn injury.
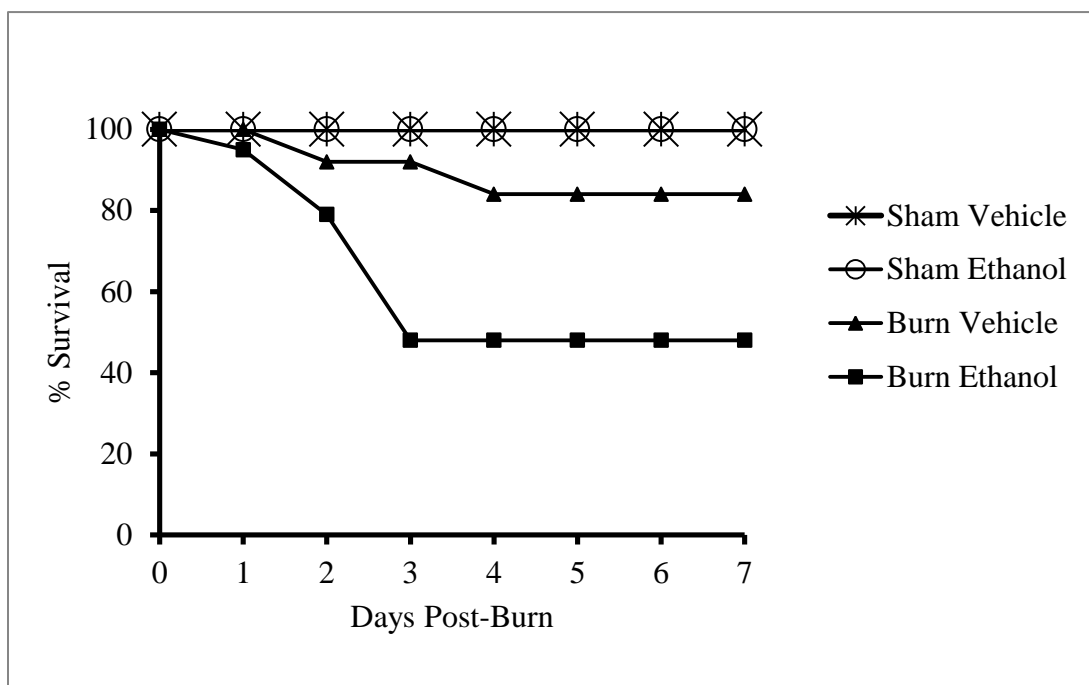
Figure 3. Decreased survival of mice exposed to ethanol prior to burn injury. Mice were exposed to ethanol or saline as a control for a total of 6 days (3 days ethanol, 4 days rest, 3 days ethanol) prior to burn injury and monitored for survival out to 7 days post-injury. $p < 0.05$, burn ethanol compared to burn vehicle by Gehan-Breslow-Wilcoxon test. Data were combined from 2 independent experiments and are expressed as percent survival. N = 4 (sham groups), n = 10-19 (burn groups).
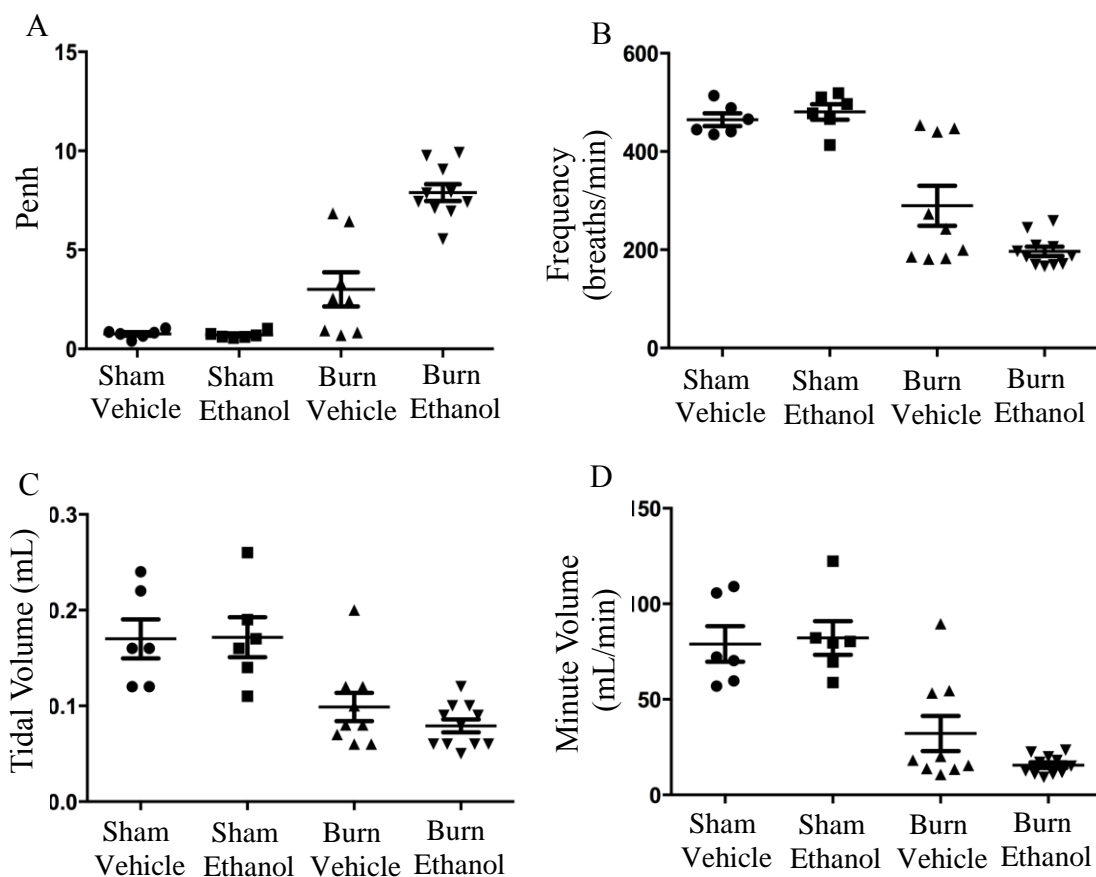
Figure 4. Ethanol intoxication impairs post-burn lung function. Mice were placed in an unrestrained whole body barometric plethysmography chamber and lung function parameters were recorded for 10 minutes. Penh, $p < 0.05$ burn ethanol versus all groups, $p < 0.05$ burn vehicle versus sham groups. Breath frequency, $p < 0.05$ burn ethanol versus all groups, $p < 0.05$ burn vehicle versus sham groups. Tidal volume, $p < 0.05$ burn ethanol compared to sham groups, $p < 0.05$ burn vehicle compared to sham groups. Minute volume, $p < 0.05$ burn ethanol compared to sham groups, $p < 0.05$ burn vehicle compared to sham groups. Data were combined from 2 independent experiments. Data points shown as individual animals. N = 6-11 animals per group.

Intoxication Reduces Lung Function in Mice Subjected

to Burn Injury

Lung function was assessed 30 minutes prior to animals being euthanized at 24 hours post-injury. Enhanced pause (Penh), a measure of bronchoconstriction and airway resistance, revealed that animals that were intoxicated at the time of burn injury had an average Penh of 8, compared to sham groups with a Penh of less than 1 and burn injury alone with an average Penh of 3 (Figure 4A). When ethanol intoxication precedes burn injury, this corresponds with an 8-fold increase in airway resistance, compared to sham groups ($p < 0.05$), and a 2.5-fold increase, compared to burn injury alone ($p < 0.05$). Moreover, our data reveal that animals with a Penh of 7 or above are at a greater risk for mortality. The frequency of breaths per minute was also significantly decreased in both burn groups. Burn injury alone had a 39% decrease in the average number of breaths per minute compared to shams ($p < 0.05$), while intoxicated and burn-injured mice had a 59% decrease compared to shams ($p < 0.05$) and a 33% decrease compared to burn alone ($p < 0.05$) (Figure 4B). Additionally, tidal volume, the amount of air that is inhaled and exhaled in a single breath, was decreased in both burn groups compared to sham groups ($p < 0.05$) (Figure 4C). Minute volume, the amount of air inhaled and exhaled per minute, was also decreased in both burn groups (Figure 4D). Compared to shams, burn injury alone had a 60% decrease in the amount of air per minute ($p<0.05$), while intoxicated and burn-injured mice had an 80% decrease ($p<0.05$). Furthermore, combined injury had a 52% decrease compared to burn alone, though this did not reach statistical significance. These data indicate burn injury alone induces abnormal breathing patterns, however,

when intoxication precedes burn injury, there is a dramatic increase in airway resistance and a pronounced reduction in lung function. Overall, intoxicated and burn injured animals have a shallow, slower breathing rate than burn injury alone, indicative of overall respiratory dysfunction.

Elevated Pulmonary Neutrophil Infiltration and Congestion

after Intoxication and Burn Injury

Similar to the single-dose binge ethanol and burn injury results previously reported by our laboratory, [104-107] histochemical analyses of sectioned lung tissue demonstrated that episodic binge ethanol intoxication prior to burn injury results in increased cellularity and alveolar wall thickening 24 hours post-injury (Figure 5A-C). Neutrophils were counted by light microscopy as previously described [104]. When intoxication preceded burn injury, there was a 10-fold increase compared to sham groups ($p < 0.05$) and an approximate 1.5-fold increase compared to burn alone (Figure 5B). Additionally, these neutrophils were localized to the interstitium and not the alveolar space. Pulmonary congestion was quantified using imaging software to measure the area of lung tissue in 10 high power fields per animal and is reported as a percentage of the entire field of view. Intoxicated and burn injured animals had a significant increase in tissue area compared to all other groups ($p < 0.05$), correlating to a decrease in air space and an increase in pulmonary congestion (Figure 5C). Notably, these changes were isolated to the distal airways. There were no apparent changes in the larger airways.

To further demonstrate that neutrophils were the key cell type contributing to the escalated cellularity, flow cytometry was performed. Flow cytometric analysis of cellular
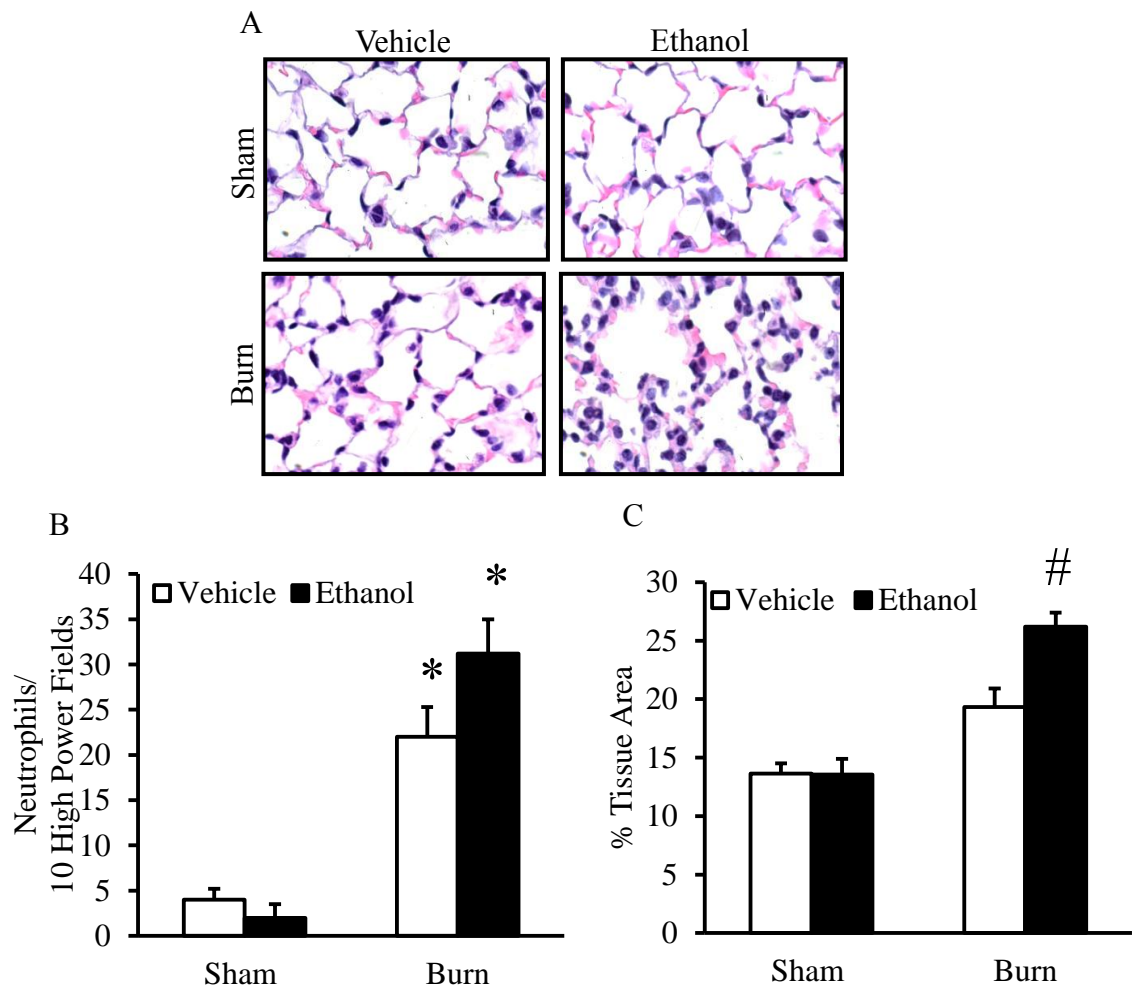
Figure 5. Episodic binge ethanol results in similar pulmonary congestion as single dose binge ethanol and burn injury. Lungs were sectioned and stained with H&E and assessed for cellular infiltration and alveolar wall thickening. A) Representative sections from each treatment group are shown at 1000x. B) Neutrophils were counted by light microscopy in H&E-stained lung sections 24 hours after intoxication and burn injury. Data are shown as the total number of neutrophils in 10 high power fields (400x). C) Quantification of pulmonary congestion 24 hours after injury. * $p < 0.05$ compared to sham groups; # $p < 0.05$ compared to all groups. Data are presented as mean values ± SEM. N = 3-6 animals per group.
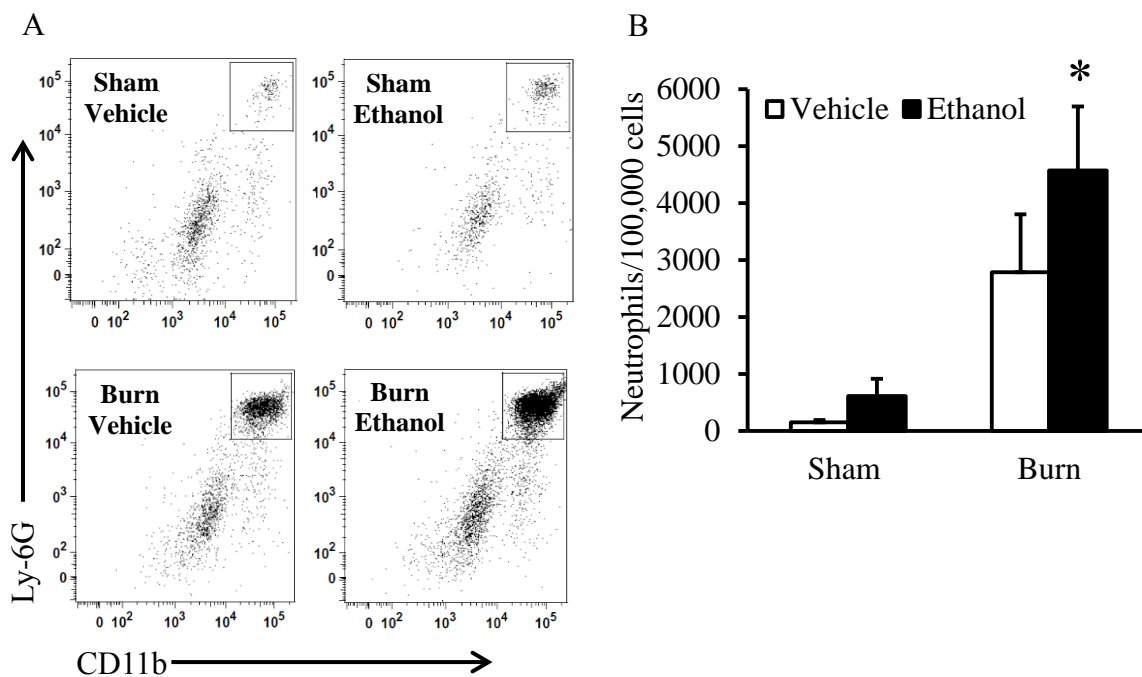
Figure 6. Ly-6G^{+}CD11b^{+} neutrophils are elevated after episodic binge ethanol and burn injury. Lung tissue was obtained 24 hours post-injury from all treatment groups. Tissue was digested into a single cell suspension and cells were analyzed by flow cytometry. A) Representative gating for Ly-6G^{+}CD11b^{+} neutrophils (box) of CD45^{+}F4/80^{-} cells (data not shown) from all four treatment groups. B) Absolute number of neutrophils in lung isolates. * $p < 0.05$ versus sham groups. Data are presented as mean of total neutrophils from 100,000 lung cells per group $\pm$ SEM. N = 3-6 animals per group.

subsets in the lung revealed dramatically increased $CD45^+CD11b^+Ly6G^+$ neutrophil cell counts in intoxicated and burn injured mice at 24 hours post-injury, compared to sham and isolated burn injury alone ($p < 0.05$) (Figures 6A&B). Mice exposed to the combined insult had a 7-fold increase ($p < 0.05$) in neutrophil numbers when compared to both sham groups and a 1.5-fold increase when compared to burn-injured animals without ethanol intoxication, confirming that neutrophils contribute to increased cellularity in the lungs of intoxicated and burn-injured mice.

It was also observed that the increase in the number of neutrophils corresponded to an increase in Penh and decreases in breath frequency, tidal volume and minute volume. Pearson's correlation coefficient was used to determine if there was a linear relationship between the number of infiltrating neutrophils and lung function measurements. We found a positive correlation between the number of neutrophils and Penh ($r = 0.9597$) and negative correlations between neutrophil numbers and breath frequency ($r = -0.9866$), tidal volume ($r = -0.9777$) and minute volume ($r = -0.9784$). These data emphasize the potential use of plethysmography as an instrument to determine the effect of neutrophil accumulation in lung tissue on overall lung function.

Ethanol Intoxication Before Burn Injury Enhances Pulmonary KC and Macrophage

Inflammatory Protein - 2 (MIP-2) Levels

Since we observed increased neutrophil infiltration, we next sought to examine levels of the neutrophil chemoattractants, KC and MIP-2. Similar to our single-dose binge ethanol and burn injury findings [104-106], the upregulation of neutrophil

A

B
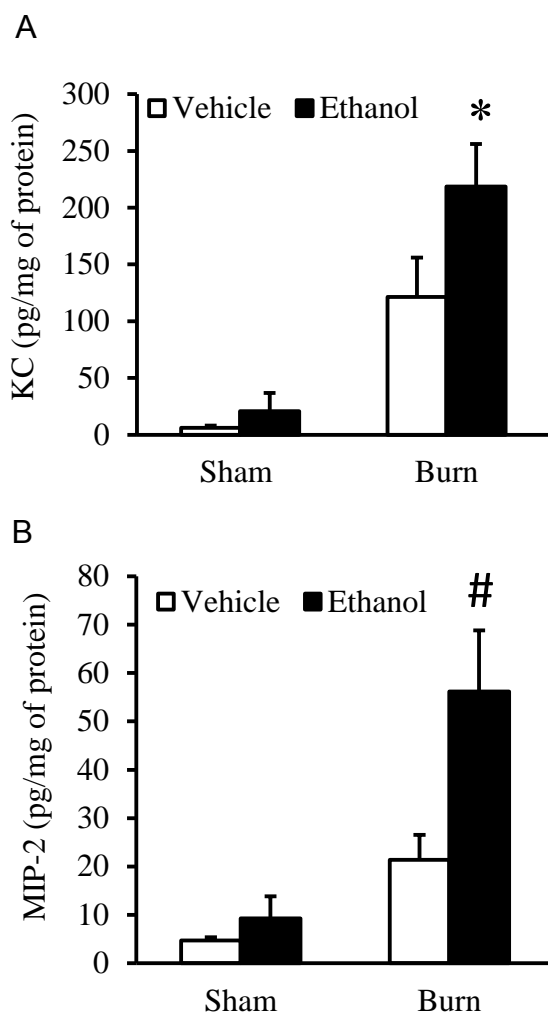
Figure 7. Heighted pulmonary neutrophil chemokine KC and MIP-2 levels after episodic binge ethanol and burn injury. Lung homogenates from all four treatment groups were analyzed for levels of A) KC and B) MIP-2. * $p < 0.05$ versus sham groups; # $p < 0.05$ versus all treatment groups. Data are presented as the mean in picograms per milligram of protein ± SEM. N = 3-6 animals per group.

chemokines KC and MIP-2 highlight a mechanism behind the increase in pulmonary neutrophil accumulation in episodic binge ethanol exposed and burn-injured mice (Figure 7). Combined injured animals had an 11-fold more KC than both sham groups ($p < 0.05$) and 1.8-fold more KC than burn injury alone (Figure 7A). Additionally, MIP-2 was significantly upregulated compared to all treatment groups, with a 6-fold increase in MIP-2 compared to sham groups ($p < 0.05$) and a 2.5-fold increase compared to burn injury alone ($p < 0.05$) (Figure 7B).

Summary

Intoxication at the time of burn injury increases bacterial translocation from the intestines into the lymphatic system and bloodstream. Excessive levels of IL-6 and endotoxins not removed by the liver may circulate to the vascular bed of the lungs and initiate pulmonary inflammation and congestion [95-100]. Prior to this study, it was not known how multiple doses of ethanol would affect burn-induced pulmonary inflammation. Ethanol intoxication alone has been shown to suppress immune responses in many organs, including the lungs [8, 75, 154, 155]. Whether episodic ethanol intoxication before burn injury would yield heightened or diminished pulmonary inflammatory effects had yet to be determined. It was also not known how intoxication prior to injury affects lung function. Here, we have demonstrated that episodic binge ethanol prior to burn injury causes heightened pulmonary inflammatory responses and congestion, paralleling single-dose binge ethanol exposure. Importantly, we have found that these histologic inflammatory responses cause physiological derangements in

intoxicated and burn-injured animals, including increased airway resistance and abnormal breathing patterns. These findings highlight an underlying mechanism contributing to the drastic mortality rate observed in mice exposed to both ethanol and burn injury.

In conclusion, these data emphasize the importance of immediate burn care treatment within the few hours after injury, to stabilize breathing patterns and to maintain respiratory function, especially when patients are intoxicated at the time of injury. Non-invasive, unrestrained whole-body plethysmography will be a useful tool in future animal studies to help identify therapeutic reagents that can improve respiratory function in all burn patients.

CHAPTER 4

LOSS OF ALVEOLAR MACROPHAGES CORRELATES WITH ELEVATED
NEUTROPHIL NUMBERS IN THE LUNG FOLLOWING INTOXICATION AND
BURN INJURY

Abstract

Clinical evidence reveals that half of all burn patients brought to the emergency

department are intoxicated at the time of injury. This combined insult results in

amplified neutrophil accumulation in the lung and pulmonary edema, with an overall

increased risk of lung failure and mortality, relative to either insult alone. We and others

believe that this excessive pulmonary inflammation, that also parallels decreased lung

function, is attributed, in part, to AM function. Restoration of lung tissue homeostasis is

dependent on the eradication of neutrophil infiltration and removal of apoptotic cells,

both major functions of AMs. With lung function impairment causing a likely decrease

in gas exchange, we chose to examine the fate of these multi-functional cells. Thirty

minutes after binge ethanol intoxication, mice were anesthetized and given a 15% total

body surface area dorsal scald injury. At 24 h, we found a 50% decrease in the number of

AMs ($p<0.05$) and 7-fold more TUNEL$^+$ apoptotic cells ($p<0.05$) in the lungs after

intoxication and injury, relative to control. Analysis of annexin V and propidium iodide

on BAL AMs revealed a 2-fold increase in the percent of dead AMs ($p<0.05$) and a 3-

fold increase in the percent of apoptotic AMs, above that of controls. Interestingly, AMs

that were recovered from intoxicated and injured mice had 5-fold more phagocytic AMs,

relative to AMs from controls (p<0.05) and also spontaneously produced 5-fold more

tumor necrosis factor α than controls (p<0.05). Intratracheal clodronate liposome

reduction of AMs correlated with a rise in lung neutrophil numbers in intoxicated and

injured mice, relative to empty liposome treatment. In summary, these data support AMs

role in managing neutrophil numbers and inflammation in the lung after intoxication and

burn injury and the significant loss of AMs may delay resolution of inflammation,

resulting in the elevated mortality rate observed in intoxicated and burn-injured patients.

Introduction

ARDS is a common morbidity among severe burn-injured patients, with or

without inhalation injury [83, 84]. Infiltration of inflammatory cells and increased

pulmonary edema lead to impaired gas exchange and increase the risk of pulmonary

failure [83, 102, 103], resulting in an estimated 42% of the mortality after burn injury

linked to pulmonary complications [85, 86]. Alcohol is the most abused substance in the

United States [133] and is a factor in many unintentional injuries, including burn injuries,

making alcohol the 3rd leading cause of preventable death [63]. The consumption of

alcohol prior to injury can lead to worsened outcomes and clinical data suggests that

nearly half of all burn patients that are taken to the emergency room have a positive blood

alcohol content [88, 89, 92]. Notably, of those who consume alcohol, the majority of the

drinkers are binge drinkers, not chronic dependent drinkers [59].

We and others have established in a mouse model of intoxication and burn injury

that lung inflammation mirrors similarities to the characteristic pathology of ARDS.

Within the distal airways of the lung we found increased alveolar wall thickening and

neutrophil accumulation into the interstitium, that paralleled heightened levels of neutrophil chemokines KC and MIP-2, as well as pro-inflammatory cytokine IL-6 levels, relative to either ethanol exposure or burn injury alone [99, 104-107, 156]. The increased number of neutrophils infiltrating into the lung interstitium correlated to a decrease in lung function. This pulmonary inflammation therefore may have causative role in increased mortality associated with alcohol exposure prior to burn injury [156].

AMs are the lungs first line of defense against inhaled particles or pathogens and elegantly coordinate the on-set and resolution of inflammation [157]. The transition from steady-state healthy conditions to an inflammatory state is made possible by the plasticity of macrophages to readily activate into a reversible inflammatory profile as either a pro-inflammatory, M1 macrophage or an anti-inflammatory, M2 macrophage, depending on mediators present within the microenvironment. AMs have a phenotype distinct from other tissue-resident macrophage populations and can be characterized as CD11c^{+}CD11b^{-} Siglec-F^{+}F4/80^{+}, with constitutive expression of mannose receptor CD206 and low to negative expression of major histocompatibility complex class II (MHC II) [20, 21, 158]. The upregulation of specific receptors on AMs can define AM function in different stages of inflammation. Scavenger receptor MARCO is described as a marker of pro-inflammatory M1 macrophages and aids in the clearance of apoptotic cells (termed efferocytosis) [159] [32, 160]. Additionally, CD11b is also an important receptor in efferocytosis [161]. During the resolution phase of inflammation, CD206 has been characterized as a marker of a M2, anti-inflammatory profile [34, 162-164], thus an up or down regulation of CD206 on AMs from baseline levels could suggest a transition to an

activated profile. Lastly, M2 marker interleukin (IL)-10 receptor (IL-10R) on AMs is also important in regulating inflammation, where the ligation of IL-10R indirectly inhibits the TLR4 signaling pathway, decreasing pro-inflammatory cytokine release [33].

During an inflammatory response in the lung, excessive levels of mediators produced by macrophages or neutrophils can result in tissue damage if not properly regulated [41]. Therefore, lung inflammation needs to be a highly monitored process. Resolution is achieved through pathogen clearance, downregulation of neutrophil chemokines and the removal of apoptotic cells, such as neutrophils, all potential functions AMs [165]. Specifically, macrophage efferocytosis can down regulate NO release and upregulate IL-10 and TGFβ [43-46]. Burn injury and apoptosis studies revealed an increase in apoptosis in both lymphoid and parenchymal tissue, including the thymus, spleen, and lungs, at 3 and 8 h post-injury; however, the specific cell subsets undergoing apoptosis were not analyzed in these studies [113-115]. Moreover, another feature of ARDS is the increase in apoptosis of epithelial cells in the lung tissue, described in both humans and in mouse models [110-112]. The role of AMs in coordinating on-going inflammation and the timely initiation of resolution emphasizes that the activation profile and fate of AMs during inflammation is critical to restoring lung homeostasis.

Since intoxication at the time of injury results in greater pulmonary complications and mortality rates than burn injury alone, we chose to examine the role of AMs in only intoxicated and burn-injured mice, in comparison to sham vehicle control. In this study, we examined the role of AMs in pulmonary inflammation after intoxication and burn injury. Our results suggest that at 24 h after injury there is a 50% reduction in the number

of AMs present within the lung tissue, but AMs that were isolated from the tissue exhibited an efferocytosis function. Upregulation of MARCO and CD11b are consistent with findings of increased efferocytosis by AMs. Additionally, we found heightened numbers of apoptotic cells in the lungs and identified AMs as at least a small population of these apoptotic cells. Finally, clodronate liposome reduction of AMs prior to intoxication and injury correlated with an increase in neutrophil numbers, in comparison to intoxicated, injured and empty liposome treated mice. We conclude that AMs role in clearing apoptotic cells and limiting the number of neutrophils in the lung is subdued by an increase in the apoptosis of AMs.

Materials & Methods

Mice

Male (C57BL/6) mice were purchased from Jackson Laboratories (Bar Harbor, ME) and used at 8-10 weeks old. Mice were housed in sterile micro-isolator cages under specific pathogen-free conditions in the Loyola University Chicago Comparative Medicine facility. All experiments were conducted in accordance with the Institutional Animal Care and Use Committee. Mice weighing between 22 to 27 g were used in these studies.

Murine Model of Binge Ethanol and Burn Injury

A murine model of single dose binge ethanol intoxication and burn injury was employed using oral gavage as described previously [138, 150, 151]. Animals were given 400 μl of 10% (v/v) ethanol solution (1.6 g/kg) or water control by gavage at a dose designed to elevate the blood alcohol concentration to 150 mg/dL at 30 min after ethanol

exposure [142]. Thirty minutes following the ethanol exposure, the mice were

anesthetized (100 mg/kg ketamine and 10 mg/kg xylazine) and their dorsum shaved. The

mice were placed in a plastic template exposing 15% of the total body surface area and

subjected to a scald injury in a 92-95°C water bath or a sham injury in room-temperature

water [138]. The scald injury results in an insensate, full-thickness burn [152]. The mice

were then resuscitated with 1.0 ml saline and allowed to recover on warming pads. All

experiments were performed between 8 and 9 am to avoid confounding factors related to

circadian rhythms. Animals were euthanized at 24 hours.

<div align="center">Histopathologic Examination of the Lungs</div>

The upper right lobe of the lung was inflated with 10% formalin and fixed

overnight as described previously [104], embedded in paraffin, sectioned at 5 μm, and

stained with hematoxylin and eosin (H&E). Sections were evaluated using light

microscopy (Zeiss AxioVert, Zeiss, Thorndale, CA) and histology photographs were

taken at 400x magnification. Neutrophils were counted in a blinded fashion in 10 high

power fields (400X).

<div align="center">Cytokine Measurements in Lung Homogenates</div>

The right middle lung lobe was snap-frozen in liquid nitrogen and then

homogenized in 1 ml of BioPlex cell lysis buffer according to manufacturer's protocol

(BioRad, Hercules, CA). The homogenates were filtered and analyzed for cytokine

production using a BioPlex multiplex bead array [106, 107]. The results were normalized

to total protein using the BioRad protein assay (BioRad).

Isolation of Cells from Lung Tissue

The upper left lung lobe was removed and cut into small pieces with a razor. The lung tissue was then transferred to a C-tube (Miltenyi Biotec, Auburn, CA) and processed using digestion buffer containing 1mg/ml of Collagenase D and 0.1 mg/ml DNase I (Roche, Indianapolis, IN) in HBSS and a GentleMACS dissociator (Miltenyi Biotec), according to manufacturer's instructions. The homogenates were then filtered through 70 um nylon cell strainers to obtain a single cell suspension [21]. Red blood cells (RBCs) were lysed using ACK lysis buffer (Life Technologies, Grand Island, NY). Cells were counted using trypan blue to exclude dead cells.

Bronchoalveolar Lavage

The lungs of mice were lavaged 5 times with 1 mL of cold PBS to obtain the bronchoalveolar lavage (BAL) fluid [76]. All lavage washes were pooled per animal. Cells were spun at 1200 rpm for 3 min at 4°C. RBCs were lysed using ACK lysis buffer, washed and spun at 1200 rpm for 3 min at 4°C. Cells were resuspended up to 400ul in PBS and counted using a hemocytometer. Cells were either analyzed by flow cytometry, cultured in chamber slides or cytocentrifued onto slides.

Flow Cytometry Analysis of Alveolar Macrophages

To assess alveolar macrophages, $1x10^6$ lung cells or $1x10^5$ BAL cells were first incubated with anti-CD16/32 (clone 93,eBioscience, San Diego, CA) to block unspecific binding to the Fcγ II/III receptor. Cells were then immunostained with rat anti-mouse antibodies: CD11c APC-eFluor 780 (clone N418, eBioscience), CD11b eFluor 450 (clone M1/70, eBioscience), Siglec-F PE-CF594 (clone E50-2440, BD Biosciences, San Jose,

CA), CD206 PE (clone C068C2, Biolegend, San Diego, CA), Ly-6G (Gr-1) PE-Cy7

(clone RB6-8C5, eBioscience), F4/80 APC (clone BM8, eBioscience), MHC II (I-A/I-E)

V500 (clone M5/114.15.2, BD Biosciences), TLR4/MD-2 APC (clone MTS510,

eBioscience), IL-10R PE (clone 1B1.3a, BD Biosciences), MARCO FITC (clone ED31,

AbD Serotec, Raleigh, NC) [21]. Antibody incubation was carried out for 30 minutes at

4^oC. Cells were washed and fixed as described [143, 153]. MHC II was used as a M1

marker and CD206 was used a M2 marker [21]. In separate experiments, apoptosis and

cell death was also assessed on BAL alveolar macrophages using an Alexa Fluor® 488

Annexin V/Dead Cell Apoptosis Kit (Life Technologies), according to the

manufacturer's protocol. Samples were run on a BD Fortessa cytometer (BD

Biosciences). Data analysis was performed using Flow Jo FCS analysis software (Tree

Star Inc., Ashland, OR). BAL alveolar macrophages were also analyzed for apoptosis

using a CellEvent™ Caspase-3/7 Green Flow Cytometry Kit (Life Technologies),

according to manufacturer's protocol, in combination with Siglec-F PE (BD

Biosciences). Samples were run on an Amnis ImageStreamX flow cytometer (Millipore,

Billerica, MA) and analyzed on IDEAS software (Amnis Millipore, Seattle, WA).

<div align="center">Intracellular Staining of iNOS and ARG1</div>

BAL cells were isolated and plated at 50,000 cells in 200ul complete medium (RPMI

without phenol red with 10% FBS and 5% penicillin-streptomycin-glutamine (PSG)) per

chamber slide well. Slides were incubated 1.5 h at $37^°$C to let macrophages adhere.

Supernatant was removed and stored at $-80^°$C for future cytokine analysis studies using a

BioPlex multiplex bead array. Cells fixed with 4% PFA for 20 minutes at room

temperature and then permeabilized with 0.2% Triton X-100 for 30 min at 37°C,

followed by 10 min at room temperature. To block non-specific binding, cells were

incubated with superblock for 5mins at room temperature and stained overnight 4°C with

mouse anti-mouse Arginase 1 (ARG1) (Abcam, Cambridge, MA) and rabbit anti-mouse

inducible nitric oxide synthase (iNOS) (Abcam). Secondary antibodies donkey anti-

mouse IgG 488 (Abcam) and donkey anti-rabbit IgG 594 were applied for 1.5 h at room

temperature. Slides were air dried and mounted with Prolong Gold Dapi (Life

Technologies).

Analysis of Alveolar Macrophages

BAL cells were cytocentrifuged onto slides using a Shandon Cytospin 2. Briefly,

50,000 BAL cells were resuspended in total of 200ul PBS and cytocentrifuged at

400RPM for 5 min. Slides were stained with HEMA 3 differential stain and analyzed

using light microscopy (EVOS, Life Technologies). Photographs of cells were taken at

100x and 400x magnification. Phagocytic alveolar macrophages were counted in a

blinded fashion in 5 high power fields (400X). Additionally, cytocentrifuged cells were

stained with rabbit anti-mouse active-caspase 3 antibody (Abcam), followed by

secondary antibody donkey anti-rabbit IgG 594. Briefly, cells were fixed with 4%

paraformaldehyde (PFA), permeabilized with 0.1% Triton-100x in 2% BSA and blocked

with 10% normal donkey serum. In a humidity chamber, cells were incubated with rabbit

anti-mouse active-caspase 3 overnight at 4°C, followed by donkey anti-rabbit IgG 594 for

1 h at room temperature. Slides were air dried and mounted with Prolonged Gold Dapi

(Life Technologies). Immunofluorescent photographs were taken at 1000x using a

Zeiss AxioVert microscope.

TUNEL Immunofluorescent Staining in Lung Tissue

The upper right lobe of the lung was inflated with 10% formalin and fixed

overnight as described previously embedded in paraffin, sectioned at 5 μm [104]. A

Click-it® Plus *in situ* terminal deoxynucleotidyl transferase-dUTP nick end labeling

(TUNEL) Alexa Fluor 488 assay was performed according to manufacturer's protocol

(Life Technologies) to detect apoptotic cells. Lung sections were evaluated using

fluorescent microscopy (EVOS, Life Technologies) and photographs were taken at 100x

and 400x. TUNEL^{+} cells were counted in a blinded fashion in 10 low power fields

(100X) using a Java-based imaging program ImageJ (National Institutes of Health,

Bethesda, MD). The images were converted to binary to differentiate TUNEL^{+} from non-

fluorescent cells and then analyzed for the number of TUNEL^{+} cells in each field of view.

Alveolar Macrophage Immunofluorescent Staining for Siglec-F

The upper left lobe was inflated with 25% optimal cutting temperature (OCT)

freezing medium, frozen in OCT over dry ice and stored at -80°C. Tissue was

cryosectioned at 6 μm and sections were air-dried for 1 hour at room temperature. Slides

were fixed for 5 min in 4% PFA and blocked with superblock for 5 min. In a humidity

chamber, sections were incubated overnight at 4°C with rat anti-mouse purified Siglec-F

(Clone E50-2440, BD Biosciences), followed by secondary antibody goat anti-rat Alexa

Fluor® IgG (H+L) 555 (Life Technologies) for 1 h at room temperature. Slides were air

dried and mounted with prolonged dapi gold (Life Technologies). For double staining of

Siglec-F and TUNEL, slides were first stained for Siglec-F, followed by TUNEL

staining, according to the manufacturers protocol (Life Technologies). Sections were

evaluated using immunofluorescent microscopy (Zeiss AxioVert, Zeiss, Thorndale, CA)

and photographs were taken at 400x and 1000x magnification.

Depletion of Alveolar Macrophages

AMs were depleted using clodronate encapsulated liposomes (Encapsula

NanoSciences, Brentwood, TN). Briefly, mice were anesthetized (100 mg/kg ketamine

and 10 mg/kg xylazine) and given intratracheal administration (75ul) of clodronate

liposomes or control, empty liposomes. Three days after clodronate administration, mice

underwent our model of binge ethanol and burn injury and were euthanized at 24 h after

injury.

Serum Measurements

Blood was collected via cardiac puncture and the serum was isolated at stored at

-80°C. Serum aliquots were used to measure IL-6 by enzyme linked immunosorbent

assay (ELISA) (BD Biosciences, Franklin Lakes, NJ).

Plethysmography

Pulmonary function was assessed at 24 hours post-injury by using barometric

plethysmography (Buxco Research Systems). BAC levels had returned to baseline

undetectable levels at this time point [76]. Mice were placed in an unrestrained whole

body barometric plethysmography chamber and allowed to acclimate to the environment

before lung function parameters [99] were recorded for 10 minutes on a breath-by-breath

basis. Enhanced pause (Penh), breath frequency (f), tidal volume (TVb) and minute

volume (MVb) were analyzed.

Statistical Analysis

Statistical comparisons were made between the sham vehicle and burn ethanol treatment groups. Unpaired T-test was used and values were considered statistically significant when $p < 0.05$. Data is reported as mean values ± the standard error of the mean (SEM).

Results

Alterations In Alveolar Macrophage Populations After Intoxication And Injury

We confirmed the phenotype of AMs obtained through either enzymatic dissociation of lung tissue or from the BAL fluid (see Appendix A). Our observations of a decrease in the density of the AM population (Appendix A, Figure 31G), but an increase in the granularity of AMs that are present (Appendix A, Figure 32D) after intoxication and injury supported the examination of the absolute number and activation profile of AMs. Quantification of AMs revealed that in intoxicated and injured mice there was a 50% decrease in the number of AMs from dissociated lung tissue ($p<0.05$) (Figure 8A), as well as a 50% decrease in the number of BAL cells recovered from BAL fluid ($p<0.05$) (Figure 8B), in comparison to sham mice. While it was not significant, there was a 1.5-fold increase in the number of $CD11c^+CD11b^+F4/80^{lo}Siglec\text{-}F^+$ intermediate AMs after intoxication and injury (Figure 8C). Expression of surface receptors using mean fluorescence intensity (MFI) revealed no significant change in the level of MHC II (Figure 9A). This was not surprising since we would not expect antigen presentation without an active lung infection in the airways. There was also no significant change in
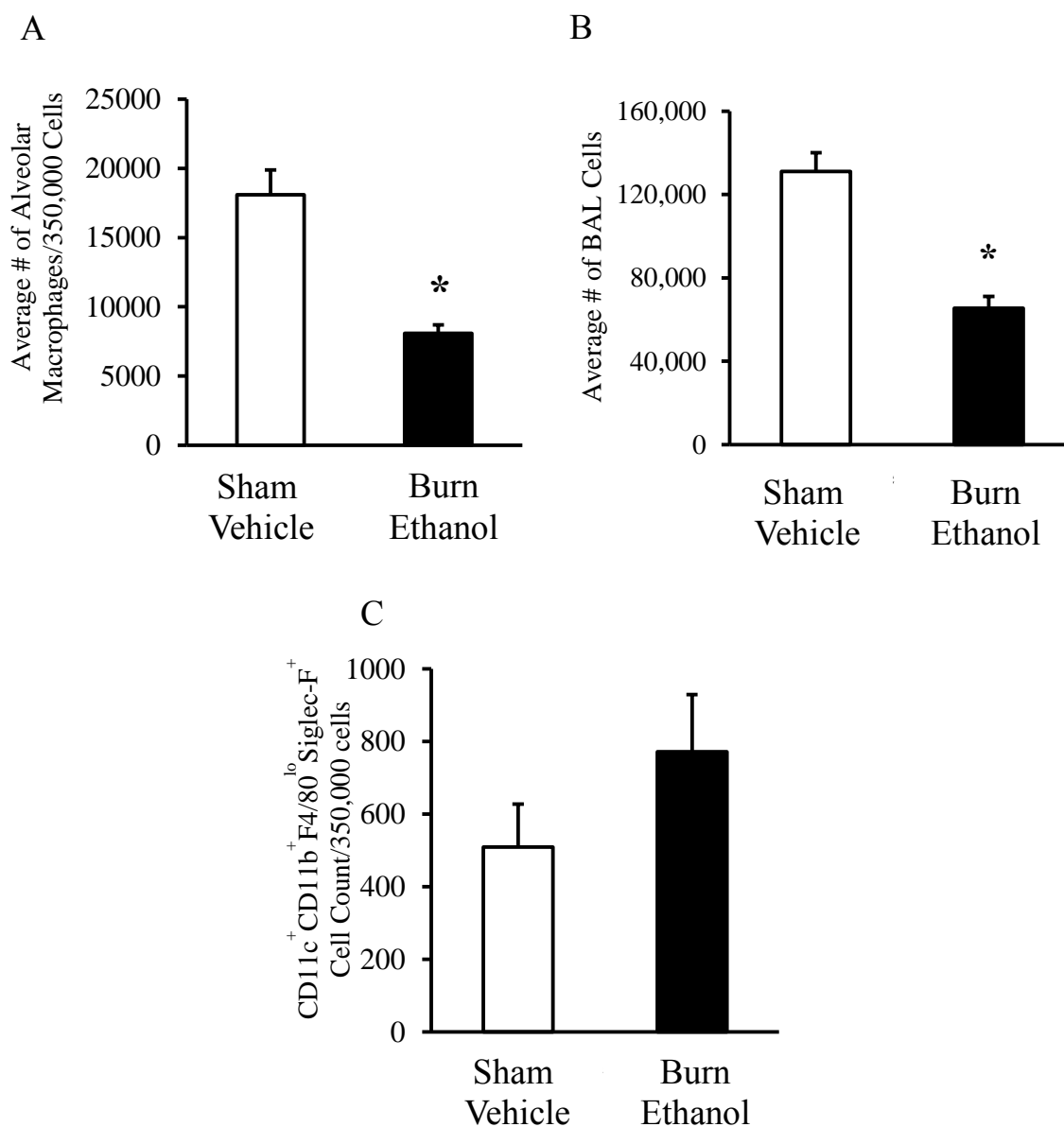
Figure 8: A) Decreased number of CD11c$^+$CD11b$^-$Siglec-F$^+$ AMs after intoxication and injury. Data are representative of cell counts per 350,000 total lung cells. B) Number of cells recovered from BAL fluid after intoxication and injury. Lungs were lavaged 5x with a total of 5mL of PBS. Total BAL cells were counted and presented as the average number of total cells recovered from BAL. C) Number of CD11c$^+$CD11b$^+$F4/80^{lo}Siglec-F$^+$ intermediate AMs in dissociated lung tissue. Data are representative of cell counts per 350,000 total lung cells.* p < 0.05. By unpaired T-test. Data shown as mean +/- SEM. N=4-6 animals per group.
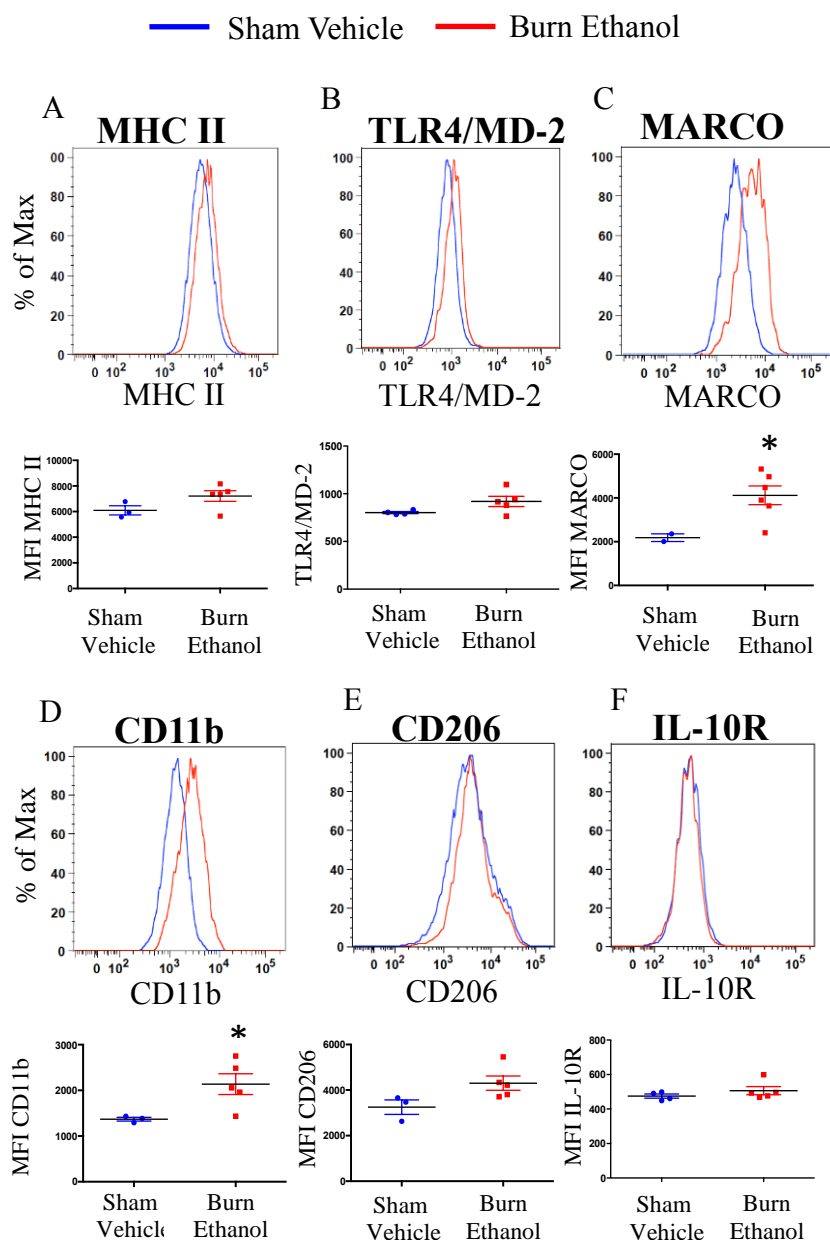
Figure 9. AMs upregulate cell surface receptors after intoxication and burn injury. Lung tissue was dissociated into a single cell suspension and AMs were gated as CD11c$^+$CD11b$^-$Sigle-F$^+$ and analyzed by flow cytometry. Histogram over lay of average MFI on AMs in sham vehicle (blue) and burn ethanol (red) groups and scatter plot graph representation of MFI on AMs from individual animals for A) MHC II B) TLR4/MD-2 C) MARCO D) CD11b E) CD206 and F) IL-10R. * p < 0.05. By unpaired T-test. Data are shown as mean ± SEM. N = 3-6 animals per group.

the level of TLR4/MD-2 at 24 h after injury (Figure 9B). However, scatterplot representation of TLR4/MD-2 MFI on AMs from individual intoxicated and injured mice showed variability in its expression, with a trend toward upregulated TLR4/MD-2, further confirmed by a slight increase in the histogram overlay. This suggests that AMs may be activated by TLR4 ligands, such as LPS or endotoxins. We also observed a significant upregulation of MARCO and CD11b ($p < 0.05$), receptors that are both important for efferocytosis (Figure 9 C&D). In contrast, there was no change in the expression of M2 markers CD206 or IL-10R (Figure 9 E&F).

These phenotypic changes towards an inflammatory profile led us to examine the intracellular levels of additional M1 and M2 markers, iNOS and ARG1. BAL cells isolated at 24 h post-injury were briefly cultured in chamber slides and immunofluorescent staining was used to evaluate these markers (Figure 10A). Results indicated there was not an increase in iNOS expression in comparison to ARG1, a phenotypic characteristic of pro-inflammatory macrophages (Figure 10B&C). iNOS has been shown to be important in killing intracellular bacteria [166], therefore the absence of an active lung infection in our model likely would not elicit an upregulation of iNOS by AMs.

<div align="center">Increased lung apoptosis 24 h after intoxication and injury</div>

AMs comprise only 10% of the total cells found in the alveoli, yet their function in maintaining a pathogen-free environment is critical for lung homeostasis. The loss of AMs after intoxication and injury led us to investigate the fate of these regulatory cells 24 h post-injury, predicting that the decrease in AMs correlated to an increase in AM

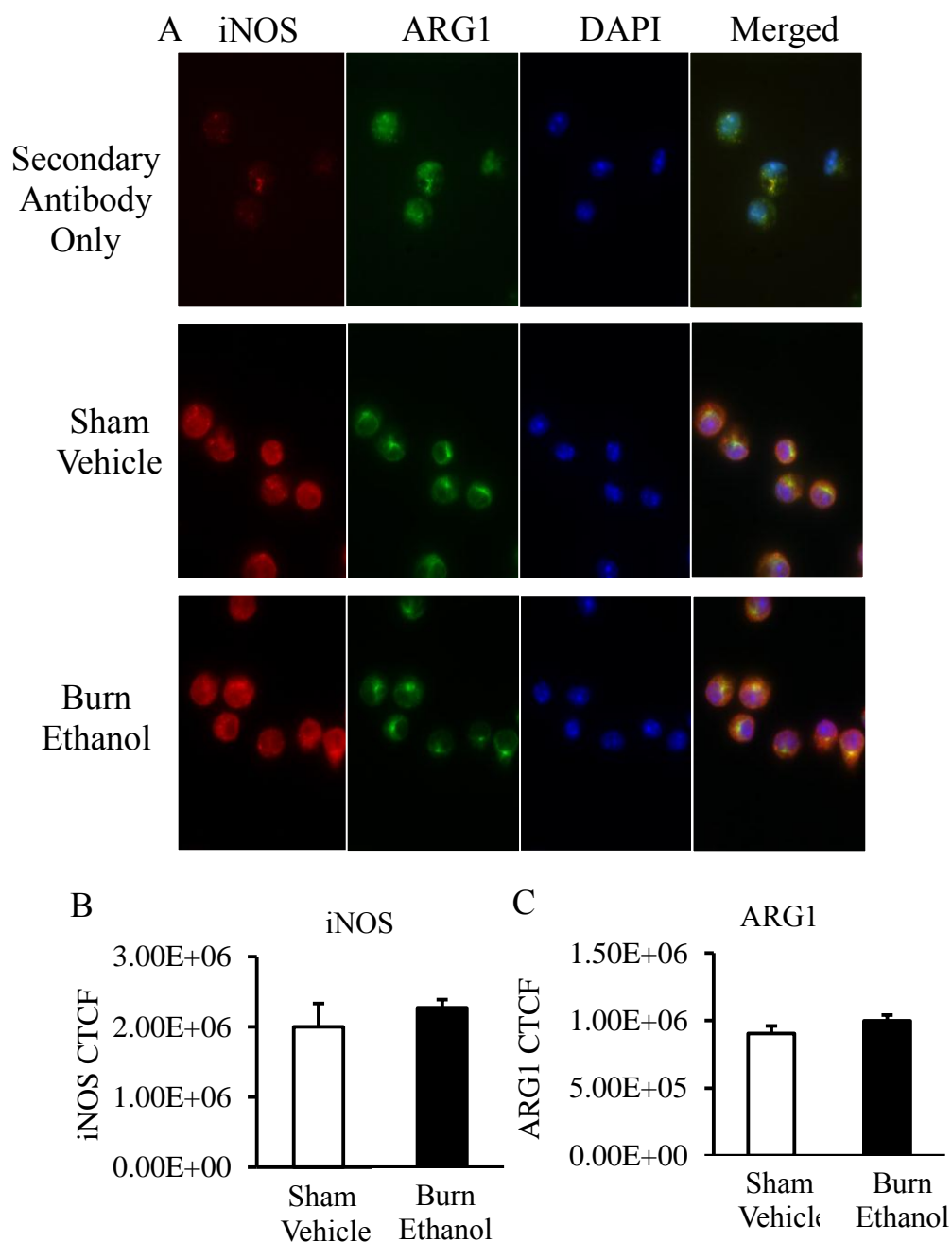Figure 10. AMs express similar levels of iNOS and ARG1. BAL AMs from each group were cultured in chamber slides for 1.5 h. Adherent cells were fixed and stained for iNOS (red), ARG1 (green, punctate staining) and nuclei (blue). A) Representative images from each treatment group. Corrected Total Cell Fluorescence (CTCF) was quantified for B) iNOS and C) ARG1. Data are shown as mean ± SEM. N=3-4 animals per group.

apoptosis. Using immunofluorescent TUNEL staining, we assessed lung tissue for apoptotic cells. We observed numerous fluorescent punctate cells in lung tissue from intoxicated and injured mice (Figure 11A) quantification revealed that this group had 7-fold more apoptotic cells than sham mice ($p < 0.05$) (Figure 11B). We also stained lung tissue from intoxicated and injured mice for both Siglec-F and TUNEL to determine if AMs were a population of apoptotic cells, but we failed to observe co-localization of Siglec-F$^+$ and TUNEL$^+$ cells in lung tissue (Figure 12A). Using an imaging flow cytometer, we examined Siglec-F$^+$ BAL AMs for apoptosis marker caspase-3/7 and observed Siglec-F$^+$ cells were negative for caspase-3/7 expression. Cells with caspse-3/7^{lo} expression exhibited low to no surface expression of Siglec-F, but potentially had cytoplasmic expression of Siglec-F. Furthermore, caspase-3/7^{hi} cells did not express Siglec-F (Figure 12B-D). Since $> 92\%$ BAL cells are AMs [8], this could suggest AMs lose Siglec-F as they undergo apoptosis and this may be the reason why we are unable to detect co-localization of the Siglec-F marker and TUNEL in lung tissue. At this time, we have yet to use other AM markers to identify TUNEL$^+$ cells in lung tissue. The imaging flow cytometry data did not reveal a difference in caspase-3/7$^+$ cells between treatment groups, but since this cytometer acquires images of cells, analysis had to be limited to only 500-1000 cells per sample. The literature also suggests there is not a universal marker for apoptosis and it is recommended apoptosis should be measured using various methods [167].

BAL cells were next analyzed for apoptosis marker, annexin V and dead cell marker, propidium iodide (Figure 13A&B). Intoxicated and injured animals had a 2-fold

A

Burn Ethanol

B
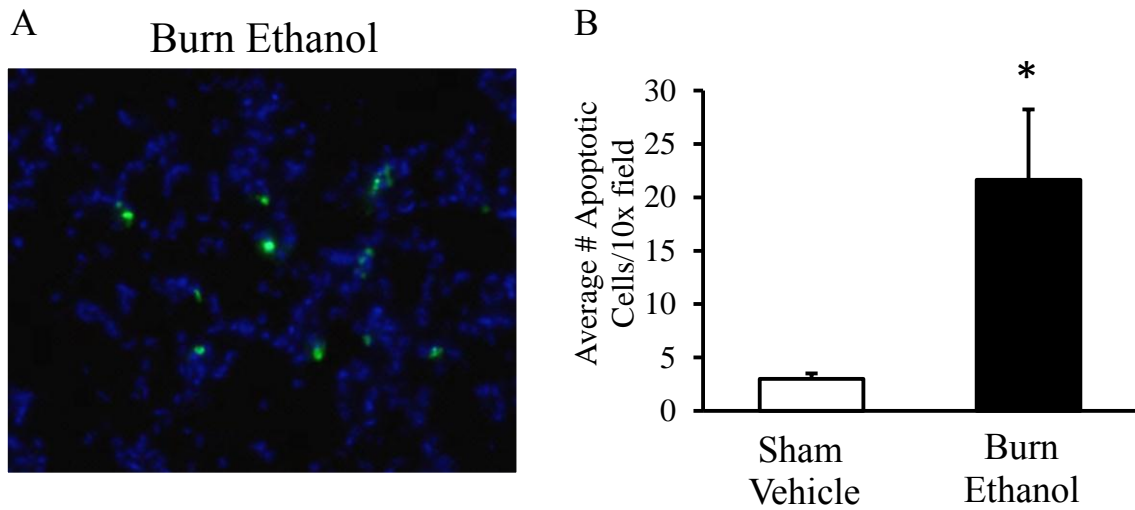
Figure 11. Increased apoptotic cells in the lung after intoxication and injury. An immunofluorescent *in situ* TUNEL assay was used to identify apoptotic cells in lung tissue. A) Representative images of TUNEL^{+} cells (green) after intoxication and injury, nuclei are blue, 200x magnification. B) Average number of apoptotic cells per 10x field after intoxication and injury. * $p < 0.05$. By unpaired T-test. Data are shown as mean ± SEM. N=2-4 animals per group.

A

Burn Ethanol

B

Siglec-F$^+$

Caspase 3/7$^-$

C

Siglec-F$^+$

Caspase 3/7^{lo}

D

Siglec-F$^+$

Caspase 3/7^{hi}
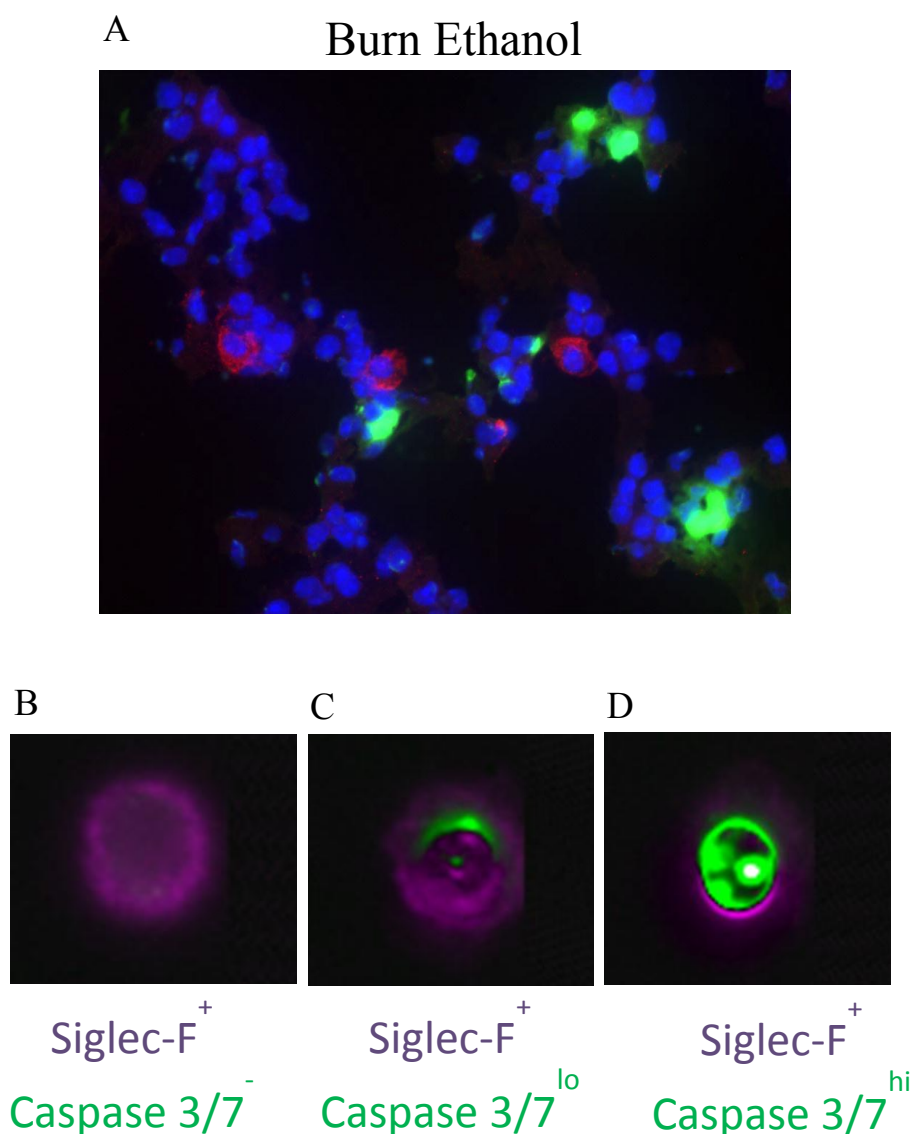
Figure 12. No co-localization of TUNEL$^+$ and Siglec-F$^+$ cells in lung tissue after intoxication and injury. A) Double staining of TUNEL$^+$ apoptotic cells (green) and Siglec-F$^+$ alveolar macrophages (red) in lung tissue. 400x magnification. Representative image demonstrating no co-localization between TUNEL$^+$ and Siglec-F$^+$ cells after intoxication and injury. B-D) Siglec-F (purple) and caspase-3/7 (green) staining of BAL cells were assessed using an Amnis imaging flow cytometer. B) Siglec-F$^+$ cells negative for caspase-3/7, C) Siglec-F^{lo} cells with low caspase-3/7 and D) Siglec-F$^-$ cells with high caspase-3/7.
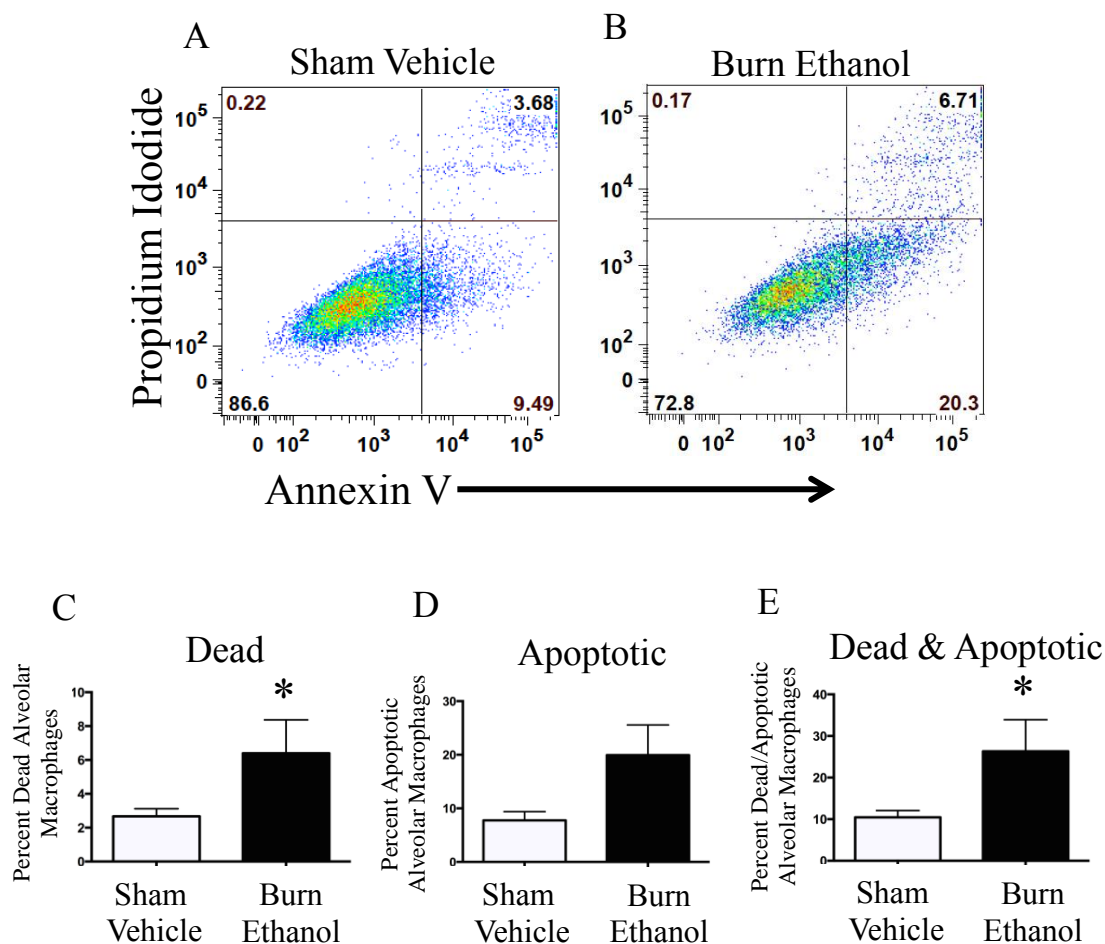
Figure 13. Heightened alveolar macrophage apoptosis and cell death after intoxication and injury. Flow cytometry was used to assess cell death and apoptosis of BAL cells using propidium iodide and annexin V staining. Representative gating of propidium iodide and annexin V positive BAL cells in A) sham vehicle and B) burn ethanol treatment groups. Percent C) dead D) apoptotic or E) total dead and apoptotic cells out of total number of alveolar macrophages. *p< 0.05. By unpaired T-test. Data shown as mean ± SEM. N=4 animals per group.

increase in percent of dead cells (p<0.05) (Figures 13C) and a 3-fold increase in the

percent of apoptotic cells (Figures 13D), in comparison to sham mice. Overall,

intoxicated and injured animals had a 2.5-fold higher incidence of dead or apoptotic BAL

cells (p<0.05), in comparison to sham animals (Figures 13E). This translated to 10% of

BAL cells from sham animals being lost to cell death or apoptosis, while intoxicated and

injured mice had 25% lost to cell death or apoptosis. With the BAL fluid containing >

92% AMs, regardless of treatment group, these data suggest AMs are susceptible to

apoptosis after intoxication and injury.

TUNEL^{+} cells were also quantified in tissue that had been lavaged to obtain the

BAL fluid, in comparison to non-lavaged lung tissue. If alveolar macrophages were

undergoing apoptosis, then we would predict to see a decrease in the number of apoptotic

cells after the tissue had been lavaged in intoxicated and injured mice. Interestingly,

there was no difference in the number of TUNEL^{+} cells between total lung tissue and

lavaged lung tissue (data not shown), but flow cytometry analysis of lavaged tissue

showed lavaging the tissue only removed 5% of AMs, in comparison to non-lavaged

lung. The literature suggests that the majority of AMs are sessile and are not easily

removed from the lungs after lavage [10]. In our laboratory, BAL fluid consistently

yields less than 200,000 AMs in sham mice and less than 100,000 cells from intoxicated

and injured mice. With only 1-2 million total AMs in mouse lungs, the removal of less

than 100,000 cells calculates to the isolation of only 5-10% of total AMs in the lungs.

This further supports our flow cytometry data that lavaging the lungs only removed 5%

of AMs, therefore, it is not unusual that the removal of BAL cells from lung tissue would

not yield major differences in the number of apoptotic cells, especially since only 25%

of the removed cells would be dead or apoptotic. Taken together, these data suggest that

AMs are only one population of the TUNEL$^+$ cells. Other cells undergoing apoptosis in

the lungs are likely epithelial and endothelial cells.

<div align="center">Active efferocytosis by AMs</div>

Phagocytic removal of apoptotic cells is an important function of alveolar

macrophage to restore lung tissue to homeostasis. Loss of AMs and an increase in

apoptosis by non-AM cell populations led us to question whether the increase in

apoptotic cells was due to the lack of AMs available to clear apoptotic cells. First, we

determined whether AMs actively efferocytosed apoptotic cells. Since AMs from

intoxicated and injured mice displayed more granularity and upregulated efferocytosis-

mediating receptors, we predicted AMs would be more phagocytic. Analysis of the

morphology of AMs from both treatment groups revealed that sham animals had healthy,

uniform alveolar macrophages (Figure 14A&C), while AMs from intoxicated and injured

animals had more phagocytic alveolar macrophages (Figure 14 B&D-F, arrows). The

appearance of phagocytic AMs ranged from small translucent vesicles (Figure 14D) to

larger bodies within AMs (Figure 14E&F). We also observed blebbing of the cell

membrane on some cells (Figure 14E, arrow head), which would support an increase in

apoptosis by AMs, but we were unsure if this was a result of cytocentrifugation and did

not count these cells. Quantification of the percent of phagocytic macrophages showed

20% of AMs from intoxicated and injured mice are in the process of efferocytosis,

A **Sham Vehicle**

B **Burn Ethanol**

Sham Vehicle   **Burn Ethanol**

C   D   E   F
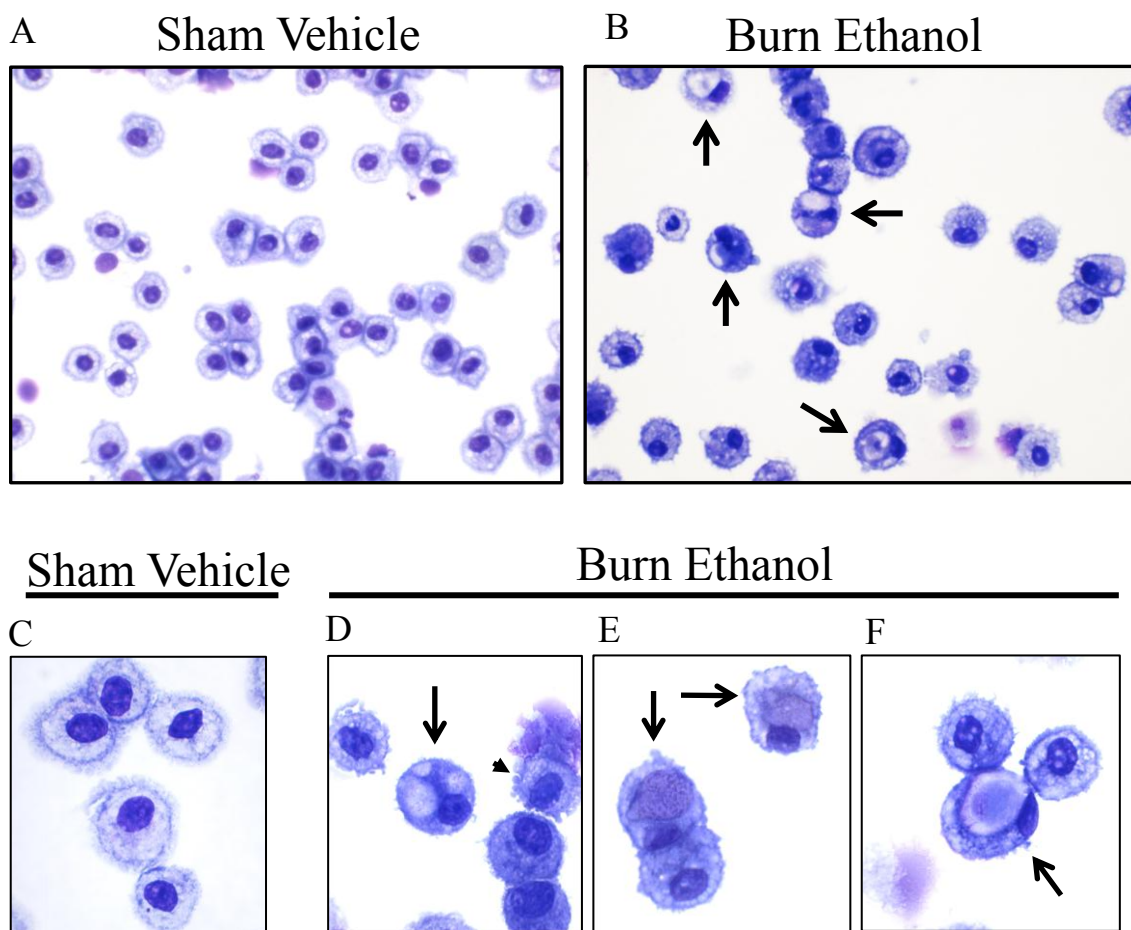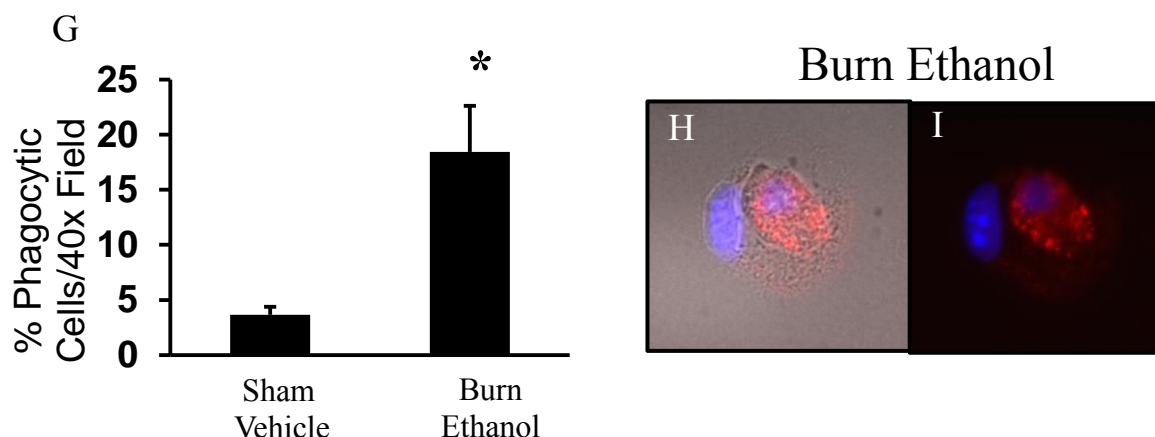
Figure 14. Increased percent of phagocytic alveolar macrophages after intoxication and injury. BAL cells were cytocentrifuged onto slides and stained with a HEMA 3 differential stain. Images demonstrate the predominance of alveolar macrophages in BAL from A) sham vehicle and B) burn ethanol treatment groups. Arrows indicate active alveolar macrophages in the process of efferocytosis after intoxication and injury. 400x magnification. Higher magnification of BAL cells in C) sham vehicle, and D-F) burn ethanol in various stages of phagocytic activity. We postulated these stages were D) macropinocytosis E) early stage of engulfment and F) later stage of engulfment. Arrows indicate active alveolar macrophages in the process of efferocytosis after intoxication and injury and arrow head indicates cell with blebbing membrane. 1000x magnification. G) Quantification of the percent of phagocytic cells per 400x field. Active-caspase-3 (red) and dapi (blue) staining of BAL cells was assessed using fluorescent microscopy H) with differential interference contrast (DIC) and I) without DIC. The DIC channel outlines a caspase-3[+] cell engulfed by another cell. *p< 0.05. By unpaired T-test. Data are shown as mean ± SEM. N= 3-4 animals per group.

a 5-fold increase comparison to sham mice (p<0.05) (Figure 14G). We predicted the

larger bodies within AMs were apoptotic cells and confirmed this using antibody against

active-caspase-3 (Figure 14H-I). This was further supported by our findings *in situ* of

Siglec-F$^+$ AMs interacting with small cells with minute nuclei, potentially indicative of

dead cells (Figure 15A&B).

<div align="center">Cytokine production by AMs</div>

To determine cytokine production by AMs after intoxication and injury,

supernatant was collected from cultured AMs from both sham and intoxicated and injured

mice. Results demonstrated that without additional stimulation, AMs from intoxicated

and injured mice spontaneously produce 5-fold more TNFα than sham animals (p<0.05)

(Figure 16). Other cytokines, such as IL-6, KC, IL-1β, MCP-1 and IL-10 were not

present in the supernatant. These data suggest AMs are not a main source of the IL-6 and

KC found in the lungs of mice subjected to intoxication and injury. Furthermore,

cytokine analysis of BAL fluid did not show significant changes in KC, MCP-1 or GM-

CSF (Figure 17). While it was not significant, intoxicated and injured mice did have an

approximate 3-fold increase in the average amount of IL-6, in comparison to sham mice

(Figure 17A). These data, taken together with cultured AM cytokine analysis, could

imply airway cells are a source of elevated lung IL-6. No change in KC in the airways is

not surprising considering neutrophil infiltration is into the interstitium and not into the

alveolar space, suggesting other cells, such as endothelial cells may be a source of lung

KC.
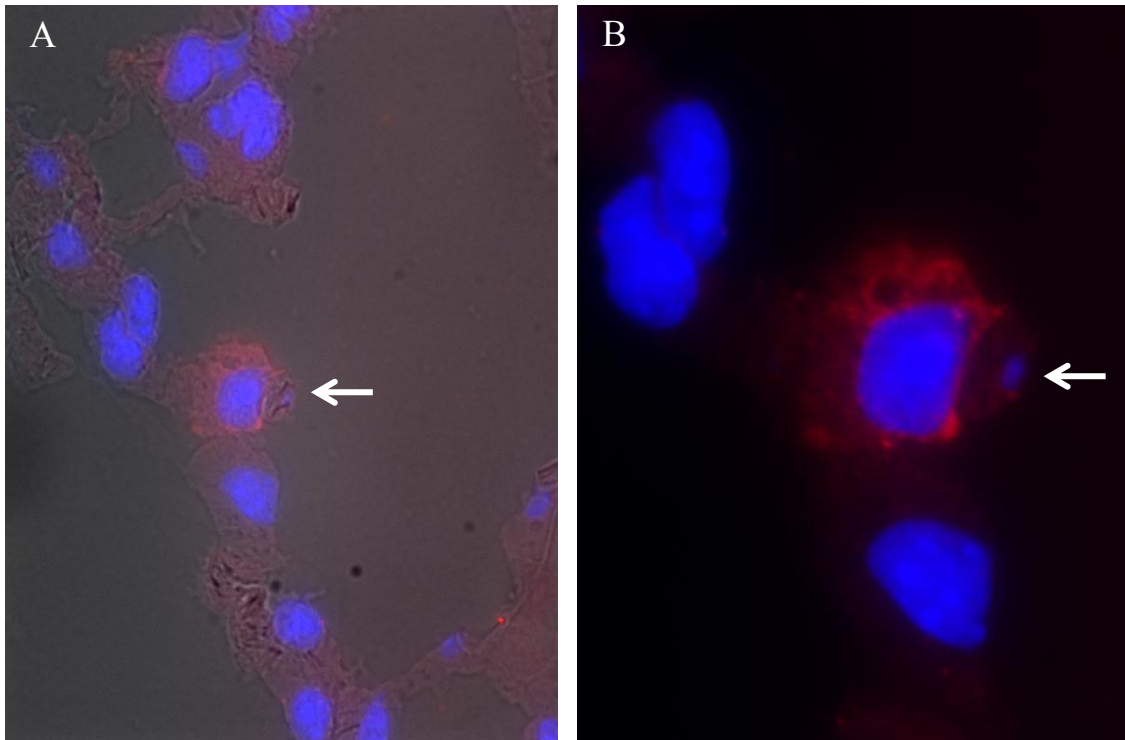
Figure 15. *In vivo* efferocytosis by Siglec-F$^+$ AMs in lung tissue after intoxication and injury. Lung tissue from intoxicated and burn injured-mice was stained for Siglec-F$^+$ (red) and assessed for AMs efferocytosis of other cells. Representative image of Siglec-F$^+$ AM in close proximity to small, nucleated cell is shown at A) 400x and B) 1000x. White arrows point to small, nucleated cell.
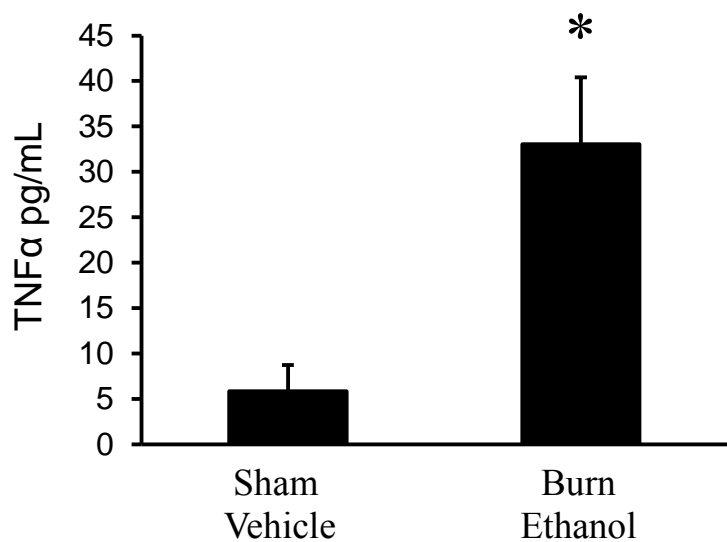
Figure 16. Elevated AM production of TNFα. AMs were cultured for 1.5 h at 37°C and supernatant was removed and assessed for cytokines by multi-plex bead array. Data represented as picograms per milliliter. * p < 0.05. By unpaired T-test. Data are presented as mean ± SEM. N = 3-6 animals per group.
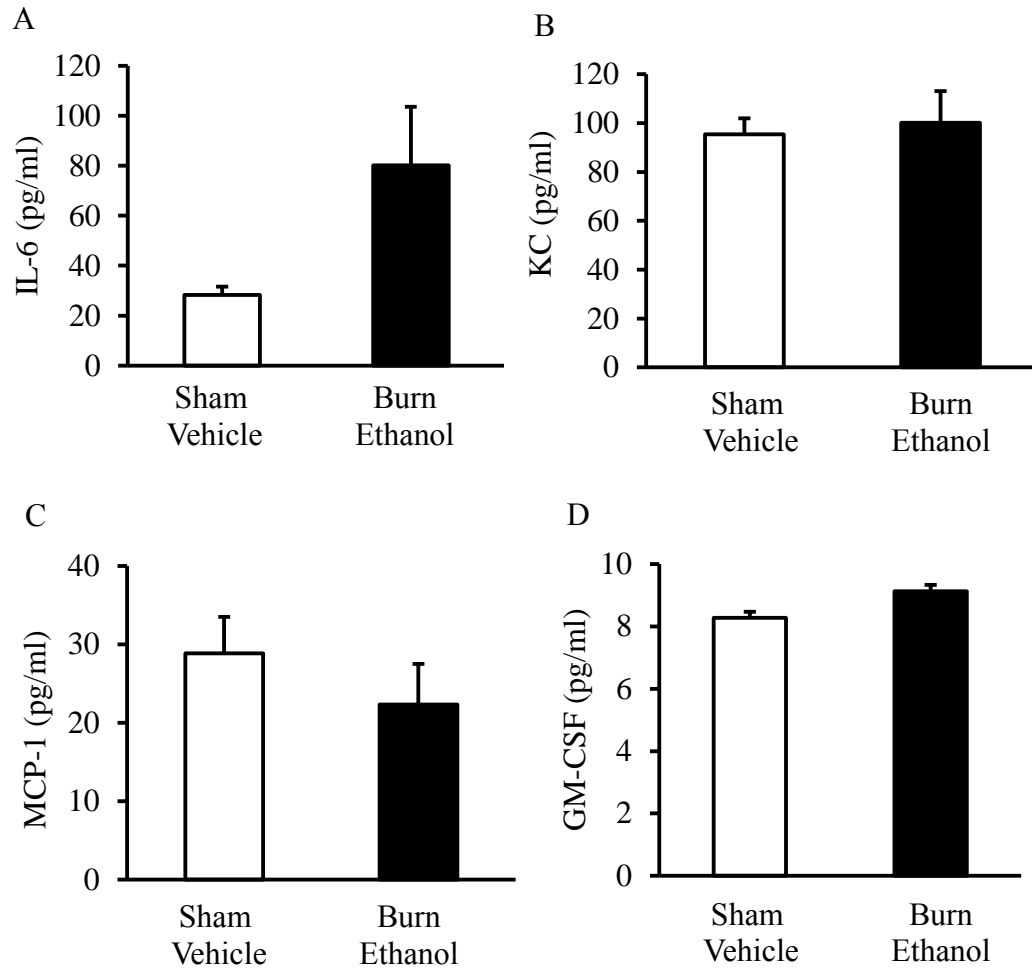
Figure 17. BAL fluid cytokine and chemokine levels. Lungs were lavaged 5x with 1mL PBS and BAL fluid was analyzed for A) IL-6, B) KC, C) MCP-1 and D) GM-CSF. Data represented as picograms per milliter. Not significant by unpaired T-test. Data are presented as mean ± SEM. N = 3-4 animals per group.

Neutrophil numbers in the lung after clodronate depletion of AMs

The role of AMs in pulmonary inflammation after intoxication and injury was further investigated by locally depleting AMs using clodronate liposomes in both sham and intoxicated and injured animals. Clodronate or empty liposomes were administered i.t. 3 days prior to injury. Clodronate liposomes specifically reduced CD11c^{+}CD11b^{-} Siglec-F^{+} AMs from the lungs in both sham and injured mice at 24 h after injury, in comparison to empty liposome treated mice ($p<0.05$) (Figure 18A&B). Examination of lung tissue sections revealed that intoxicated and injured mice treated with clodronate liposome had 2-fold more neutrophils, in comparison to intoxication, injury and empty liposome treated mice (Figure 19C-E). This increase was not seen in sham mice given empty or clodronate liposomes (Figure 19A&B). Flow cytometry analysis further supports these data showing a 1.5-fold increase in CD11b^{+}Ly-6G^{+} neutrophils in the lungs of intoxicated, injured, and clodronate treated mice, in comparison to those of empty liposome treated mice (Figure 19F). This elevation in neutrophil numbers significantly correlated to a decrease in AM numbers in intoxicated and injured mice treated with clodronate liposome, relative to that of intoxicated injured mice given empty liposome ($r = -0.8983$) (Figure 19G). Interestingly, we did not observe significant changes in lung tissue levels of KC after the depletion of AMs (Figure 19H). This further supports the importance of other cells types, such as endothelial cells, as a major source of this neutrophil chemokine. Serum levels of IL-6 were also not altered by the depletion of AMs (Figure 19I).
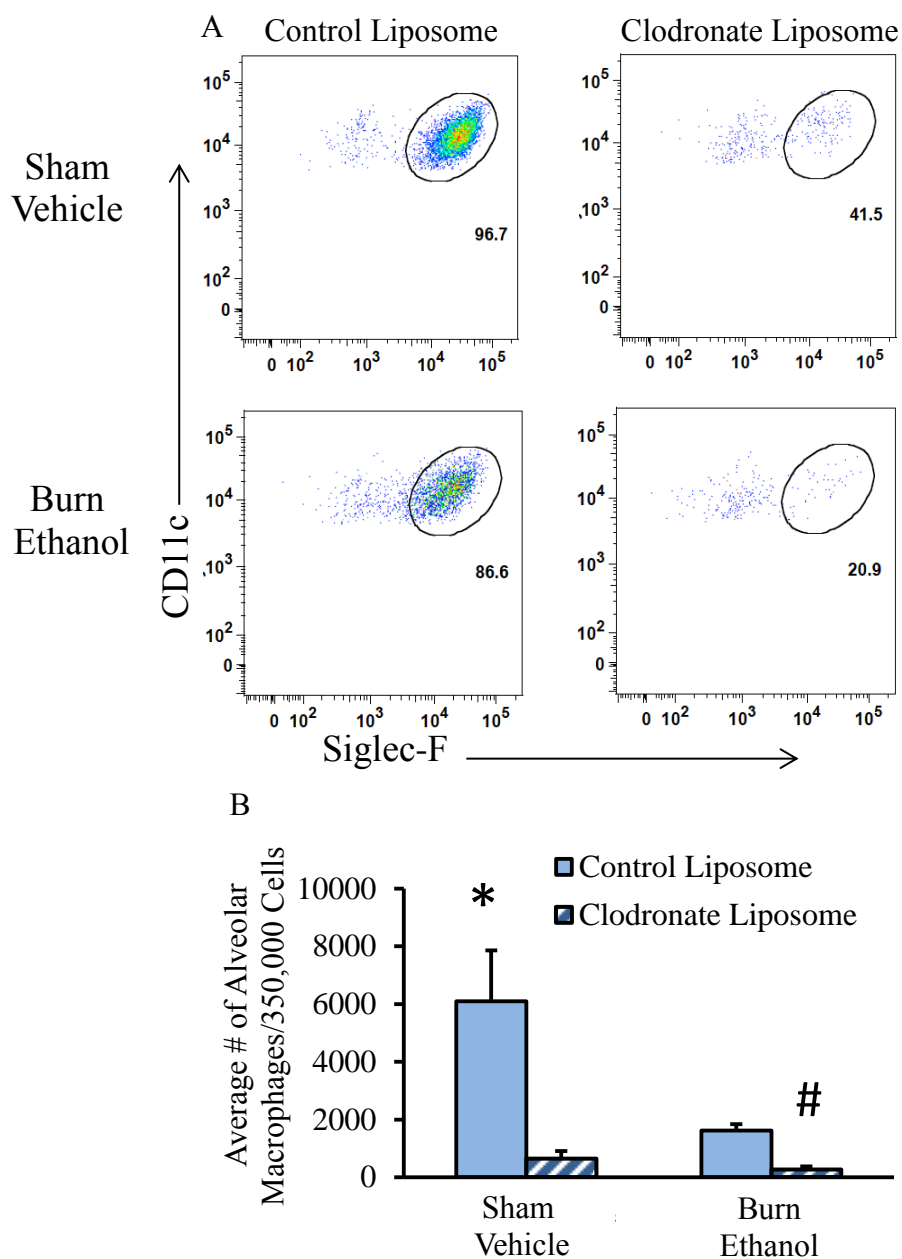
Figure 18. Clodronate liposome treatment depletes AMs. Lung tissue was obtained 24 h post-injury from all treatment groups. Tissue was enzymatically dissociated into a single cell suspension and cells were analyzed by flow cytometry. A) Representative gating for Siglec-F^{+}AMs of CD11c^{+}CD11b^{-} cells (data not shown) from all four treatment groups. B) Absolute number of AMs in lung isolates. *p < 0.05 versus all groups, by One-way ANOVA. # p < 0.05 versus burn ethanol + clodronate liposome, by unpaired T-test. Data are presented as mean of number of AMs per 350,000 lung cells ± SEM. N = 3-6 animals per group.
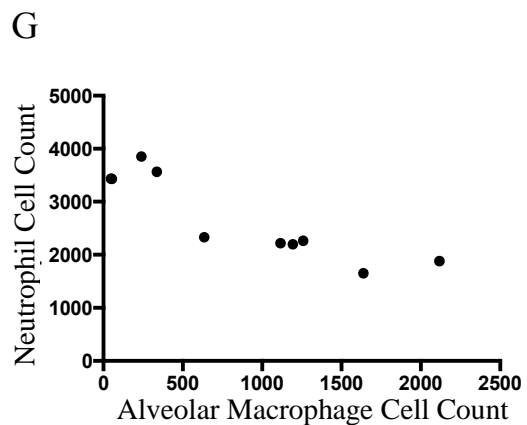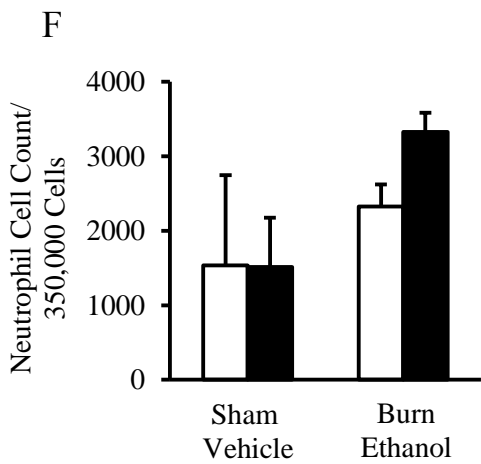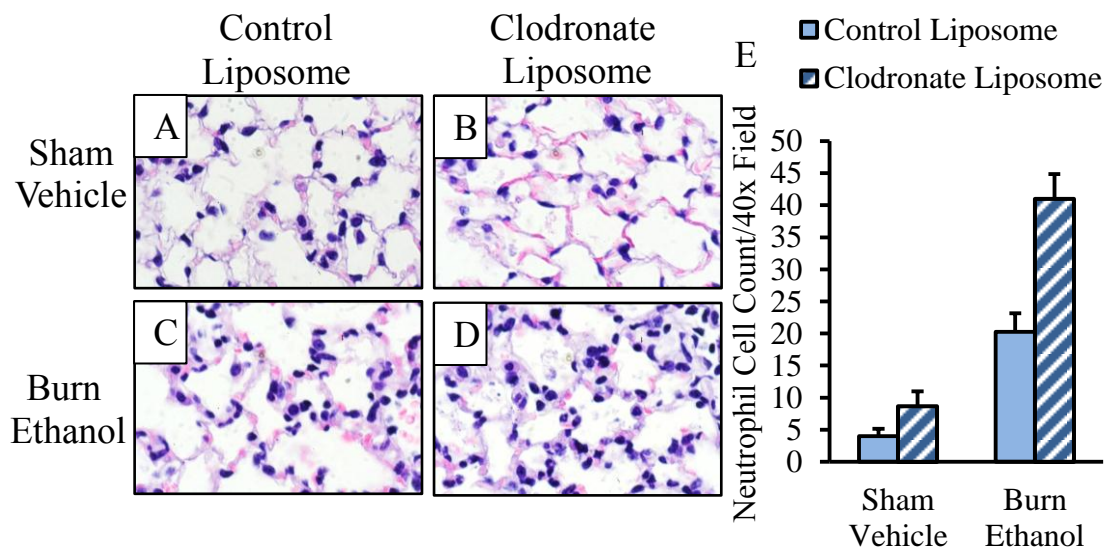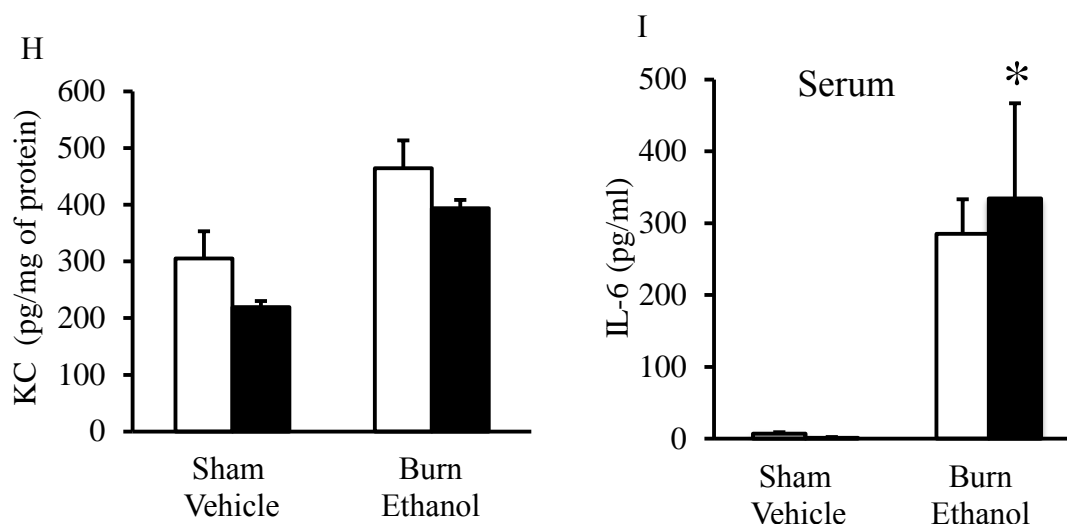
Figure 19. Assessment of pulmonary inflammation in AM depleted, intoxicated and burn-injured mice. A-D) Lungs were sectioned and stained with H&E and assessed for cellular infiltration. Representative sections from each treatment group are shown at 1000x. E) Neutrophils were counted by light microscopy in H&E-stained lung sections 24 h after intoxication and burn injury. Data are shown as the total number of neutrophils in 5 high power fields (400x). Not statistically significant. F) Flow cytometric analysis of dissociated lung tissue Ly-6G^{+}CD11b^{+} neutrophils. Data representative as absolute number of neutrophils per 350,000 cells. G) Pearson correlation of AM cell counts to neutrophil cell counts from the lungs of intoxicated and burn injury mice, with or without clodronate treatment , r = -0.8983. H) Lung homogenates from all four treatment groups were analyzed for levels of KC. I) Serum from all four treatment groups were analyzed for IL-6. *p <0.05 versus sham vehicle + empty liposome. Data are presented as mean ± SEM. N = 3-6 animals per group.

We have established there is a significant correlation between neutrophil infiltration and decreased lung function [156]. In these studies we show that there is also a significant correlation between the loss of alveolar macrophages and heightened neutrophil numbers in lung tissue. We predicted that depletion of AMs with clodronate liposomes prior to intoxication and injury would further impair lung function. In contrast, there was no significant difference in Penh, breath frequency, tidal volume, or minute volume (Figure 20), in comparison to injured mice treated with empty liposomes. Our recent observations of lung function in intoxicated and injured mice were from studies in which a multi-day episodic binge ethanol exposure regimen was utilized. Repeated exposure to ethanol before injury may result in greater lung impairment than a single dose of ethanol exposure. Moreover, in this experiment, numbers of AMs were drastically reduced by 75% after just intoxication, injury and empty liposome treatment, in comparison to sham mice given empty liposome. The additional loss of a small percentage of remaining AMs after clodronate liposome treatment therefore may not result in greater lung impairment.

Finally, we analyzed lung tissue for TUNEL$^+$ cells. We discovered that clodronate treatment alone, 3 days after it was administered, resulted in remnants of apoptotic cells, in comparison to empty liposome treated mice (Figure 21A&B). Consistent with our previous observations (Figure 21C&E), intoxicated and burn injured mice given empty liposomes had more TUNEL$^+$ cells, in comparison to empty liposome treated sham mice. Unfortunately, treatment of sham or intoxicated and injured animals with clodronate liposomes yielded TUNEL$^+$ debris throughout the lung tissue (Figure 21 D&F),
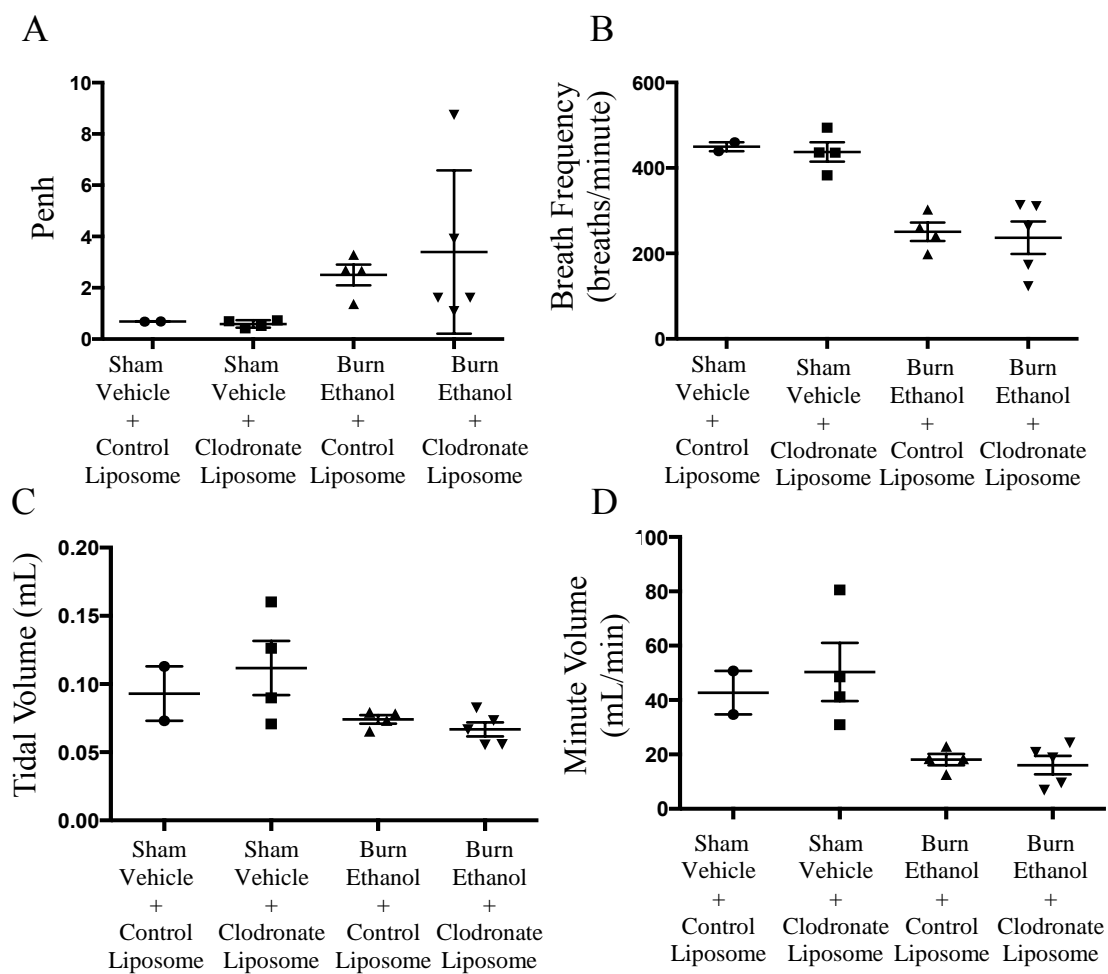
Figure 20. Clodronate liposome depletion of AMs does not increase lung impairment. Mice were placed in an unrestrained whole body barometric plethysmography chamber and lung function parameters were recorded for 10 minutes. A) Penh, B) Breath frequency, C) Tidal volume and D) Minute volume. Data points shown as individual animals. Data are presented as mean ± SEM. N = 2-5 per group.
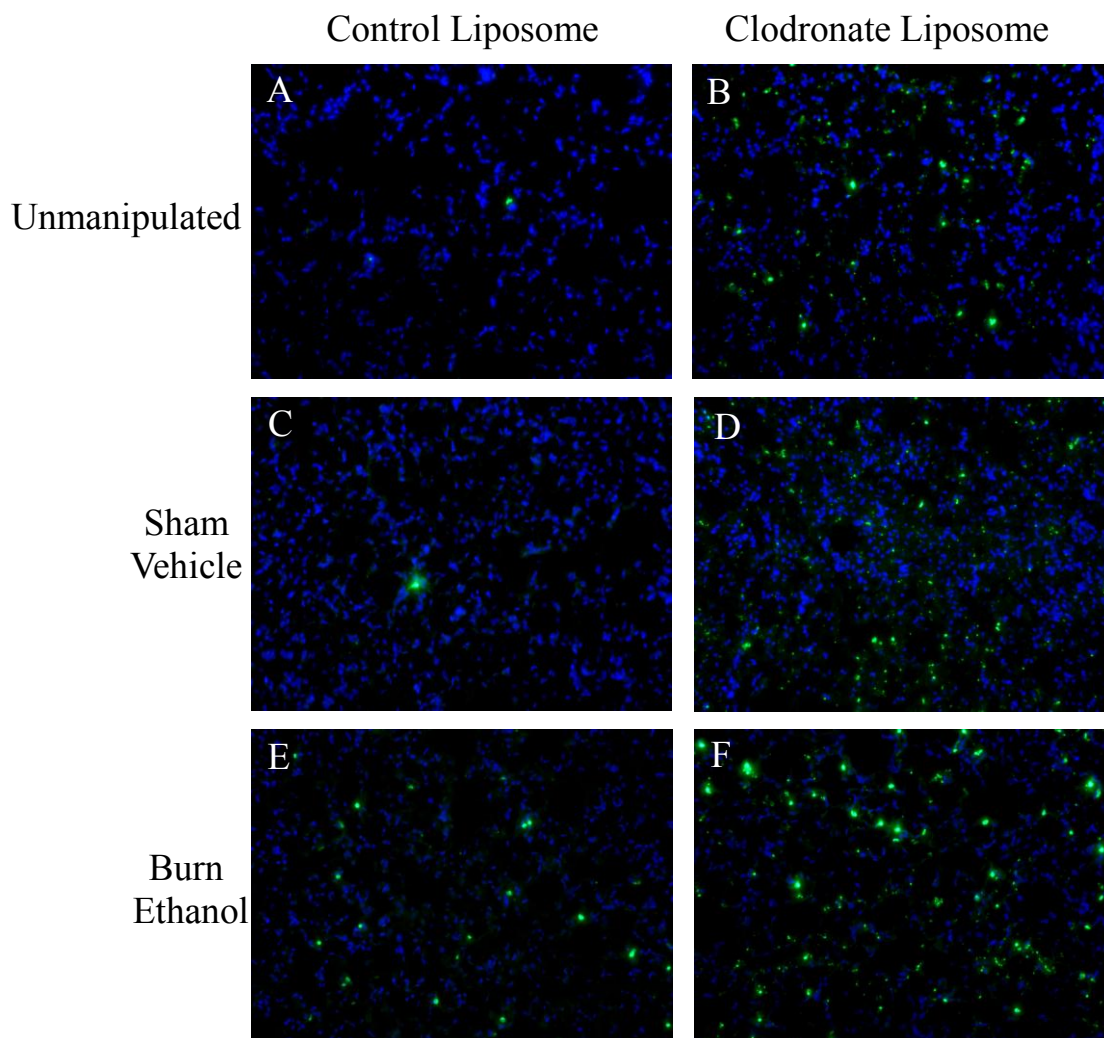
Figure 21. Clodronate liposome increases apoptotic debris in lung tissue. An immunofluorescent *in situ* TUNEL assay was used to identify apoptotic cells in lung tissue. Representative images of TUNEL^{+} cells (green) in each treatment group. Left panel, control liposome treated A) unmanipulated C) sham vehicle and E) burn ethanol. Right panel, clodronate liposome treated B) unmanipulated D) sham vehicle and F) burn ethanol. 200x magnification.

Highlighting a limitation of clodronate liposome depletion of AMs to study apoptosis. In intoxicated and injured mice treated with clodronate liposome, lung tissue had both TUNEL[+] debris and punctate cells, further suggesting that the increase in apoptotic cells is not representative of only AM apoptosis but also of other lung cell types (Figure 21F).

Summary

Higher SSC granularity, altered expression of TLR4/MD-2, and increased production of TNFα together suggest AMs from intoxicated and injured mice have an activated, pro-inflammatory phenotype. The elevated secretion of TNFα and the increased surface expression of MARCO and CD11b on AMs, both important receptors in phagocytosis and efferocytosis, coincide with elevated numbers of apoptotic cells in lung tissue after injury. Furthermore, morphological analysis revealed a percentage of AMs from intoxicated and injured mice could effectively take up apoptotic cells. We determined AMs are a small population of these apoptotic cells, but the majority of apoptotic cells are likely epithelial or endothelial cells.

The literature suggests that efferocytosis by AMs initiates the transition from an inflammatory phase towards a resolution phase. Our data revealed there is a 50% reduction in the total number of AMs and, of the AMs that were present, less than 20% were active in efferocytosis. Minimal AM efferocytosis in the presence of elevated numbers of apoptotic cells consequently can hinder the process of transitioning to a resolution phase. Clodronate experiments confirmed AMs also have a role in limiting neutrophil numbers into the lungs after intoxication and injury. The negative correlation between decreased AM numbers and increased neutrophil numbers proposes elevated

neutrophil infiltration after intoxication and injury is a result of AM deficiency in the lung tissue. We speculate lack of mediators released in response to efferocytosis by AMs (i.e. IL-10 or TGFβ) is responsible for the increase in neutrophil accumulation. Overall, our data demonstrate that both the loss of AMs and a heightened pro-inflammatory profile on remaining AMs, may prolong pulmonary inflammation after intoxication and injury, underlining a mechanism for impaired lung function and increased incidences of mortality.

CHAPTER 5

MESENCHYMAL STEM CELLS ATTENUATE PULMONARY INFLAMMATION
AFTER INTOXICATION AND BURN INJURY

Abstract

Clinical evidence reveals that 50% of burn patients are under the influence of alcohol at
the time of hospital admission and that the combined insult of alcohol and burn injury
causes increased risk of pulmonary complications leading to multiple organ failure and
death. Our previous work demonstrated that a mouse model of alcohol and burn injury
resulted in prolonged pulmonary inflammation characterized by amplified neutrophil
accumulation and dramatic increases in pro-inflammatory cytokines and chemokines
relative to burn injury and sham groups. Recent studies indicated the role of AMs in
amplifying pulmonary inflammation after intoxication and injury. Mesenchymal stem
cells (MSCs) have been shown to attenuate acute lung inflammation, specifically by their
ability to modulate the phenotype of AMs. Therefore, we explored exogenous MSCs as a
post-injury therapy in a mouse model of intoxication and burn injury. Eight week-old
C57BL/6 male mice were subjected to binge alcohol exposure Thirty minutes following
the final ethanol exposure, mice were given a 15% total body surface area dorsal scald
injury. One hour after injury, intoxicated and burn-injured mice were given an
intravenous injection of CFSE labeled bone marrow-derived MSCs ($5x10^5$ i.v.). We
detected a small percentage of CFSE$^+$ MSCs in the lungs at 24 h post injury and assessed

lung tissue for pulmonary inflammation. We found that intoxicated and injured mice treated with MSCs had a decrease in infiltrating neutrophils into the lungs that paralleled reduced neutrophil chemoattractant KC (CXCL1) and pro-inflammatory IL-6 levels in lung tissue. Our data suggest that one way in which MSCs attenuated pulmonary inflammation is by the activation of anti-inflammatory AMs. Together, these data demonstrate that exogenous administration of MSC to mice after intoxication and burn injury reduced pulmonary inflammation, highlighting MSCs as therapeutic targets that can improve survival in all burn patients.

Introduction

Binge drinking is an increasingly prevalent activity in the United States and is the most common form of alcohol consumption [61]. It is defined by a blood alcohol concentration of 0.08% or by the number of alcoholic drinks an individual has with in a 2 hour time period (4 for women, 5 for men), and is the most common drinking pattern among patients with traumatic injury, including burn injury [66, 87]. Clinical evidence reveals that half of the burn patient population is under the influence of alcohol at the time of injury [88, 89]. This combined insult results in greater fluid resuscitation, a longer hospital stay and an increase in the number of days spent on mechanical ventilation, leading to a greater risk pulmonary complications and mortality [89, 92, 168]. Our laboratory and others have used a murine model of ethanol intoxication followed by a moderate size burn injury to study how intoxication exacerbates inflammation in various organ systems, including the lungs. With this combined insult, the lungs display characteristics of acute respiratory distress syndrome, including elevated levels of

alveolar wall thickening, neutrophil accumulation and increased pro-inflammatory

cytokine interleukin-6 (IL-6) levels, relative to either ethanol exposure or burn injury

alone [99, 104-107]. This amplification of pulmonary inflammation has also been

correlated to a decrease in physiological lung function and an increase in mortality [156].

The lungs are often the first organs to fail after traumatic injury [84], hence, managing

the excessive inflammatory response seen after remote injury will likely reduce elevated

morbidity and mortality in intoxicated and burn-injured patients.

Resident alveolar macrophages play a critical role in both the onset and resolution

of pulmonary inflammation [157, 162, 169]. The activation of tissue resident

macrophages by endogenous danger signals or by the detection of pathogens through

pattern recognition receptors stimulate macrophages to release pro-inflammatory

cytokines that initiate the inflammatory process, such interleukin-1β, tumor necrosis

factor α (TNFα), and interferon-γ [157]. During the course of inflammation, the up

regulation of anti-inflammatory mediators or the phagocytosis of apoptotic cells by

macrophages, activate macrophages into an alternative M2, anti-inflammatory phenotype,

facilitating the resolution of inflammation [51, 52, 170]. Alveolar macrophages are the

first line of defense against inhaled particles or pathogens. This environment, with a

direct connection to open-air, leads to a distinct phenotype with atypical macrophage cell

surface markers, in comparison to other macrophage populations. Alveolar macrophages

can be characterized by dendritic cell marker CD11c and eosinophil marker Siglec-F, but

are negative for classical macrophage marker CD11b [20, 21, 158]. Additionally, the

constant exposure to inhaled or blood-born pathogens results in alveolar macrophages

constitutively expressing mannose receptor CD206 [21, 169], an important receptor that

assists in the clearance of foreign antigens [171]. CD206 has also been characterized as a

marker of alternative macrophage activation [34, 162-164]. Thus, an upregulation of

CD206 on alveolar macrophages from baseline line levels may suggest a transition to an

M2 phenotype. With the excessive pulmonary inflammation observed after intoxication

and injury, triggering the anti-inflammatory, resolving and/or reparative macrophage

phenotype could be critical to restoring lung homeostasis.

Bone marrow and tissue resident mesenchymal stem cells (MSCs) have been

characterized as modulators of acute inflammation by virtue of their ability to influence

the phenotype of macrophages [119]. Exogenous MSC interaction with macrophages and

their release of paracrine soluble factors have been shown to suppress inflammation and

polarize macrophages into an alternative, anti-inflammatory phenotype [119-123].

Notably, experimental studies using murine models of allergic asthma demonstrated the

localized benefits of MSC treatment in the lungs. In one murine study, short-term

localization of exogenous human MSCs (hMSCs) within the lungs was sufficient to

inhibit allergic inflammation. Through clodronate liposome depletion of alveolar

macrophages, this study established that the anti-inflammatory effect of MSCs was

dependent on alveolar macrophages and their indirect role in the upregulation of IL-10

[172]. Recent reports additionally showed hMSCs can reduce allergic inflammation and

improve lung function through TGFβ signaling and the upregulation of M2 alveolar

macrophages, [173]. Additionally, incubating the RAW264.7 macrophage cells line with

MSC conditioned medium has been shown to induce the expression of the M2 marker

CD206 in [174]. Moreover, many studies also suggest the intravenous administration of MSCs results in the entrapment of MSCs within the lungs. Due to their large size, MSCs becomes trapped within the pulmonary vasculature with only a fraction of these cells passing through and migrating to other organs [124-126]. The resulting reduction in capillary flow allows MSCs to secrete anti-inflammatory mediators specifically into the lung niche, reducing inflammation [175]. This limitation of MSC therapy, combined with the ability of MSCs to attenuate inflammation through the anti-inflammatory polarization of macrophages, suggests MSCs would be particularly advantageous to attenuating elevated lung inflammation after intoxication and injury.

The purpose of this study was to determine whether the intravenous infusion of exogenous bone marrow-derived MSCs will reduce pulmonary inflammation after intoxication and burn injury and if this parallels a shift in alveolar macrophage phenotype. Since intoxication at the time of injury results in greater pulmonary complications and mortality rates than burn injury alone, we examined the effect of MSC treatment on only intoxicated and burn-injured mice, in comparison to sham vehicle control. *In vitro*-expanded MSCs were given intravenously to intoxicated and burn-injured mice 1 hour after injury. Pulmonary inflammation was assessed by neutrophil infiltration, neutrophil chemokine CXCL1 (KC) and IL-6 levels in lung tissue, while alveolar macrophage phenotype was analyzed by flow cytometry. Our results suggest MSCs can reduce pulmonary inflammation, possibly by polarizing alveolar macrophage to an anti-inflammatory phenotype, highlighting MSCs as a novel therapeutic agent to treat lung-specific inflammation in severe burn patients.

Materials & Methods

Mice

Male (C57BL/6) mice were purchased from Jackson Laboratories (Bar Harbor, ME) and used at 8-10 weeks old. Mice were housed in sterile micro-isolator cages under specific pathogen-free conditions in the Loyola University Medical Center Comparative Medicine facility. All experiments were conducted in accordance with the Institutional Animal Care and Use Committee. Mice weighing between 22 to 27 g were used in these studies.

Mesenchymal Stem Cell Culture

Gibco® Mouse (C57BL/6) bone marrow (BM)-derived MSCs (Life Technologies, Grand Island, NY) were expanded *in vitro* per manufacturer protocol. Briefly, MSC growth medium consisted of 10% FBS and 10mg/ml genatmicin in MEMα Medium with GlutaMAX™-I, ribonucleosides and deoxyribonucleosides. MSCs were plated at a density of 5,000 cells per cm^2 in T75 flasks and incubated at 37°C, 5% CO_2 and 90% humidity. Medium was changed every 2 days until cultures were 70-80% confluent. MSCs were detached from flasks using pre-warmed trypsin, fluorescently labeled with carboxyfluoresceindiacetate, succinimidyl ester (CFSE), following manufacturer protocol (Life Technologies) and resuspended in sterile Dulbecco's phosphate buffered saline (PBS) [176]. Additionally, MSCs were analyzed by flow cytometry for MSC markers. Briefly, MSCs were incubated with anti-mouse antibodies C-kit APC-eFluor 780 (clone ACK2, eBioscience), CD31PE (clone 390, eBioscience), Sca-1 PerCP Cy5.5 (clone D7, eBioscience), CD34 eFluor 660 (clone RAM34, eBioscience), and CD44 PE-Cy7 (clone

IM7, eBioscience). Antibody incubation was carried out for 30 minutes at 4°C. Cells were washed and fixed as described [143, 153]. Data analysis was performed using Flow Jo FCS analysis software (Tree Star Inc., Ashland, OR). Passage 3 cells were used in all experiments.

Murine Model of Binge Ethanol and Burn Injury

A murine model of single dose binge ethanol intoxication and burn injury was employed using oral gavage as described previously [138, 150, 151]. Animals were given 400 μl of 10% (v/v) ethanol solution (1.6 g/kg) or water control by gavage at a dose designed to elevate the blood alcohol concentration to 150 mg/dL at 30 min after ethanol exposure [142]. Thirty minutes following the ethanol exposure, the mice were anesthetized (100 mg/kg ketamine and 10 mg/kg xylazine) and their dorsums shaved. The mice were placed in a plastic template exposing 15% of the total body surface area and subjected to a scald injury in a 92-95°C water bath or a sham injury in room-temperature water [138]. The scald injury results in an insensate, full-thickness burn [152]. The mice were then resuscitated with 1.0 ml saline and allowed to recover on warming pads. All experiments were performed between 8 and 9 am to avoid confounding factors related to circadian rhythms. One hour after injury, intoxicated and burn-injured animals either received an intravenous tail vein injection of 5x10^5 CFSE-labeled MSCs or PBS as a control in 200ul [124]. Animals were euthanized at 24 hours.

Histopathologic Examination of the Lungs

The upper right lobe of the lung was inflated with 10% formalin and fixed overnight as described previously [104], embedded in paraffin, sectioned at 5 μm, and

stained with hematoxylin and eosin (H&E). Sections were evaluated using light

microscopy (Zeiss AxioVert, Zeiss, Thorndale, CA) and histology photographs were

taken at 400x magnification. Neutrophils were counted in a blinded fashion in 10 high

power fields (400X). The upper left lobe was inflated with 25% OCT freezing medium,

frozen in OCT over dry ice and store at $-80^{o}C$. Tissue was cryosectioned at 6 μm and

assessed for CFSE fluorescent MSCs.

<div align="center">Cytokine Analysis of Lung Homogenates</div>

The right middle lung lobe was snap-frozen in liquid nitrogen and then

homogenized in 1 ml of BioPlex cell lysis buffer according to manufacturer's protocol

(BioRad, Hercules, CA). The homogenates were filtered and analyzed for cytokine

production using a BioPlex multiplex bead array. The results were normalized to total

protein using the BioRad protein assay (BioRad) [106, 107].

<div align="center">Flow Cytometry Analysis of Alveolar Macrophages</div>

The upper left lung lobe was removed and cut into small pieces with a razor

blade. The lung tissue was then transferred to a C-tube (Miltenyi Biotec, Auburn, CA)

and processed using digestion buffer containing 1mg/ml of Collagenase D and 0.1 mg/ml

DNase I (Roche, Indianapolis, IN) in HBSS and a GentleMACS dissociator (Miltenyi

Biotec), according to manufacturer's instructions (Shults et al. 2015). The homogenates

were then filtered through 70 um nylon cell strainers to obtain a single cell suspension.

Red blood cells were lysed using ACK lysis buffer (Life Technologies, Grand Island,

NY). Cells were counted using trypan blue to exclude dead cells. To assess alveolar

macrophages, $1x10^{6}$ lung cells were first incubated with anti-CD16/32 (clone

93,eBioscience, San Diego, CA) to block unspecific binding to the Fcy II/III receptor.

Cells were then immunostained with rat anti-mouse antibodies: F4/80 APC (clone BM8, eBioscience), CD11b eFluor 450 (clone M1/70, eBioscience), Siglec-F PE-CF594 (clone E50-2440, BD Biosciences, San Jose, CA), CD206 PE (clone C068C2, Biolegend, San Diego, CA). CFSE$^+$ cells were identified using a FITC channel. Antibody incubation was carried out for 30 minutes at 4°C. Cells were washed and fixed as described [143, 153]. MHC II was used as a M1 marker and CD206 was used a M2 marker [21]. Samples were run on a BD Fortessa cytometer (BD Biosciences). Data analysis was performed using Flow Jo FCS analysis software (Tree Star Inc.).

Serum Measurements

Blood was collected via cardiac puncture and the serum was isolated at stored at -80°C. Serum aliquots were used to measure IL-6 by enzyme linked immunosorbent assay (ELISA) (BD Biosciences, Franklin Lakes, NJ) or liver alanine aminotransferase (ALT) and aspartate aminotransferase (AST) levels using a DRI-CHEM 7000 (HESKA, Loveland, CO).

TUNEL Immunofluorescent Staining

The upper right lobe of the lung was inflated with 10% formalin and fixed overnight as described previously [104], embedded in paraffin, sectioned at 5 μm. An *in situ* TUNEL assay was performed according to manufacturer's protocol (Life Technologies). Sections were evaluated using fluorescent microscopy (EVOS, Life Technologies) and TUNEL$^+$ were counted in a blinded fashion in 10 low power fields (100X).

Statistical Analysis

Statistical comparisons were made between the sham vehicle, burn ethanol + PBS, and burn ethanol + MSC treatment groups. One-way analysis of variance (ANOVA) was used with Tukey's post-hoc test and values were considered statistically significant when $p < 0.05$. Data is reported as mean values ± the standard error of the mean (SEM).

Results

Mesenchymal stem Cells are Present the Lungs 24 h after Administration

Gibco® Mouse (C57BL/6) BM-derived MSCs were purchased from Life Technologies. These cells were described to have tri-potential differentiation into at least osteogenic, adipogenic, and chondogenic lineages, as well as express a flow cytometry phenotype of Sca-1^+CD34$^+$CD44$^+$CD29$^+$c-kit$^-$, which is characteristic of BM-derived MSCs. To confirm the phenotype of these MSCs, we analyzed confluent MSCs (passage 3) using flow cytometry (Figure 22). We found the MSCs were Sca-1^+CD34$^+$CD44$^+$CD29$^+$, negative for CD31, and had less than 5% positive for c-kit (Figure 22A-F). Additionally, in adoptive transfer experiments, MSCs were labeled with CFSE (Figure 23A) and administered to mice an hour after burn injury. At 24 h, CFSE$^+$ MSCs were identified in the lungs of intoxicated and burn injured mice using flow cytometry (Figures 23B&C). Lung cells were negatively selected for alveolar macrophage/eosinophil marker Siglec-F and granulocyte/neutrophil marker CD11b (data not shown), and analyzed for CFSE$^+$ cells compared to macrophage/monocyte marker F4/80 (Figure 1). Additionally, CFSE$^+$ cells were negative for dendritic cell marker CD11c (data not shown). Our results indicated there were approximately 100 CFSE$^+$
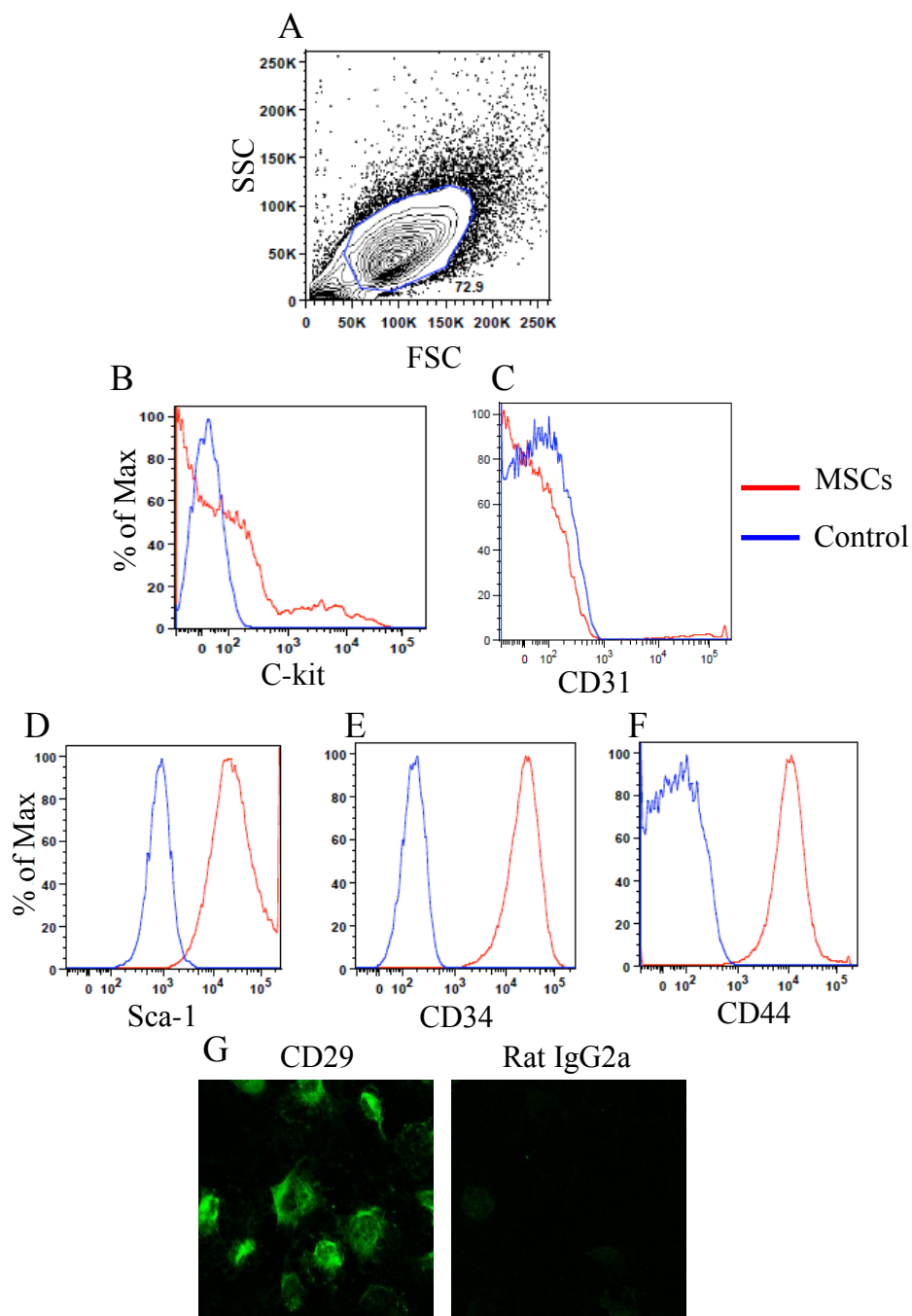
Figure 22. Flow cytometry analysis of MSCs confirms phenotype. A) Representative gating (Blue) for MSCs. B-G) MSCs (red) expression was compared against controls (blue) for B) c-kit, C) CD31, D) Sca-1, E) CD34 and F) CD44. G) Immunofluorescent staining confirming CD29 expression, in comparison to a Rat IgG2a control antibody.

A   CFSE^{+} MSCs

B — Burn Ethanol + PBS

C — Burn Ethanol + MSCs
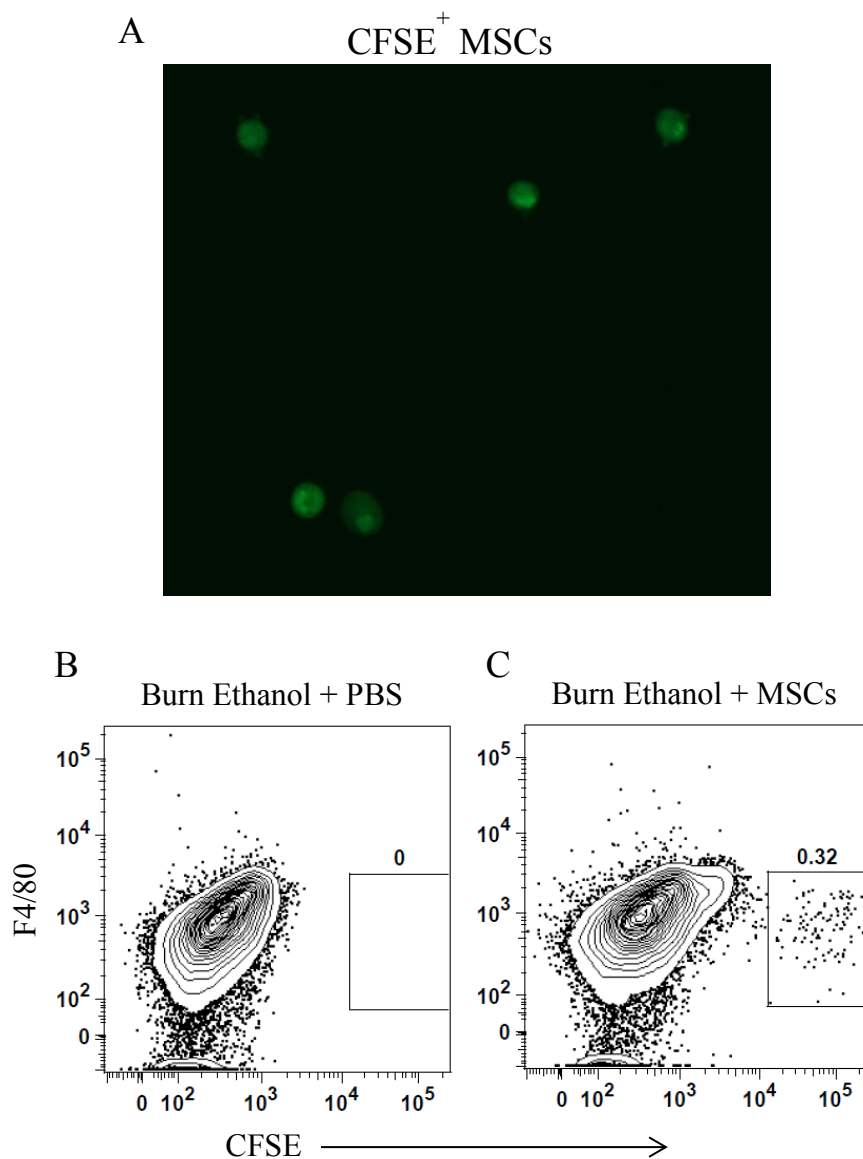
Figure 23. MSCs localize in lung tissue. CFSE^{+} MSCs were identified in dissociated lung tissue from intoxicated and injured mice at 24 h using flow cytometry. A) Confirmation of MSCs fluorescence prior to tail vein injection. B&C) Total dissociated lung cells were negatively selected for Siglec-F and CD11b (data not shown), followed by the identification of F4/80^{-} CFSE^{+} cells (box) in B) burn ethanol + PBS and C) ethanol + MSCs.

MSCs recovered per 3.5 x 10^5 total lung cells. Lack of Siglec-F, CD11b, F4/80 and CD11c expression supports the identification of individual CFSE^{+} cells and not CFSE^{+} cells engulfed by macrophage/monocytes, granulocytes, or dendritic cells. These data confirm that MSCs are in a position to attenuate pulmonary inflammation by their ability to localize in the lungs and remain there at least 24 h after infusion.

MSC Treatment Reduces Pulmonary Inflammation after Intoxication and Burn Injury

As previously shown by our laboratory, histochemical analyses of sectioned lung tissue demonstrated that ethanol intoxication prior to burn injury results in a 1.5 fold increase in cellularity, primarily by neutrophils, in comparison to burn injury alone at 24 hours after injury [104-107, 156]. Administration of MSCs 1 hour after injury decreased cellular infiltration and reduced pulmonary congestion after intoxication and injury (Figure 24A). Neutrophils within the lung interstitium were counted by light microscopy as previously described [104]. The increase in neutrophil infiltration into the lungs after intoxication and injury was attenuated with MSCs treatment and overall reduced neutrophil infiltration by 33% (Figure 24B). Additionally, the lung, liver, and skin (approximate to wound interface) were assessed for the presence of CFSE[+] MSCs. At 24 h after injury we were unable to identify CFSE^{+} cells in either tissue using immunofluorescence. However, we were able to identify CSFE^{+} cells in the lung using flow cytometry. Analysis of lung tissue indicated an average of 100 CFSE[+] MSCs per 350,000 total cells (~0.3%) (Figure 23C) remained in the lung at 24 h. Supporting these data, Eggenhofer and colleagues found the majority of viable MSCs were within the lungs at 1 h and at 24 h, their presence in the lungs was significantly reduced [124].
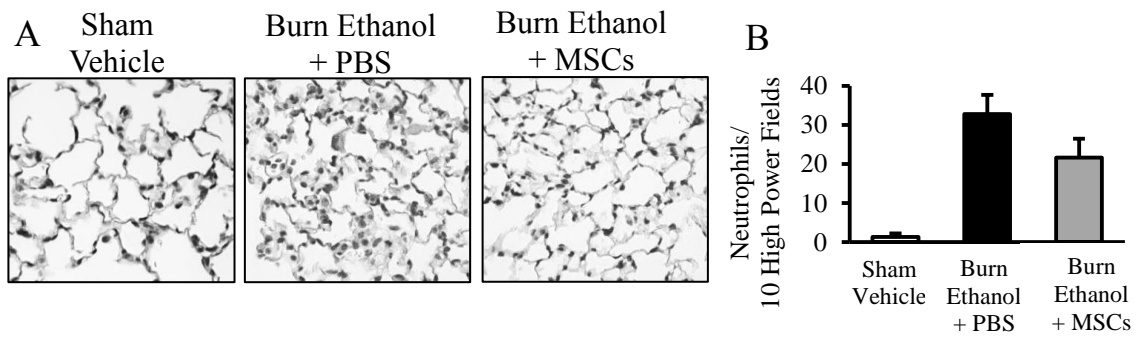
Figure 24. Histological assessment of pulmonary inflammation. Lungs were sectioned and stained with H&E and assessed for cellular infiltration. A) Representative sections from each treatment group are shown at 400x. B) Neutrophils were counted by light microscopy in H&E-stained lung sections 24 h after intoxication, injury and MSC treatment. Data are shown as the total number of neutrophils in 5 high power fields (400x). Not significant. Data are presented as mean values ± SEM. N = 3-4 animals per group. Representative of 2 independent experiments.

Decreased Pulmonary KC and Interleukin-6 (IL-6) Levels

Since we observed decreased neutrophil infiltration with MSC treatment, we next examined pulmonary neutrophil chemoattractant, KC and pro-inflammatory cytokine IL-6 levels. Consistent with previous studies, there was an 11-fold increase in KC ($p < 0.05$) in lung tissue, of intoxicated mice subjected to burn injury in comparison to control animals (Figure 25A) [104-106, 156] .This paralleled a 5.6 fold increase in IL-6 levels ($p < 0.05$) (Figure 25B). MSC treatment reduced KC levels by a 50% and IL-6 levels by 70% (Figure 25A&B). These data support our observation that MSC treatment decreases neutrophil infiltration into lung tissue, overall reducing pulmonary congestion. Surprisingly, we found no difference in the level of the anti-inflammatory interleukin-10 (IL-10) between experimental groups, even after MSC treatment and reductions in IL-6 (data not shown).

Serum IL-6 Attenuated with Mesenchymal Stem Cells

Dramatic increases in circulating IL-6 levels have been detected with intoxication and injury, relative to either insult alone [139] and a high serum level of IL-6 in burn injured patients has been correlated with increased chance of morbidity and mortality [101]. Here, we also found that intoxication and burn injury significantly upregulates serum levels of this cytokine ($p < 0.05$) and found that treating intoxicated and burn-injured animals with MSCs reduced serum IL-6 by 50% (Figure 26). The liver is likely one of the primary sources of IL-6 after intoxication and injury. We, therefore, analyzed levels of liver IL-6, as well as markers of hepatic damage, liver aminotransferases AST and ALT. Consistent with previously data [99, 177], intoxication and burn injury

A

B
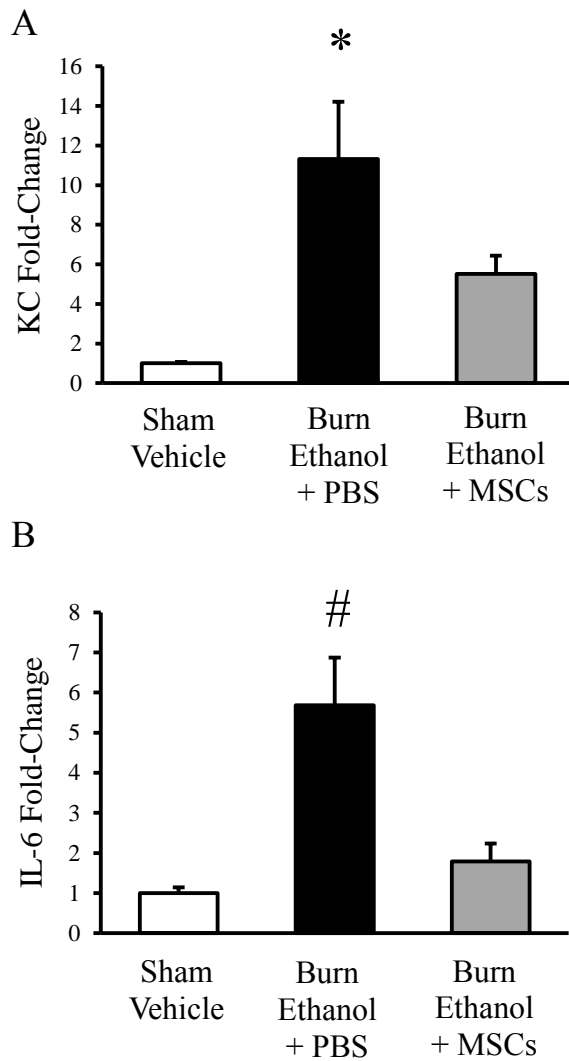
Figure 25. MSCs attenuate pulmonary KC and IL-6 levels. Lung homogenates were analyzed for levels of A) KC and B) IL-6. * $p < 0.05$ versus sham vehicle; # $p < 0.05$ versus all groups. By One-way ANOVA. Data are presented as fold-change ± SEM. N = 3-4 animals per group. Representative of 2 independent experiments.
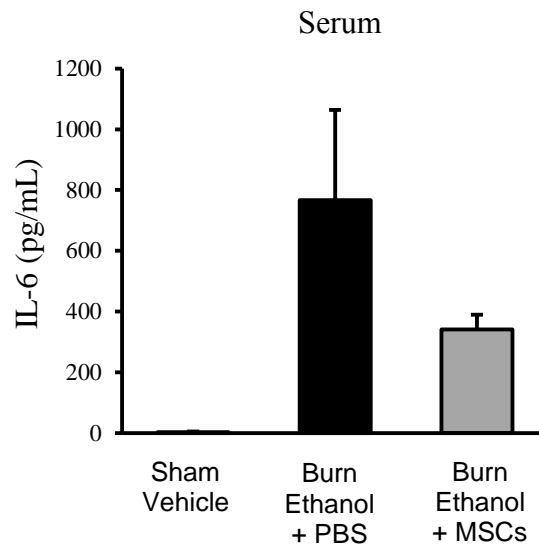
Figure 26. MSCs reduce serum levels of pro-inflammatory IL-6. Serum was collected from each treatment group and analyzed for IL-6. Not significant. Data are presented as the mean in picograms per milliter ± SEM. N = 3-6 animals per group.

Table 2: MSCs do not alter liver cytokine and serum aminotransferase levels.

	Sham Vehicle	**Burn Ethanol + PBS**	**Burn Ethanol + MSCs**
IL-6	8.9 ± 1.12	17.3 ± 0.05*	16.9 ± 0.18*
ALT	24.3 ± 12.9	217 ± 38.2*	174 ± 50.3
AST	145.3 ± 88.2	1035.8 ± 209.0*	815.5 ± 229.2

Liver homogenates were analyzed for levels of IL-6. IL-6 is presented as the mean in picograms per milliter ± SEM. Serum was collected from each treatment group and analyzed for AST and ALT. AST and ALT are presented as the mean units per liter ± SEM. * $p < 0.05$ versus sham vehicle. N = 3-6 animals per group.

elevated hepatic levels of IL-6 ($p < 0.05$), ALT ($p < 0.05$), and AST ($p < 0.05$), relative

to control animals. While MSC treatment restored pulmonary parameters, it failed to

diminish the levels of these factors in the liver (Table 2). Since MSC treatment

significantly reducing both lung IL-6 and systemic IL-6, but not liver IL-6, this suggests

that the MSCs have a direct effect on lung tissue. Additionally, these data propose that

the liver is not the only source of systemic IL-6 after intoxication and burn injury and that

the lungs may also contribute to systemic levels.

Elevated CD206^{hi} Alveolar Macrophages 24 hours

after Mesenchymal Stem Cell Treatment

We have shown that the administration of MSCs to intoxicated and injured

animals reduces inflammation in the lungs, but not on the liver. We postulated this may

be due to MSC activation of alveolar macrophages towards an anti-inflammatory

phenotype [121, 172, 173]. Therefore, we next analyzed alveolar macrophages by flow

cytometry for M1 and M2 markers, MHC II and CD206, respectively. Lung tissue was

digested into a single cell suspension and stained for alveolar macrophage cell surface

markers. As shown in Chapter 4, Siglec-F$^+$CD11c$^+$CD11b$^-$ alveolar macrophages have

low to negative levels of MHC II and constitutive expression of CD206 (Figure 27B)

[21]. To determine if MSCs altered the phenotype of alveolar macrophages in

intoxicated and burn-injured animals we analyzed alveolar macrophages after

intoxication, injury and MSC treatment and observed an increase in a population of

alveolar macrophages with heightened expression of CD206 (Figure 27A-C). We

quantified the percent of CD206^{hi} alveolar macrophages out of total alveolar
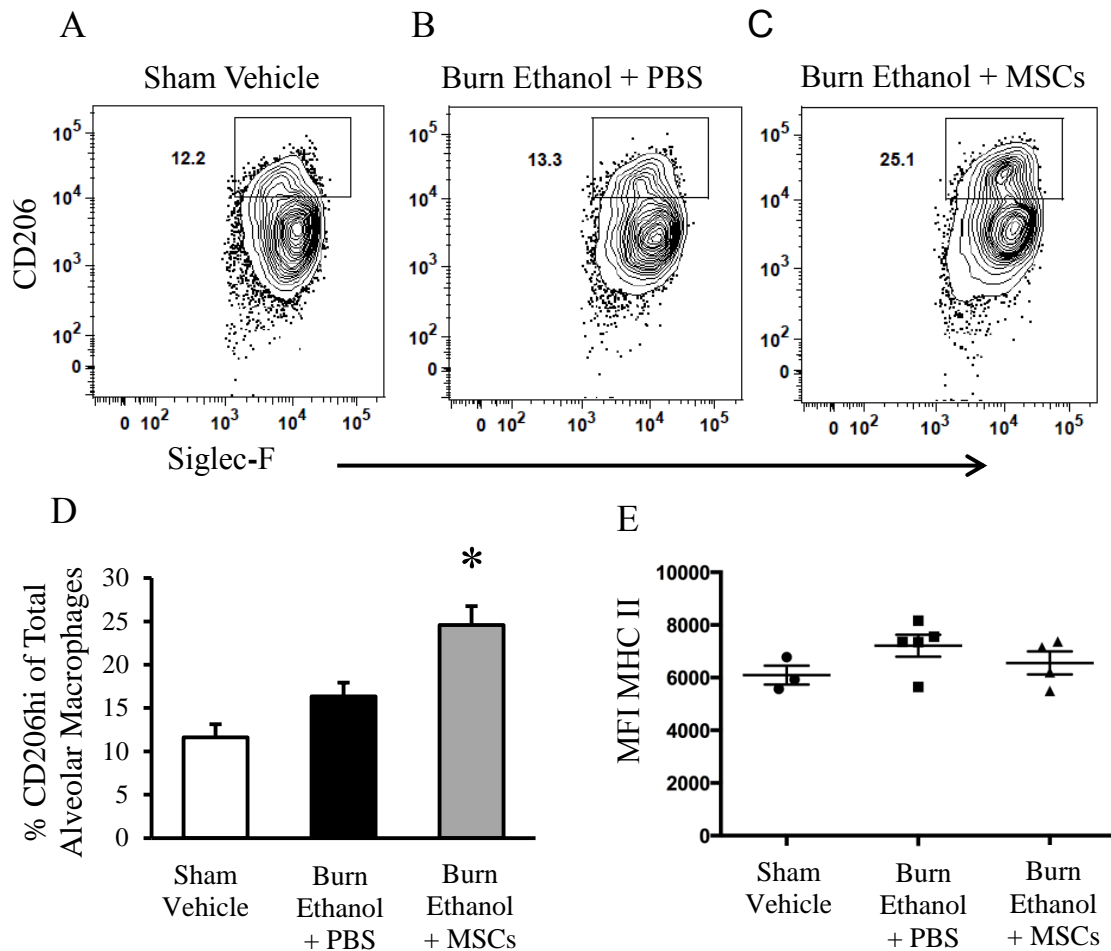
Figure 27. CD206^{hi} AMs are upregulated after MSCs treatment. Lung tissue was dissociated into a single cell suspension and cells were analyzed by flow cytometry. A-C) Representative gating for CD11c$^+$CD11b$^-$Siglec-F$^+$CD206^{hi} alveolar macrophages (box) from each treatment group. D) Percentage of CD206^{hi} cells of total alveolar macrophages. E) Scatterplot representation of mean fluorescence intensity (MFI) of MHC II on alveolar macrophages from each treatment group. * $p < 0.05$ versus all groups. By One-way ANOVA. Data are presented percentage CD206^{hi} cells per group $\pm$ SEM. N = 3-5 animals per group.

macrophages and found a 1.5-fold increase ($p < 0.05$) in these cells after intoxication, injury and MSC treatment, in comparison to intoxication and injury alone (Figure 27D). However, we found no change in the level of MHC II expression between all treatment groups at 24 h (Figure 27E). This was not surprising considering pulmonary inflammation after intoxication and injury likely mirrors sterile inflammation where we would not expect antigen presentation. These findings suggest MSCs may diminish pulmonary inflammation through the direct or indirect activation of alveolar macrophages into an M2 phenotype, overall highlighting MSCs as a viable therapy to locally suppress pulmonary inflammation in intoxicated and burn-injured patients.

<div align="center">Decreased Apoptosis in Lung Tissue</div>

The average number of TUNEL$^+$ apoptotic cells in lung tissue was quantified after intoxication, injury and MSCs. We found a 33% decrease in the number of TUNEL$^+$ cells with MSC treatment, however, mice treated with MSCs still had a 4.5-fold increase in apoptotic cells in comparison to sham (Figure 28A). We also found no difference in the number of alveolar macrophages after MSC treatment (Figure 28B). This suggests that the reduction in pulmonary inflammation as a result of MSC infusion may attenuate the cell death of a portion of lung cells, such epithelial or endothelial cells, but not alveolar macrophages. The studies herein did not determine how early after injury there is a decrease in the alveolar macrophage population, but the literature has shown apoptosis in the lungs as early as 3 h after burn alone in rats [116]. One study also demonstrated the majority of MSCs are within the lungs at 1 h after administration [124], therefore if we inject MSCs 1 h after injury, the majority of MSCs are in the lungs at 2 h after injury and

apoptosis in the lungs after intoxication and injury may have already been initiated by this time point.

Summary

The above studies demonstrate that the intravenous administration of exogenous MSCs have the ability to reduce both lung and systemic IL-6, a cytokine that has been described to play a causative role in the excessive pulmonary inflammation after intoxication and injury [107]. To this end, neutrophil chemokine KC levels and neutrophil infiltration into the lungs were also reduced after MSC treatment. Whether this was a direct outcome of decreased IL-6 levels was not determined in this study. Additionally, the entrapment of MSCs within the lung capillary bed may have led to the activation of alveolar macrophages into an anti-inflammatory phenotype resulting in a decrease in both systemic IL-6 and pulmonary inflammation, identifying the lungs one source of this pro-inflammatory cytokine. Taken together, these data suggest that the anti-inflammatory properties of MSCs, through either the direct or indirect interaction with resident alveolar macrophages may be helpful in initiating the resolution of pulmonary inflammation and either decreasing apoptosis or stimulating efferocytosis to remove apoptotic cells after intoxication and injury. These studies highlight MSCs as a useful therapeutic to specifically target lung inflammation. More studies are warranted to determine their effectiveness in a clinical application in the context of systemic inflammation.
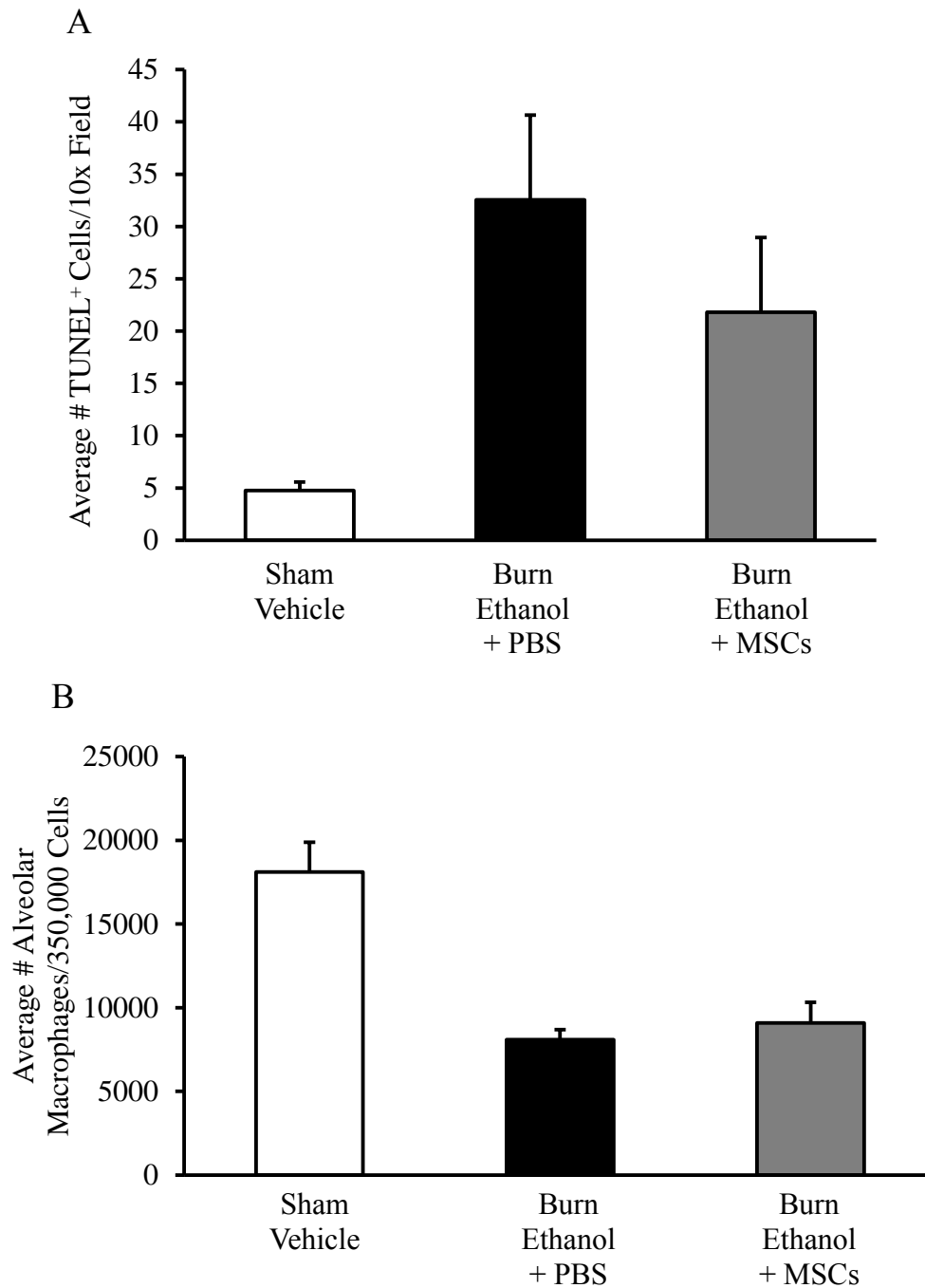
Figure 28. Decreased apoptotic cells in the lung after intoxication, injury and MSC treatment. An immunofluorescent *in situ* TUNEL assay was used to identify apoptotic cells in lung tissue. A) Average number of apoptotic cells per 10x field. Not Significant. B) Average number AMs per 350,000 lung cells. Not Significant. Data are shown as mean ± SEM. N=3-4 animals per group.

CHAPTER 6

DISCUSSION

In review, clinical studies indicate patients who are intoxicated at the time of burn injury have an increased risk of pulmonary complications and failure. Previous studies in our laboratory described elevated levels of neutrophils, neutrophil chemokines, KC and MIP-2, and IL-6 within lung tissue of intoxicated and burn-injured mice, relative to either insult alone. However, it had not been determined what underlying mechanism in the lung caused these changes or if they affected physiological lung function. With the knowledge that AMs are key orchestrators of both the initiation and resolution of inflammation, we hypothesized elevated pulmonary inflammation was a result of alterations in the AM population. To study the role of AMs in pulmonary inflammation and the effect of inflammation on lung function after intoxication and injury, we used a mouse model of binge ethanol exposure and scald injury. The results described in this dissertation correlate heightened pulmonary inflammation with impaired lung function and identify AMs as important regulators of both inflammation and targets of therapeutic interventions.

Lung inflammation can cause physiological derangements in intoxicated and burn-injured animals, including increased airway resistance and abnormal breathing patterns. Non-invasive, unrestrained whole-body plethysmography is a convenient method to evaluate normal breathing patterns in mice [178]. Unlike invasive

methods using a tracheotomy and mechanical ventilation to study plethysmography,

non-invasive techniques do not require anesthesia or surgery. This significantly reduces

stress and allows individual animals to be assessed multiple times, a useful feature for

time course studies [178-180]. In non-invasive plethysmography, Penh is a

dimensionless parameter that has been viewed as a measure of bronchoconstriction and

airway resistance, though several studies claim Penh is an unreliable measure of

respiratory mechanics [181, 182]. However, other studies suggest Penh should be used as

a measure of overall lung function, highlighting changes in respiratory breathing patterns

[178, 183, 184]. Verheijden, et. al. recently compared non-invasive plethysmography

(Penh) to invasive plethysmography (Resistance) in a severe model of allergic airway

inflammation. Their data revealed an increase in both Penh and resistance with severe

allergic airway inflammation. Notably, a Penh of 8 corresponded to a significant increase

in resistance, compared to controls, suggesting that in severe models of inflammation,

Penh is a reflective measure of resistance. Additionally, it was determined an increase in

Penh paralleled an increase in bronchoalveolar lavage cells in the airways [183],

furthering supporting our data that pulmonary congestion with intoxication and burn

injury leads to functional lung complications.

We observed that ethanol intoxication at the time of injury leads to a longer pause

between breaths (Penh), correlating with a decrease in the frequency of breaths per

minute. With this data, one would expect this slower breathing pattern, an indicator of

increased lung resistance, would result in deeper breaths, represented by an increase in

tidal volume. In contrast, we observed a decrease in tidal volume and minute volume, an

indication that the mice are not able to compensate for the increase in lung resistance.

This breathing pattern may mirror agonal breathing, which is characterized by infrequent, shallow breaths and has been observed in severely injured humans. This pattern is precipitated by hypoxemia regardless of arterial carbon dioxide levels or pH, which may be the case in our injured animals since agonal breathing in humans is typically viewed as the terminal stage of respiration, occurring immediately before death [185]. When the plethysmography measurements were taken at 24 hours in our experiments, majority of the animals appeared either moribund or lethargic in the plethysmography chamber. With 47% of death occurring between 24 and 72 hours, the breathing pattern we detected in mice at 24 hours strongly suggests it can be characterized as agonal breathing, indicating a mechanism behind the large percentage of mortality in the following 48 hours.

The location of the dorsal burn injury in this model could also restrict chest wall movement during both the inflammatory and the wound healing phases, promoting the observed decrease in breaths per minute, overall leading to decreased gas exchange. Humans with chest, back or torso circumferential burns have breathing patterns with rapid shallow breaths, not slow shallow breaths, as we have observed in our model [86]. These differences, however, may be attributed to the immediate care provided to human burn patients. Torso circumferential burns can limit respiration and require a chest escharotomy where incisions are made in the burn wound, releasing constricted and non-elastic damaged tissue, to restore chest movement. The mice in our model do not receive circumferential burns, removing the need for escharotomy in the model, but the injury

location may still lead to an altered breathing pattern. Tidal breathing is usually interrupted every few minutes by a deep breath or yawn, which is needed to expand underinflated alveoli. Restricted chest wall movement can cause burn patients to lose this ability. Without this interruption in tidal volume, the alveoli eventually collapse in a process known as atelectasis, resulting in decreased blood flow, oxygen exchange and the ability of the lungs to expand [86, 186]. Our data demonstrate that the loss of lung compliance with burn injury, even in the absence of inhalation injury, is further decreased when intoxication precedes burn injury. The restricted chest movement and subsequent collapse of alveoli may also explain the differences in breathing patterns in our mouse model, in comparison to human burn patients. However, the 3-fold increase in Penh with burn alone does not correspond to significantly increased mortality rates. This suggests ethanol, not the location of the burn, leads to impaired lung function and elevated mortality rates. Overall, these findings highlight pulmonary inflammation as an underlying mechanism that contributes to the drastic mortality rate observed in mice exposed to both ethanol and burn injury.

Apoptosis of type I and type II epithelial cells and neutrophil infiltration are postulated as two main causes of ARDS [187]. Heighten infiltration or ineffective removal of apoptotic neutrophils can prolong the inflammatory response, while damage to epithelial cells and the capillary-alveolar interface can lead to increased lung permeability. The resolution of pulmonary inflammation is influenced by the recognition of apoptotic cells and efferocytosis by AMs [43, 170]. A defect in this process can

substantially prolong the inflammatory response, leading to greater tissue damage. A functioning population of AMs is therefore needed to regulate pulmonary inflammation.

The studies herein demonstrate intoxication and injury results in increased numbers of apoptotic cells in lung tissue 24 h post-injury. AMs from intoxicated and injured mice display functional components, MARCO and CD11b, both important in efferocytosis. Morphological analysis of AMs also supports the capacity of a percentage of AMs to effectively take up apoptotic cells, even after intoxication and injury. Therefore, it does not seem intoxication at the time of injury completely inhibits the function of AM efferocytosis. Whether ethanol reduces the percent of efferocytosis after burn injury was not determined in this these studies. However, previous studies in our laboratory found ethanol exposure decreased AM phagocytosis of *P. aeruginosa* and that this was facilitated by a decrease in macrophage Fcγ- receptor after *in vitro* or *in vivo* alcohol exposure [8, 76]. Efferocytosis is a separate and distinct process from the phagocytosis of pathogens, therefore it is plausible alcohol can have differential effects on both of these functions.

There are two main pathways in the initiation of apoptosis. First, pro-apoptotic stimuli can signal the intrinsic pathway of mitochondrial BCL-2 and cytochrome c release. Second, activation of death receptors, such as Fas and TNF-family receptors, initiate the extrinsic pathway of apoptosis. Both of these pathways lead to caspase-3/7 activation and the subsequent cleavage of cellular protein and DNA fragmentation that results in apoptosis [188]. Here we showed AMs isolated from intoxicated and burn-injured mice spontaneously produced 5-fold more TNFα, a prominent death receptor

activator. The literature suggests both apoptotic and necrotic cells are TUNEL$^+$ [167], but only apoptotic cells are caspase-3/7$^+$. Our findings of active-caspase-3/7$^+$ cells being efferocytosed by AMs, supports an apoptosis pathway of cell death, and not necrosis, in lung cells after intoxication and injury.

Clinical data revealed that burn injury alone leads to increased levels of endotoxins in the bloodstream, peaking between 7 and 12 hours after injury [108]. Elevated levels of circulating endotoxin after burn injury has also been correlated to increased incidences of multiple organ failure [109]. While the effect of ethanol and burn injury on circulating endotoxin levels has not been determine, we postulate that increased bacteria translocation from the gut would result in heightened levels of LPS, or other bacterial products, into the blood stream. Previously, our laboratory demonstrated TLR4 signaling, but not TLR2, contributes to elevated pulmonary inflammation after intoxication and injury [106]. LPS, a TLR4 ligand, has been shown to activate endothelial cell production of pro-inflammatory mediators, including neutrophil chemokines [189]. Interestingly, our data indicate AMs and airways cells are not primary sources of KC. Taken together, LPS-induced activation of capillary endothelial cells may facilitate heightened levels of neutrophil chemokines we have observed in total lung tissue. In addition to endotoxins, AM production of TNFα may also have an important role in prolonged pulmonary inflammation. In human studies, TNFα activates endothelial cells and induces the upregulation of adhesion molecules and IL-8 and IL-6 secretion, resulting in transendothelial migration of neutrophils [190-192]. Furthermore, human studies suggest apoptosis of AMs and epithelial cells in acute lung injury is induced by

endotoxins and not hypoxemia [193, 194]. Our data revealed there was a trend toward

an increase in TLR4/MD-2 expression on AMs at 24 h. We speculate that if endotoxin

levels peak by 12 h after combined injury, that perhaps endotoxin-induced apoptosis

occurred long before our 24 h analysis, and is why we observe decreased number of AMs

in lung tissue.

Published studies from our laboratory indicate that long myosin light-chain kinase

(MLCK) activation mediates increased intestinal permeability after intoxication and burn

injury [97, 98]. Inhibition of MLCK activation, either through membrane permeant

inhibitor of MLCK (PIK) or studies using MLCK knockout (KO) mice, showed a

decrease in intestinal damage and bacterial translocation into the mesenteric lymph

nodes. Preliminary studies examined levels of apoptotic cells in the lungs of intoxicated

and burn-injured MLCK KO mice. We found that decreased tight junction disruption

after intoxication and bury injury resulted in a 75% decrease in apoptotic cells in the

lung, in comparison to wild type counterparts (p <0.05) (Figure 29). These data support

our hypothesis that systemic mediators, such as LPS or endotoxins, influence pulmonary

inflammation and apoptosis. Future studies are warranted to compare the role of AMs in

inflammation in MLCK KO mice to wild type mice.

The literature suggests that efferocytosis by AMs initiates the transition from an

inflammatory phase towards a resolution phase by stimulating the release of IL-10 and

TGFβ [43-46]. TGFβ has specifically been shown to inhibit TNFα-induced, IL-8

dependent migration of neutrophils through the endothelium [195]. We did not examine

levels of TGFβ, but this would be an interesting future direction for these studies. We
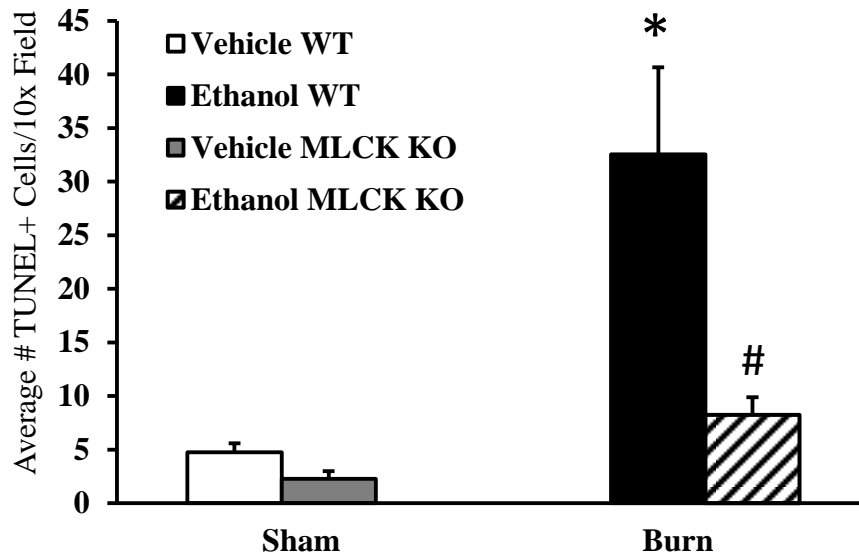
Figure 29: Decreased number of apoptotic cells in the lung after intoxication and injury in MLCK KO mice. An immunofluorescent *in situ* TUNEL assay was used to identify apoptotic cells in lung tissue. Average number of apoptotic cells per 10x field after intoxication and injury. *p < 0.05 versus sham vehicle WT, #p < 0.05 versus burn ethanol WT by One Way ANOVA. Data are shown as mean ± SEM. N=3-4 animals per group.

have analyzed lung IL-10, but have not seen changes in this cytokine 24 h after

intoxication and burn injury. We also did not detect a change in the IL-10R expression,

suggesting if exogenous IL-10 were administered, it may be able to activate an

inflammatory phenotype on AMs. Loss of AMs, in addition to minimal AM efferocytosis

of the abundant apoptotic cells, may result in deficient levels of anti-inflammatory

mediators that can initiate the resolution phase. Thus, this can prolong the pro-

inflammatory phase. The heightened expression of scavenger receptor MARCO and

production of TNFα by AMs supports a pro-inflammatory phenotype. Excessive

inflammatory mediator production has been shown to inhibit apoptosis of neutrophils and

prolong their stay in tissue [196]. Our laboratory also demonstrated intoxication, prior to

burn injury and infection, decreased in neutrophil apoptosis and prolonged their stay in

the airways [143]. These factors support an extended pro-inflammatory phase that can

result in tissue damage and impair lung function. Collectively, these data also indicate

AMs 24 h post-injury may be activated by LPS. In response, they may upregulate

MARCO, express both ARG1 and iNOS, and secrete TNFα. Using recent macrophage

nomenclature guidelines these data suggest we can potentially classify AMs from

intoxicated and injury mice as M(LPS) [34] (Figure 30).

Clodronate experiments confirmed AMs also have a role in limiting neutrophil

numbers into the lungs after intoxication and injury. The negative correlation between

decreased AM numbers and increased neutrophil numbers proposes elevated neutrophil

accumulation after intoxication and injury is a result of AM deficiency in the lung tissue.

Our data show that both the loss of AMs and a heightened pro-inflammatory profile on
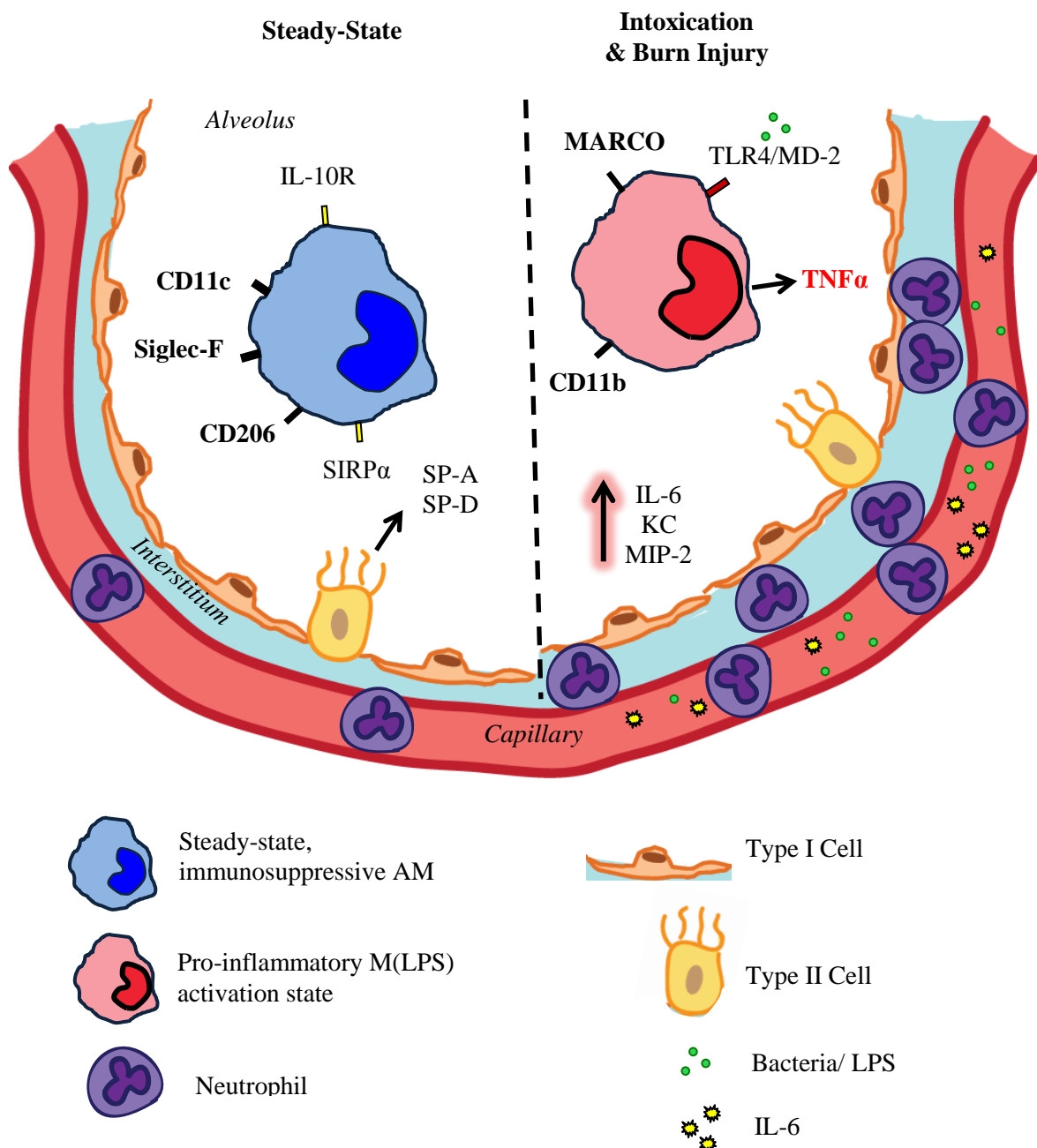
Figure 30: AMs have a pro-inflammatory M(LPS) phenotype after intoxication and injury. In steady-state conditions, AMs maintain tolerance and suppress inflammatory responses through inhibitory receptors CD206 and SIRPα, that binds SP-A and SP-D. As a result of heightened levels bacteria/LPS and IL-6 in the blood stream after intoxication and injury, there is increased alveolar wall thickening, neutrophil accumulation into the interstitium and an increase in neutrophil chemoattractants KC and MIP-2, and IL-6 in lung tissue. The studies indicate AMs acquired an M(LPS) phenotype. We postulated LPS activates through TLR4/MD-2. *Co-illustration credit C.L. Shults*

remaining AMs, may prolong pulmonary inflammation after intoxication and injury,

underlining a mechanism for impaired lung function and increased incidences of

mortality.

Kinetic studies of AM life-span reveal AMs are long-lived cells with a half-life of

30 days and minimal self-renewal in steady-state lung conditions [12]. During lung

injury, loss of AMs results in the local proliferation of AMs and is the main mechanism

of repopulation [13-15]. In Appendix A (Figure 31&33-34), we identified a population

of intermediate AMs. Quantification of these cells after injury demonstrated a 1.5-fold

increase in this population (Figure 8C), indicating intermediate AMs may be actively

trying to repopulate loss of AMs in the alveolar space. The rate of repopulation after

injury and function of efferocytosis was not determined, but these activities would be an

interesting study to determine the effect of alcohol on the repopulation of AMs after

injury.

Our studies emphasize the imperative role of AMs in pulmonary inflammation

after intoxication and burn injury and the restoration of these multi-functional AMs could

be critical to re-establishing lung homeostasis and improving lung function. The

identification of local lung therapeutic agents that specifically target AMs may be

beneficial to attenuating pulmonary inflammation, overall reducing mortality in burn

patients. The data in this dissertation highlight MSCs a useful therapy to specifically

treat pulmonary inflammation.   Intravenous administration of exogenous MSCs were

demonstrated to have the ability to reduce both lung and systemic IL-6, a cytokine that

has been described to play a causative role in the excessive pulmonary inflammation after

intoxication and injury [107]. To this end, neutrophil chemokine KC levels and

neutrophil infiltration into the lungs were also reduced after MSC treatment. Whether this

was a direct outcome of decreased IL-6 levels was not determined in this study. However,

the literature implies that MSC production of anti-inflammatory mediators, such as IL-10

and TGFβ, can down regulate pro-inflammatory mediators, such as IL-6. In our study, we

did not observe increased levels of lung IL-10, but Lee et al. demonstrated the anti-

inflammatory factor, tumor necrosis factor-α induced protein 6,which is secreted by

MSCs trapped in the lungs can enter the bloodstream and reduce inflammation at the

primary site of injury [175]. In our intoxication and injury model, it is possible MSC

therapy attenuated pulmonary inflammation in more than one way. The secretion of anti-

inflammatory mediators by MSCs into circulation may localize to the burn injury,

dampening the release of IL-6, thereby decreasing systemic IL-6 levels and pulmonary

inflammation. Additionally, the entrapment of MSCs within the lung capillary bed allows

MSCs to activate alveolar macrophages to an anti-inflammatory phenotype, further

contributing to the reduction of lung inflammation. Alternatively, MSC attenuation of

pulmonary inflammation through alveolar macrophages may result in a decrease in

systemic IL-6, identifying the lungs one source that contributes to elevated serum levels

of this pro-inflammatory cytokine.

To our knowledge, clinical and experimental MSC therapy in burn injury has

focused on wound repair, through either the topical transplantation or injections of MSCs

near the site of injury [127-130]. Xue et al. demonstrated the plasticity of MSCs to

differentiate into tissue-specific cells and to promote accelerated wound healing, while

others have shown an increase in neoangiogenesis and a decrease in cellular infiltration at the wound site [130, 131]. Thus far, alternative routes of MSC administration and their therapeutic applications is an understudied field in burn research [129]. We choose an intravenous method of MSC administration in attempt to localize MSCs and their anti-inflammatory properties to the lungs and believe that our study is the first to investigate the effects of intravenous administered MSCs to target pulmonary inflammation after intoxication and burn injury. We found a small percentage CFSE$^+$ MSCs in the lungs 24 h after burn injury using flow cytometry, at a ratio of 100 CFSE$^+$ MSCs per 350,000 total cells (~0.3%) (Figure 23C). However, we could not identify CFSE+ cells in the lung tissue. The small percentage of MSCs in the lungs at the time point could be due to a various factors. While the majority of intravenous MSCs are localized to the lungs, regardless of experimental model, bone fracture studies suggest viable MSCs are able to home to the site of injury and promote fracture healing. These studies used bioluminescent trafficking and confirmed a large percentage of MSCs get trapped in the lungs 1 day after transfer, but a portion of MSCs home to the bone fracture site by 3 to 14 days after administration [197-199]. This delay in migration from the lungs to the site of injury may support why we do not see MSCs near the burn wound at this 24 h time point. Furthermore, intoxication at the time of bone fracture did not inhibit the migration of MSCs given 24 h after injury [200]. Bioluminescence is a very sensitive technique that shows the general location of labeled MSCs within a test subject, but the visualization of individual fluorescently labeled cells may be more difficult to find within the several million lung alveoli. Additionally, burn injury alone results in an increase in capillary

permeability and tissue edema, with a great need for fluid resuscitation [201], while intoxicated and burn-injured patients require an even greater amount of fluid resuscitation [89]. Our laboratory found that intoxication at the time of injury increases post-burn dehydration, even after fluid resuscitation, while also causing a shift in fluid compartments that results in greater ischemic end-organ damage [202]. The increase in capillary permeability and loss of fluid from the vascular space may highly influence the fate of infused MSCs. The large size of MSCs may not only trap them within the lung capillary bed, but also retain them within constrained vasculature of intoxicated and burn-injured mice. It is also possible the migration aptitude of the Gibco® MSCs differs from freshly isolated primary bone marrow-derived MSCs. However, published studies have confirmed the immunosuppressive ability of this cell line [203]. Overall, we can conclude that even in the presence of acute dehydration and ischemia, MSCs are able to exhibit an anti-inflammatory effect on the lungs, while also reducing systemic IL-6.

In conclusion, even though AMs may only be a small percentage of cells in the lungs, their function and presence has a huge impact on normal lung function. These data presented in this dissertation support our hypothesis that intoxication and burn injury results in the loss of AMs through apoptosis, leading to elevated levels of neutrophil infiltration and impaired lung function. Finally, AMs diverse functions and their changeable activation state present an opportune therapeutic target to help control pulmonary inflammation in all burn patients.

APPENDIX A

CHARACTERIZATION OF LEUKOCYTE POPULATIONS IN THE LUNG

AFTER INTOXICATION AND INJURY

[117]

APPENDIX A

CHARACTERIZATION OF LEUKOCYTE POPULATIONS IN THE LUNG
AFTER INTOXICATION AND INJURY

Results

Lung tissue was dissociated into a single cell suspension from both sham vehicle

and burn ethanol treatment groups and analyzed by flow cytometry [21]. Total live lung

cells were gated (Figure 31A) and examined for expression of CD11b and CD11c cell

surface markers (Figure 31B). Using these 2 markers we were able to subdivide lung

cells into 4 different populations, including AMs (Figure 31B, R1), intermediate

AMs/CD11b$^+$ DCs (Figure 31B, R2), granulocytes (neutrophils) (Figure 31B, R3), and

lymphocytes/non-leukocytes (Figure 31B, R4), regardless of injury. While our main

focus was on the characterization of AMs, we confirmed the phenotype of all 4

populations and assessed whether intoxication and injury altered the frequency of these

individual subsets. First, forward scatter (FSC-cell size) and side scatter (SSC-

granularity) plots were analyzed from each treatment group (Figure 31C&F). With

intoxication and injury, we visually noted the appearance of a population of cells within

total lung (Figure 31F, white dashed circle). Based on data presented in Chapter 3, as

well as previous data by our laboratory, we predicted this population of cells was

infiltrating neutrophils. To identify AMs, we first analyzed total live cells for

CD11c$^+$CD11b$^-$ (Figure 31D&G) and noticed a decrease in the density of this population.

Further analysis of alveolar macrophages confirmed their expression of Siglec-F (Figure

31E&H). Within CD11c$^+$CD11b$^-$ population we also can identify
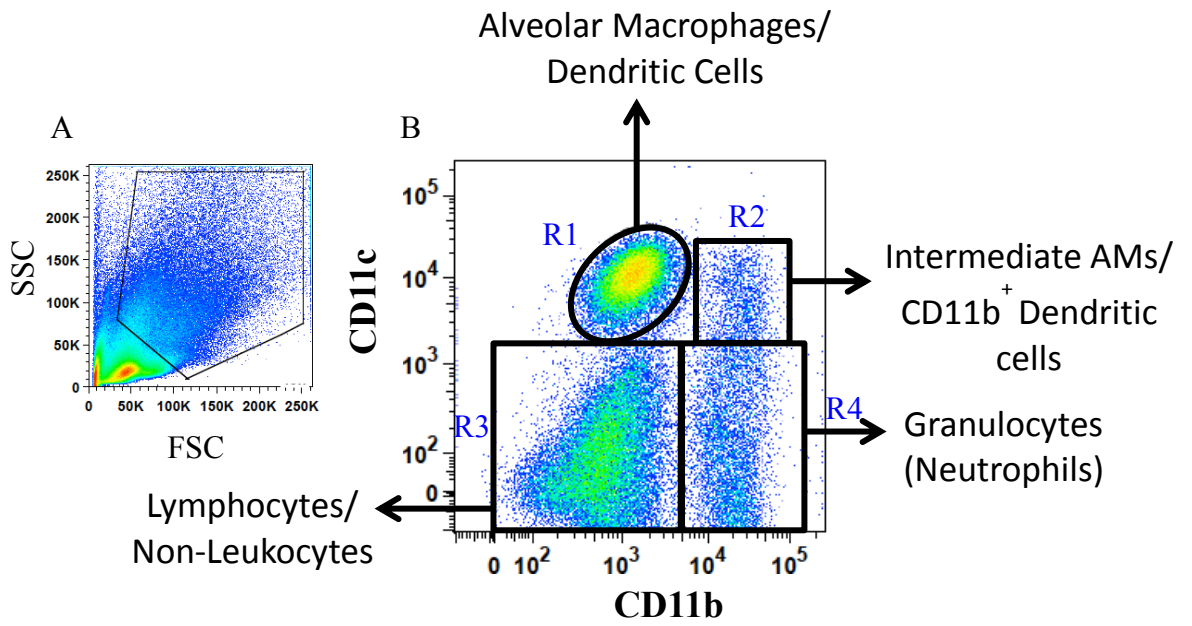
Figure 31 continued on next page

Alveolar Macrophages in Enzyme Dissociated Lung Tissue
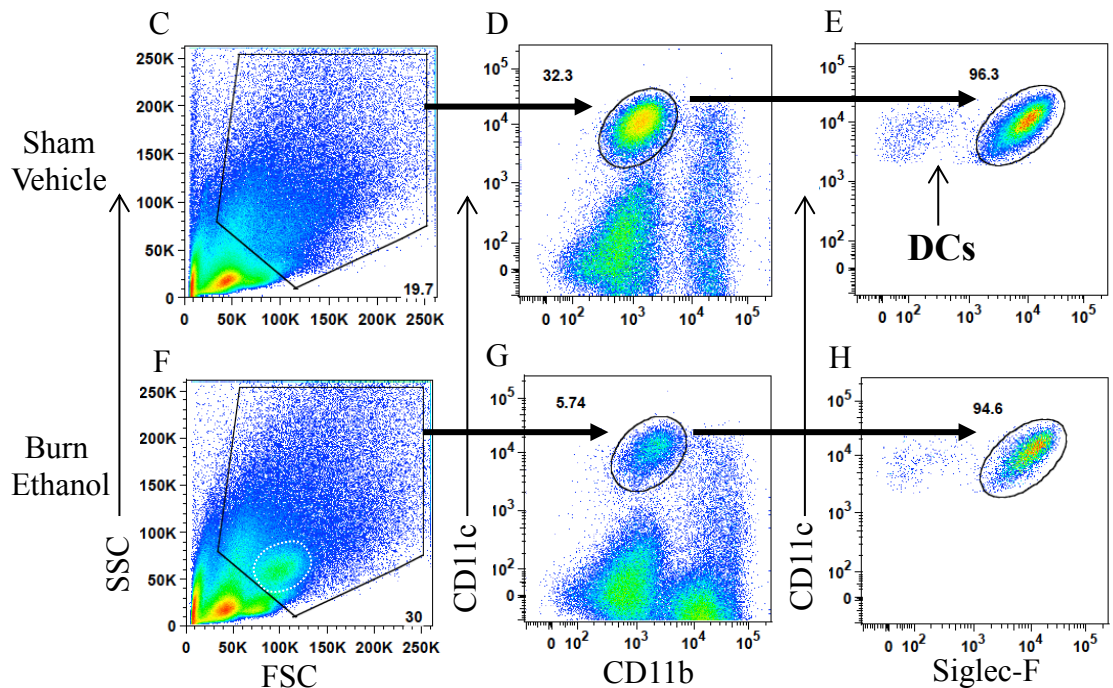
Figure 31. Flow cytometry analysis of leukocyte populations in lung tissue. Lung tissue was obtained 24 hours post-injury and enzymatically dissociated into a single cell suspension. Lung cells were stained for leukocyte cell markers. A) Total lung cells were gated to include large myeloid cells (polygon gate) and exclude smaller lymphocytes and dead cells. B) Summary of individual cell populations within the total lung gate using a CD11c versus CD11c gating method. **(R1)** CD11c$^+$CD11b$^-$ AMs **(R2)** CD11c$^+$CD11b$^+$ intermediate AMs and CD11b$^+$ DCs **(R3)** CD11c$^-$CD11b$^-$ lymphocytes/non-leukocytes and **(R4)** CD11c$^-$CD11b$^+$ granulocytes (neutrophils). C-H) Representative gating of AMs from both sham vehicle and burn ethanol groups. Flow profiles in sham vehicle were selected for C) total lung cells (polygon gate), then D) CD11c$^+$CD11b$^-$ cells (black gate), then E) Siglec-F$^+$ (CD11c$^+$) cells (black gate), small black arrows indicate DCs within the CD11c$^+$CD11b$^-$ population. Flow profiles in burn ethanol were similarly selected for F) total lung cells (polygon gate-white dash circle indicates infiltrating cells), then G) CD11c$^+$CD11b$^-$ cells (black gate), then H) Siglec-F$^+$ (CD11c$^+$) cells (black gate). Changes in the density of cell populations indicate changes in the quantity of cells in a population.

CD11c$^+$Siglec-F$^-$ DCs. Using a backgating tool we, we examined where CD11c$^+$CD11b$^+$Siglec-F$^+$ AMs were located within total lung cells in both treatment groups (Figure 32A&D). AMs in sham vehicle varied in size (FSC) and granularity (SSC), with the majority of AMs falling between 50-150K SSC (Figure 32A). However, AMs from intoxicated and burn injured mice showed an increase in SSC, majority of cells ranging from 100-225K (Figure 32D), suggesting combined injury activates AMs. We further show CD11c$^+$CD11b$^-$Siglec-F$^+$ cells are F4/80$^+$ (Figure 32C&F). Additionally, we examined Siglec-F$^+$ cells and found a population of CD11c$^+$CD11b$^+$Siglec-F$^+$ cells adjacent on the plot to AMs (Figure 32B&E). Eosinophils can be eliminated because they are Siglec-F$^+$, but not CD11c$^+$, therefore, we hypothesized this additional population of Siglec-F$^+$ cells were interstitial macrophages.

Analysis of CD11c$^+$CD11b$^+$ cells (Figure 33) revealed that the majority of the cells from sham animals had a wide range of FSC and SSC (Figure 33A), while this population from intoxication and injured mice had an increase in SSC (Figure 33C). We next analyzed this population for F4/80 and Siglec-F expression in both treatment groups. Using fluorescent minus one controls we established a F4/80$^-$Siglec-F$^-$ and a F4/80^{lo}Sigle-F$^+$population of cells (Figure 34A). F4/80$^-$Siglec-F$^-$ also expressed MHC II (Figure 34B), while F4/80^{lo}Siglec-F$^+$ expressed similar levels of CD206 as AMs (Figure 34C). The literature suggests these CD11c$^+$CD11b$^+$ cells are an intermediate macrophage population that replenish alveolar macrophages [204]. However, we believe we have shown that CD11c$^+$CD11b$^+$ cells are representative of F4/80$^-$Siglec-F$^-$MHC II$^+$ "CD11b$^+$ DCs" and F4/80^{lo}Siglec-F$^+$CD206$^+$ intermediate AMs. We are hesitant to call
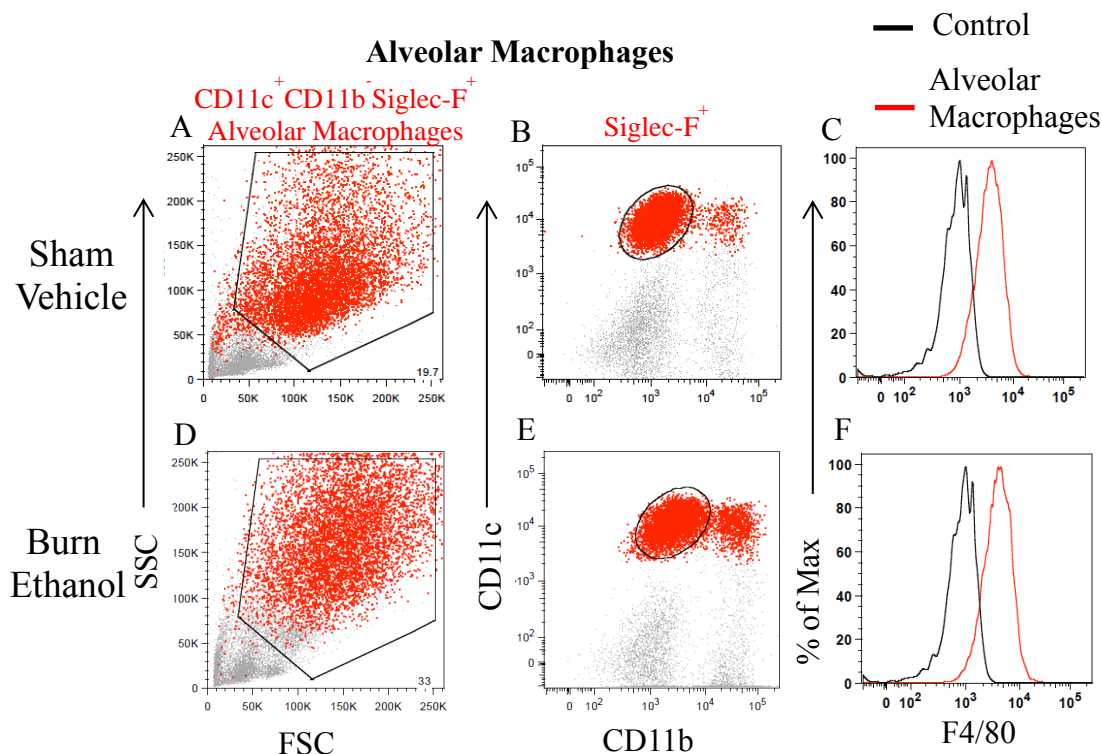
Figure 32. Forward scatter and side scatter characteristics of AMs. Forward scatter (FSC) is a measure of cell size and side scatter (SSC) is a measure of granularity. Data representative of dissociated lung tissue from (A-C) sham vehicle and (D-F) burn ethanol mice. A&D) CD11c$^+$CD11b$^-$Sigle-F$^+$ AMs (red) were analyzed for FSC and SSC in total lung cells. B&E) Location of Siglec-F$^+$ cell populations within CD11c and CD11b gating (red). There are two Siglec-F$^+$ populations of cells, CD11b$^-$ and CD11b$^+$. C&F) Confirmation of F4/80 expression on CD11c$^+$CD11b$^-$Sigle-F$^+$ AMs (red), in comparison to a fluorescent minus one control (black).
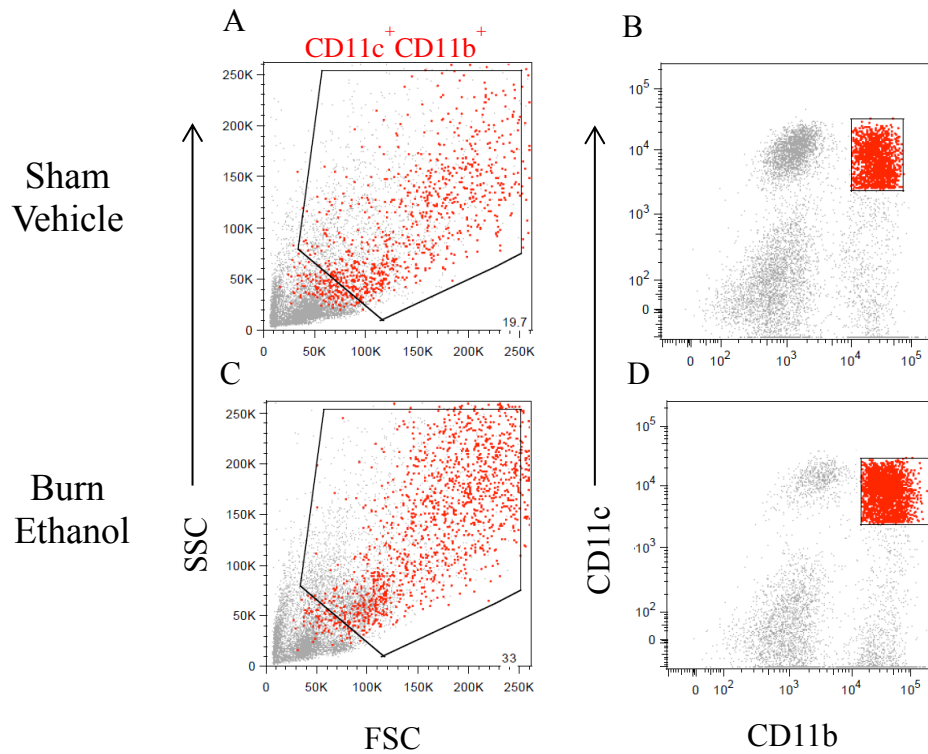
Figure 33. Forward scatter and side scatter characteristics of CD11b$^+$CD11c$^+$ cells. Data representative of dissociated lung tissue from A&B) sham vehicle and C&D) burn ethanol mice. A&C) CD11c$^+$CD11b$^+$cells (red) were analyzed for FSC and SSC in total lung cells. B&D) Gating of CD11c$^+$CD11b$^+$ cells (red) that were analyzed for FSC versus SSC in A&C.

Intermediate Alveolar Macrophages
Dendritic Cells
Alveolar Macrophages
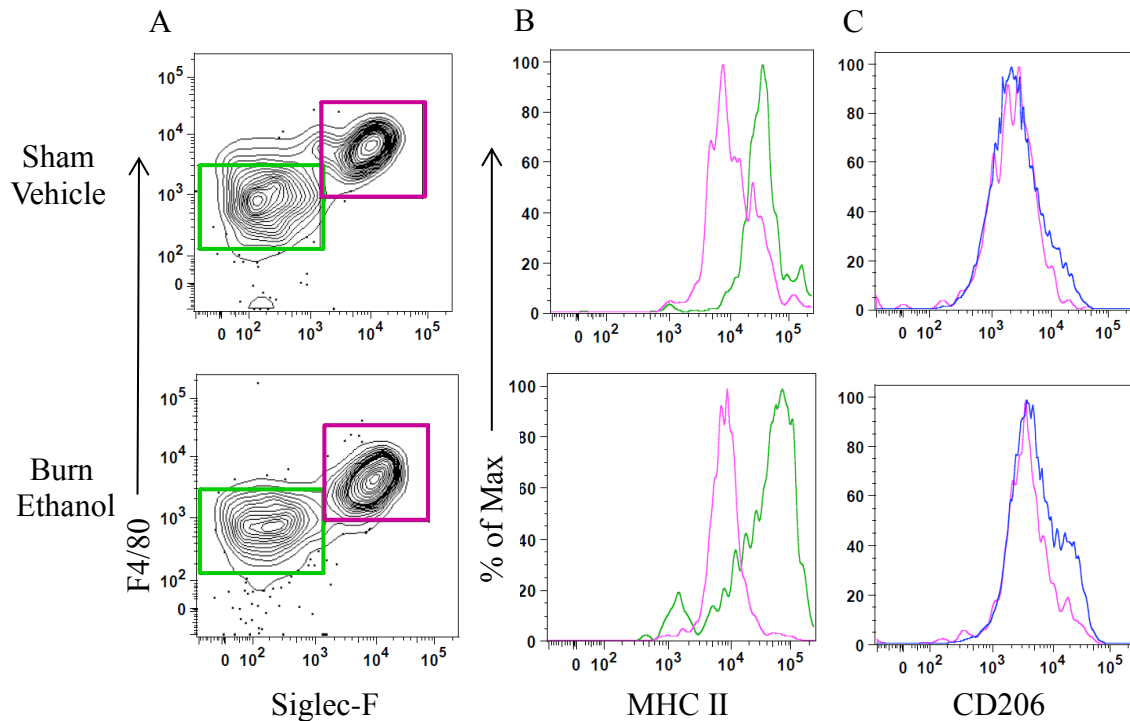
Figure 34. Characterization of CD11b$^+$CD11c$^+$ cells. CD11b$^+$CD11c$^+$ cells from dissociated lung tissue were analyzed in sham vehicle and burn ethanol mice for Siglec-F and F4/80 expression. A) Two populations were identified, Siglec-F$^+$F4/80^{lo} intermediate AMs (magenta gate) and Siglec-F$^-$F4/80$^-$ DCs (green gate). B) Expression levels of MHC II on both intermediate AMs (magenta) and DCs (green). MHC II is expressed on Siglec-F$^-$F4/80$^-$ DCs, but not on Siglec-F$^+$F4/80^{lo} intermediate AMs. C) Expression levels of CD206 on intermediate AMs (magenta) in comparison to CD11c$^+$CD11b$^-$Sigle-F$^+$ AMs (blue). CD206 levels on intermediate AMs are similar to AMs.

intermediate AMs interstitial macrophages because 1) we did not assess their location in the tissue and 2) it is thought that interstitial AMs do not express Siglec-F [21]. Additionally, clodronate depletion of AMs also eliminated intermediate AMs, but not DCs, further confirming that these are two distinct populations (Figure 35). We originally hypothesized the DC population were monocytes, but according to Misharin et al., monocytes in the lung are not MHC II$^+$ [21].

The location of CD11c-CD11b+ cells was also assessed in total lung cells (Figure 36A&D), confirming that the infiltrating population observed with intoxication and injury was CD11c$^-$CD11b$^+$Ly-6G$^+$ neutrophils (Figure 31F & 36A-C) and we have already established in Chapter 3 that there is a significant increase in CD11b$^+$Ly-6G$^+$ neutrophils after intoxication and injury. Eosinophils were not assessed, but they would likely fall in the CD11c$^-$CD11b$^+$ population during an allergic stimuli. Lastly, CD11c$^-$CD11b$^-$ cells were characterized as F4/80$^-$Ly-6G$^-$Siglec-F$^-$ lymphocytes or non-leukocytes. Based on where they fall in the FSC and SSC plot, these cells likely are a mix of lymphocytes, epithelial, endothelial cells or dead cells (Figure 36D&E).

In separate experiments, BAL cells were also obtained and their phenotype was compared against AMs from dissociated lung tissue (Figure 37). BAL cells were phenotyped as CD11c$^+$CD11b$^+$Siglec-F$^+$F4/80$^+$ (Figure 37D) and these cells represented >92% of total BAL cells, highlighting BAL cells as a mainly pure population of AMs, regardless of treatment. The small scattering of cells that would be CD11c$^+$CD11b$^+$ suggests BAL may also contain intermediate AMs. More studies on this are needed to confirm these observations. We further analyzed the baseline expression of
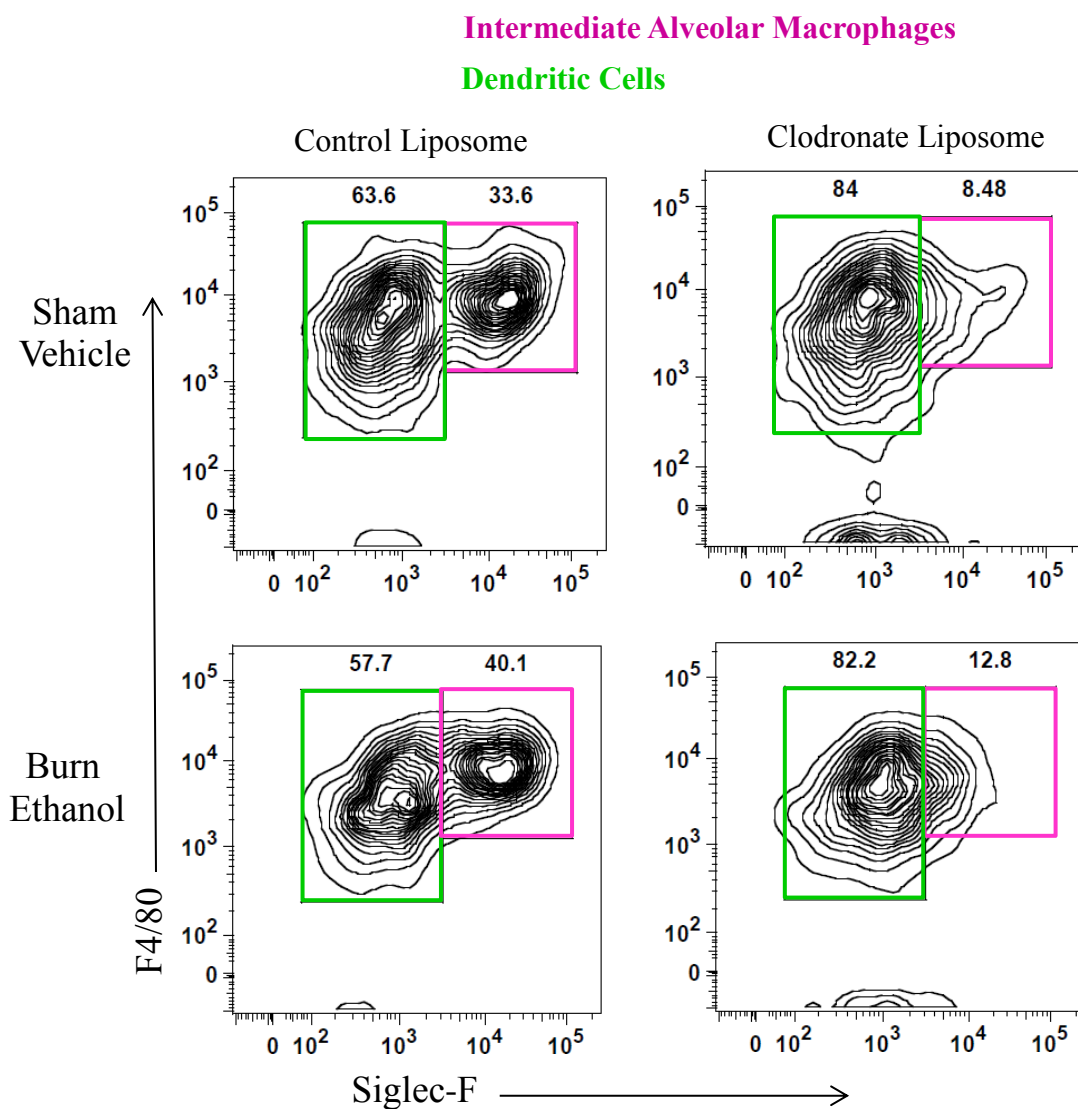
Figure 35. Clodronate liposome depletes CD11b$^+$CD11c$^+$Siglec-F$^+$F4/80^{lo} intermediate AMs. Total lung cells from dissociated lung tissue were analyzed in sham vehicle and burn ethanol mice after empty control and clodronate liposome treatment. Analysis of intermediate AMs (magenta gate) and DCs (green gate) revealed clodronate liposome selectively depleted only CD11b$^+$CD11c$^+$Siglec-F$^+$F4/80^{lo} intermediate AMs, confirming their macrophage lineage.
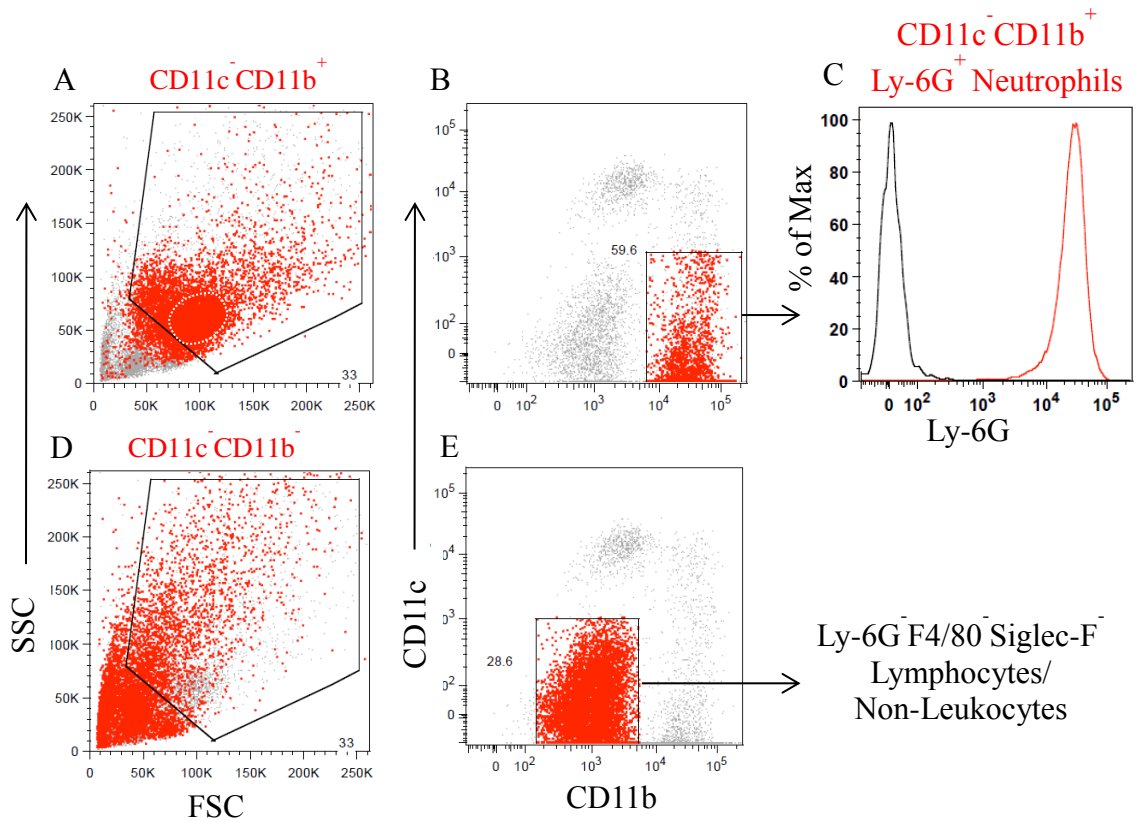
Figure 36. Forward scatter and side scatter characteristics of CD11b$^+$CD11c$^-$ and CD11b$^-$ CD11c$^-$ cells. Data representative of dissociated lung tissue from burn ethanol. A) CD11b$^+$CD11c$^-$ (red) were analyzed for FSC and SSC in total lung cells. White dashed circle indicates infiltrating population after intoxication and injury. B) Gating of CD11c$^-$ CD11b$^+$ cells (red) that were analyzed for FSC versus SSC in A. C) Confirmation of Ly-6G expression on CD11c$^-$CD11b$^+$ cells (red), in comparison to a fluorescent minus one control. This confirmed a neutrophil phenotype. D) CD11b$^-$CD11c$^-$ (red) were analyzed for FSC and SSC in total lung cells. E) Gating of CD11c$^-$CD11b$^-$ cells (red) that were analyzed for FSC versus SSC in D. These small cells are lymphocytes, non-leukocytes, or dead cells.
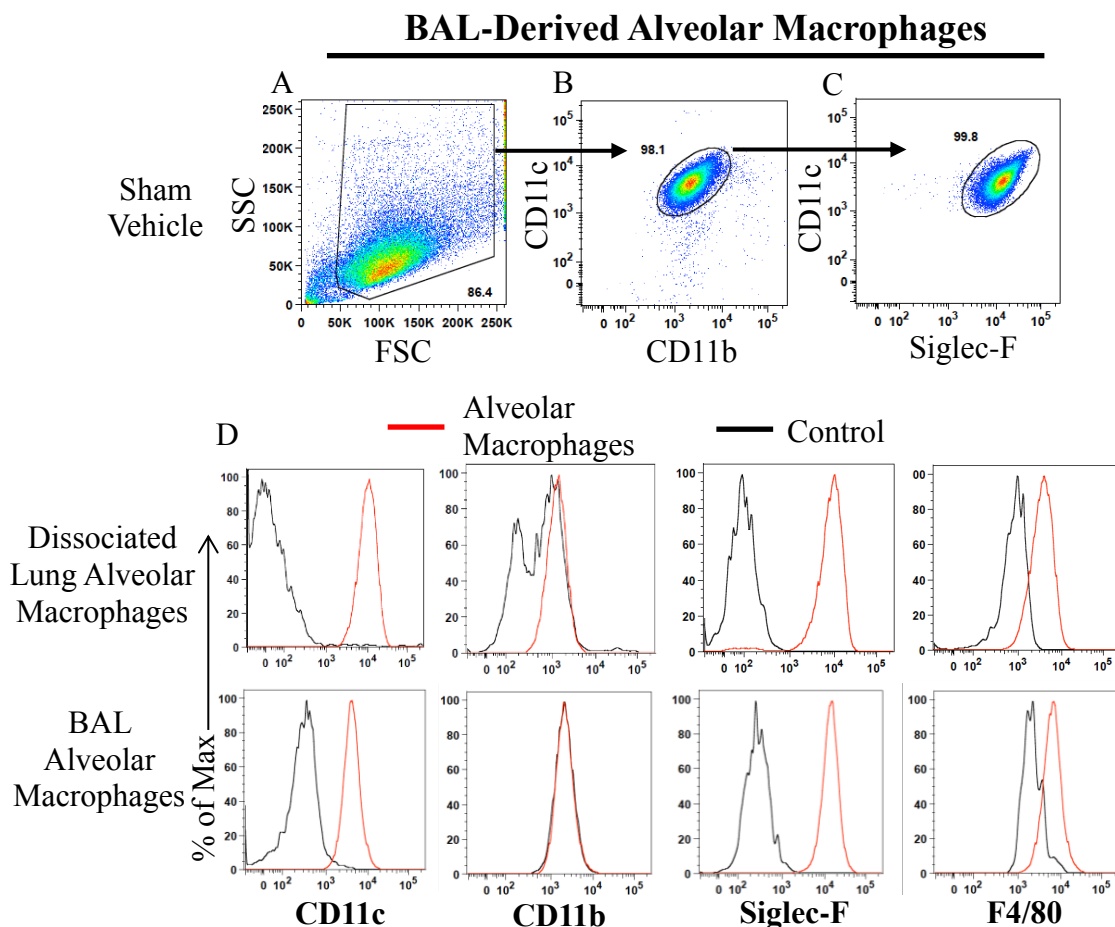
Figure 37. Comparison of AMs from dissociated lung or BAL fluid in sham vehicle. Lungs were either enzymatically dissociated into a single cell suspension or they were lavaged 5x with 1 mL PBS and cells stained for AM markers. A-C) Representative gating of AMs in BAL fluid. Flow profiles were selected for A) total lung cells (polygon gate), then B) CD11c$^+$CD11b$^-$ cells (black gate), then C) Siglec-F$^+$(CD11c$^+$) cells (black gate). D) Histogram display of surface receptor fluorescent intensity on AMs from both dissociated lung and BAL fluid, confirming the CD11c$^+$CD11b$^-$Sigle-F$^+$ F4/80$^+$ AM phenotype (red) in comparison to fluorescent minus one (FMO) controls (black). A FMO is where cells are stained for every antibody except one to determine fluorescence crossover. This is done for each antibody.

M1 markers, MARCO and MHC II, and M2 marker CD206 on both dissociated lung

AMs and BAL AMs from sham mice (Figure 38). There was no change in the expression

of MARCO or MHC II in sham animals and consistent with the literature, AMs

constitutively express CD206 [21, 169]. In summary, the nearly pure population AMs in

the BAL fluid can also be identified in dissociated lung tissue, emphasizing that both of

both BAL and dissociated lung tissue will be useful source for our AM-focused studies.
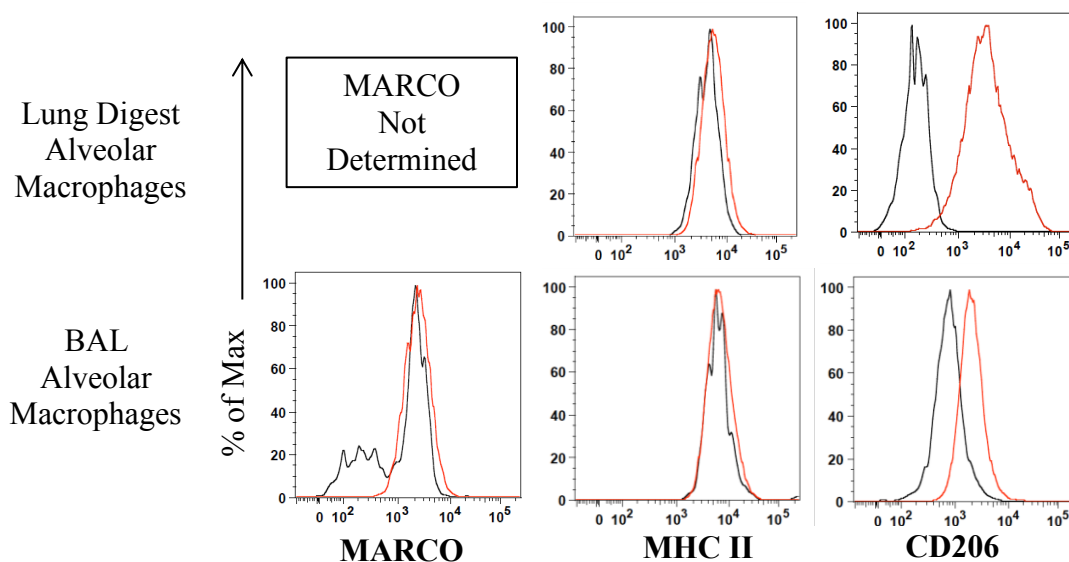
Figure 38. Baseline expression of activation receptors on AMs from dissociated lung and BAL-derived AMs in sham vehicle. Lungs were either enzymatically dissociated into a single cell suspension or they were lavaged 5x with 1 mL PBS and cells stained for AM markers. Histogram display of baseline surface receptor fluorescent intensity on sham vehicle CD11c$^+$CD11b$^-$Sigle-F$^+$ AMs (red) from both dissociated lung and BAL fluid in comparison to fluorescent minus one (FMO) controls (black).

APPENDIX B

DETAILED METHODS DESCRIPTION

APPENDIX B

DETAILED METHODS DESCRIPTION

Intoxication and Burn Injury Protocol

Materials

Hot plate

Water basins

Animal clippers with #40 surgical clip comb

Thermometer

1cc syringes with 27 gauge needle

3cc syringes with 20 gauge oral gavage needle

0.9% normal saline (sterile)

Burn injury template (check for proper size according to weight of mice)

Ketamine

Xylazine

Ethanol

Procedure

1. Fill two water basins with deionized water and heat one until 92-95°C, leaving the other at room temperature.

2. Tail mark and weigh the mice.

3. Gavage mice with 400ul of ethanol mixed in water at the desired dose or water alone. Allow 2-3 minutes between cages so there is time to shave and burn the mice at their scheduled time.

4. Thirty (30) min. after ethanol administration, anesthetize the mice by injecting a mixture of ketamine (100 mg/kg) and xylazine (10 mg/kg) in sterile saline by i.p. injection.

5. As soon as they are asleep (approx. 5 min. after anesthesia injection), thoroughly shave the backs of the mice (Oster animal clippers with #40 comb).

6. One at a time, place animals in appropriate burning template to give a 14-16% total body surface area scald injury according to their weight (see chart in procedure room), and proceed with the burn injury (or sham – dunking mice in room temp water). Make sure the shaved part of the back is "sealed" on the burning template by gently pressing the mouse down into the template.

7. Hold the template containing the animal in the water for 7 seconds. Quickly blot the mouse's back on paper towels. Removing as much hot water as possible from the animal prevents further scalding. Put the mouse back in a clean cage.

8. As soon as possible after the injury, resuscitate each mouse with 1.0 ml of 0.9% sterile saline (i.p.), pre-warmed in 37C water bath, or on warming pads.

9. Keep cages on heating pads for the next 3-4 hours.to help the mice recover from procedure. Mice can be returned to the mouse room once they are walking and fairly alert.

10. Place some food pellets on the bottom of each cage; the mice can't stretch their necks as easily to reach for food after burn injury. Replace water bottles.

Solutions:

Ketamine/Xylazine: Diluted with 0.9% saline, 100 mg/kg ketamine, 10 mg/kg xylazine,

70.0 uL/mouse i.p. (see Ketamine/Xylazine protocol for how to make)

Ethanol:

1) 20% solution is the final concentration, made from the 95% stock ethanol

(marked for use in mice only). Dilute with water from the drinking fountain.

Plethysmography

Materials

Mice

Barometric plethysmography apparatus

Mini screwdriver

1cc syringe with tubing

Timer

Procedure

2) Turn on computer and the 3 Buxco plethysmography machines.

3) Make sure all 4 chambers (1-4) are connected to machine.

4) Under Home, select calibration (wrench symbol) on the Loyola WBP file. Calibrate all 4 chambers according to instructions. Close stop cock (turn to side) at the top of each chamber during calibration. Re-open stop cock when chamber is finished being calibrated. Use mini screw driver to adjust calibration setting and a 1cc syringe attached to tubing to inject air into the chamber. Make sure to re-attach tubing to chamber after syringe is removed.

5) After calibration, select Basline and then Loyola WBP.

6) Enter in animal numbers and place mice into each chamber, making sure chambers are completely closed, stop cock is facing up and all connections are secure.

7) Under Session, select "Acknowledge All Sites".

8) Mice will have 5 min of acclimation, followed by 10 min of data recording. Set timer for 15 min per mouse set.

9) After 15 min, remove mice and put next set of mice into chambers.

10) Under Session, select "Load New Subjects". Enter in animal numbers for new set of mice. Repeat steps 6-8 until all mice are done.

11) When finished recording data, under File select "End Session". Make sure each animal recording is selected and save data.

Lung Tissue Dissociation

Materials

Collagenase D

DNase I

2% BSA/PBS

HBSS, no phenol red

gentleMACS C tubes

70 μm cell strainers

50mL conical tubes

gentleMACS Dissociator

Incubator

Centrifuge

Procedure

1. Modified from Miltenyi Biotec's Lung Dissociation Kit protocol.

2. Prepare to digest lung lobe in 2mg/mL Collagenase D and 0.1mg/mL DNase I.

3. Prepare digestion buffer by dissolving the following into HBSS:

    a. Collagense D: 100mg in 2ml in 15mL (100ul of this into 2.4mL is

       2mg/mL).

    b. DNase I: 10mg in 1ml (25ul of this into 2.4mL is 0.1mg/mL).

4. Remove lungs from mice and place upper left lobe into C tube with 2.4mL HBSS.

   Add in 100ul prepared Collegenase D and 25ul DNase I.

5. Close C tube tightly until you hear a snap and attach it upside down into slot on the gentleMacs Dissociator.

6. Run gentleMACS program m_lung_01. Detach C tube from dissociator.

7. Incubate samples in incubator at 37°C for 20-25 min, manually mixing samples every 5 min.

8. Remove tubes from incubator and use a pipet to gentle break up dissociated tissue until it's a single cell suspension (Do not use program m_lung_02. It is too harsh on cells).

9. Perform brief 15 s centrifugation to collect sample at bottom of the tube.

10. Resuspend sample and filter through a 70 μm cell strainer into a 50mL conical tube. Wash strainer with 2.5mL HBSS.

11. Discard strainer and centrifuge cells for 10 min at 300xg. Remove supernatant.

12. Resuspend in 2% BSA/PBS and count cells.

13. Cells are now ready for flow cytometry analysis.

Bronchoalveolar Lavage

Materials

Cold 1x PBS

60 Tubing

1cc syringe with 20g needle

25g needle

15mL conical tube

50mL conical tube

Procedure

1. Attach tubing to a 20g gauge needle with ¼ inch of tubing extended from needle.

2. Euthanize mouse and expose trachea and lungs. Using a 25g needle, gently pierce the trachea below the first collangenous ring, Insert tubing (that is attached to needle and syringe) into the trachea.

3. Lavage lungs 5 times with .8-.9 ml of cold PBS (keep PBS in 50mL conical tube in ice bucket).

4. Pool all washes per animal into a 15mL conical tube

5. Spin cells 1200 rpm 3min 4° C.

6. Removed supernatant (~5mL) and store at at -80ºC for future cytokine analysis studies.

7. Resuspend in 500ul RBC Lysis Buffer (ACK lysis buffer) and incubate 4 min on ice.

8. Add 5ml PBS to quench reaction and spin cells 1200 rpm 3 min.

9. Resuspend to 400ul in PBS and count cells.

10. Cells are ready for flow cytometry staining, chamber slide incubation or cytocentrifugation onto slides.

Flow Cytometry of Alveolar Macrophages

Materials

Antibodies

FACS Buffer: 1x PBS + 2% BSA

1x PBS

Eppindorf tubes

Plastic FACS tubes

Pipets

Centrifuge

Ice

Refrigerator or cold room

Waste container

Foil

Procedure

1. Obtain and count lung cells or BAL cells.

2. Add $1x10^6$ lung cells or $1x10^5$ BAL cells to eppindorf tubes.

3. Centrifuge at 1200rpm at 4^oC for 5min.

4. Decant supernatant by gently "dumping" it into a waste container.

5. Block unspecific binding to the Fcγ II/III receptor using anti-CD16/32 for 20 min at 4^oC on ice.

6. Without washing cells, directly add in 50ul of primary antibodies diluted in FACS buffer for 30 min at 4°C on ice in the dark. (Titer antibodies to determine appropriate concentrations).

7. Wash 2x with FACS buffer.

8. Transfer cells to FACS tubes and immediately run unfixed cells resuspended in 400ul PBS on the BD Fortessa cytometer OR fix cells with 500ul 1% PFA for 15 min on ice. Wash with PBS and store in refrigerator at 4°C overnight covered in foil and analyze samples the next day.

Controls:

9. Unstained Cells (from both sham vehicle and burn ethanol groups).

10. Fluorescence Minus One Control (FMO): Each fluorochrome needs 1 sample with all fluorochromes, except for that 1 fluorochrome.

Antibodies to characterize alveolar macrophages:

CD11c APC-eFluor 780 (clone N418, eBioscience)

CD11b eFluor 450 (clone M1/70, eBioscience)

F4/80 APC (clone BM8, eBioscience)

Siglec-F PE-CF594 (clone E50-2440, BD Biosciences, San Jose, CA)

CD206 PE (clone C068C2, Biolegend, San Diego, CA)

Ly-6G (Gr-1) PE-Cy7 (clone RB6-8C5, eBioscience)

MHC II BD Horizon V500 (BD Biosciences)

TLR4/MD-2 APC (clone MTS510, eBioscience)

MARCO FITC (Abd Serotec),

CD71 PerCP-eFluor 710 (clone R17217, eBiosciences)

IL-10R PE (clone 1B1.3a, BD Bioscience

Siglec-F Immunofluorescent Staining

1. Section OCT frozen lung tissue at 6μm onto slides.

2. Airdry slides for 1 hour at room temperature.

3. Fix slides 5 min in 4% PFA (15ml 16% PFA + 45ml cold PBS in a coplin jar) in the hood.

4. Wash 3x with 1x cold PBS for 5 min. Pour PBS into coplin jar, then gently put slides in PBS. Pouring PBS over slides in jar can cause delicate tissue to dislodge from slide.

5. Block with superblock for 5 min (no longer or can ruin tissue).

6. 'Dip" rinse slides (dip slides in PBS-don't leave in PBS).

7. In a humidity chamber, incubate sections overnight at 4^oC with rat anti-mouse purified Siglec-F (Clone E50-2440, BD Biosciences) at 10ug/ml diluted in antibody diluent (Immco).

8. Wash 3x with 1x cold PBS for 5 min each.

9. Incubate sections with secondary antibody goat anti-rat Alexa Fluor® 555 anti-rat IgG (H+L) (Life Technologies)1:500 diluted in antibody diluent for 1 h at room temperature.

10. Wash 3x with 1x cold PBS for 5 min each.

11. Air slides dry and mount with prolonged dapi gold (Life Technologies).

Active-Caspase 3 Staining

Materials

Humidity chamber

Coplin jars

1x PBS

Fixation : 4% Paraformaldehyde (PFA) in 1x PBS

Permeabilization: 0.1% Triton X-100 in 2% BSA/PBS

Blocking Reagent: 10% normal donkey serum + 0.1% Triton-100x

Antibody diluent: 2% BSA/PBS

Prolong Gold Dapi mounting medium

Procedure

1. Isolate BAL cells. Centrifuge 300g for 3 minutes. Lyse RBCs with ACK lysis buffer for 4 mins on ice. Wash cells. Resuspend each pellet in 300ul media and count by putting 10ul directly onto hemocytometer. After counting, measure exactly how much media each sample was resuspended in.

2. BAL cells were cytocentrifuged (50,000 cells/200ul PBS or complete medium) onto slides at 400RPM for 5 min.

3. Fix slides 5 min in 4% PFA (made in cold PBS) in coplin jars in <u>the hood</u>.

4. Wash 3x with 1x cold PBS for 5 min.

5. In humidity chamber, permiabilize with 0.1% Triton-100x in 2% BSA/PBS for 30 min at room temperature.

6. Wash 3x with 1x cold PBS for 5 min.

7. Block with 10% normal donkey serum (NDS) + 0.1% Triton-100x for 20 minutes at room temperature. Tap off serum.

8. Incubate slides overnight at 4°C with rabbit anti-active-caspase 3 (Abcam) at 10ug/ml diluted in 2% BSA/PBS.

9. Wash 3x with 1x cold PBS for 5 min each.

10. Incubate sections with secondary antibody donkey anti-rabbit 594 (Life Technologies) diluted in 2%BSA/PBS for 45 min at room temperature.

11. Wash 3x with 1x cold PBS for 5 min each.

12. Air slides dry and mount with prolonged dapi gold (Life Technologies).

ImageJ Analysis of Lung Tissue Histology

Materials

Lung H&E slides

Microscope with camera

ImageJ program

Procedure

1. Save 10 high power images per animal as jpeg files in a separate folder for each animal.

2. Import folder as an "Image Sequence" in the ImageJ program.

3. Convert to 8-bit and adjust contrast and threshold if necessary. Must apply the same settings to all sets of images.

4. Convert to binary.

5. Set measurements to be captured with threshold as area fraction.

6. Select "measure" and record.

ImageJ Analysis of TUNEL$^+$ Cells

Materials

Lung slides stained with TUNEL

Microscope with camera

ImageJ program

Procedure

7. Save 10 high power images per animal as jpeg files in a separate folder for each animal.

8. Import folder as an "Image Sequence" in the ImageJ program.

9. Convert to 8-bit and adjust contrast and threshold if necessary. Must apply the same settings to all sets of images.

10. Convert to binary.

11. Set measurements to be captured with threshold as area fraction.

12. Select analyze and "analyze particles" and set measurements to be captured:

   a. Size 5-infinity

   b. Circularity 0-100

13. Generate results and save data cell counts of TUNEL$^+$ cells.

Clodronate Depletion of Alveolar Macrophages

Materials

Clodronate liposome

Control liposome

1cc syringe with 30g needle

50 Tubing

200ul pipet

Ketamine

Xylazine

Board and rubber band

Procedure

1. Bring clodronate and control liposomes (Encapsula NanoSciences, Brentwood, TN) to room temperature. Gently mix vial contents (do not vortex).

2. Weigh and tail mark mice.

3. Anesthetized mice with100 mg/kg ketamine and 10 mg/kg xylazine.

4. Mice were suspended

5. Using a 200ul pipet, take 75ul of liposomes and pipet it into a 1cc syringe. Attached needle with tubing to syringe and intratracheally administer liposomes.

Mesenchymal Stem Cells Tail Vein Injection

Materials

Wooden box with small hole in the side

27 gauge needle with syringe

Heating Pad

Ethanol (70% v/v)

PBS

MSCs ($1x10^5$/200ul pre-warmed PBS)

Procedure

1. Place animal cage on warming pad.

2. Bend needle to a 120° angle with the syringe.

3. Place mouse under Styrofoam housing, pulling tail through the side hole.

4. Wet the tail with ethanol and rub proximal portion of the tail until a lateral tail vein is visible.

5. Insert needle into lateral vein and slowly inject MSCs or saline control.

REFERENCES

1. Treuting, P.M.a.D., S.M., *Comparative Anatomy and Histology: A Mouse and Human Atlas*. 2011: Academic Press.

2. Burns, A.R., C.W. Smith, and D.C. Walker, *Unique structural features that influence neutrophil emigration into the lung.* Physiol Rev, 2003. **83**(2): p. 309-36.

3. Kopf, M., C. Schneider, and S.P. Nobs, *The development and function of lung-resident macrophages and dendritic cells.* Nat Immunol, 2015. **16**(1): p. 36-44.

4. Knust, J., M. Ochs, H.J. Gundersen, and J.R. Nyengaard, *Stereological estimates of alveolar number and size and capillary length and surface area in mice lungs.* Anat Rec (Hoboken), 2009. **292**(1): p. 113-22.

5. Fels, A.O. and Z.A. Cohn, *The alveolar macrophage.* J Appl Physiol (1985), 1986. **60**(2): p. 353-69.

6. Bowden, D.H., *The alveolar macrophage.* Environ Health Perspect, 1984. **55**: p. 327-41.

7. van oud Alblas, A.B. and R. van Furth, *Origin, Kinetics, and characteristics of pulmonary macrophages in the normal steady state.* J Exp Med, 1979. **149**(6): p. 1504-18.

8. Karavitis, J., E.L. Murdoch, C. Deburghgraeve, L. Ramirez, and E.J. Kovacs, *Ethanol suppresses phagosomal adhesion maturation, Rac activation, and subsequent actin polymerization during FcgammaR-mediated phagocytosis.* Cell Immunol, 2012. **274**(1-2): p. 61-71.

9. Ely, K.H., T. Cookenham, A.D. Roberts, and D.L. Woodland, *Memory T cell populations in the lung airways are maintained by continual recruitment.* J Immunol, 2006. **176**(1): p. 537-43.

10. Westphalen, K., G.A. Gusarova, M.N. Islam, M. Subramanian, T.S. Cohen, A.S. Prince, and J. Bhattacharya, *Sessile alveolar macrophages communicate with alveolar epithelium to modulate immunity.* Nature, 2014. **506**(7489): p. 503-6.

11. Guilliams, M., I. De Kleer, S. Henri, S. Post, L. Vanhoutte, S. De Prijck, K. Deswarte, B. Malissen, H. Hammad, and B.N. Lambrecht, *Alveolar macrophages develop from fetal monocytes that differentiate into long-lived cells in the first week of life via GM-CSF.* J Exp Med, 2013. **210**(10): p. 1977-92.

12. Murphy, J., R. Summer, A.A. Wilson, D.N. Kotton, and A. Fine, *The prolonged life-span of alveolar macrophages.* Am J Respir Cell Mol Biol, 2008. **38**(4): p. 380-5.

13. Tarling, J.D., H.S. Lin, and S. Hsu, *Self-renewal of pulmonary alveolar macrophages: evidence from radiation chimera studies.* J Leukoc Biol, 1987. **42**(5): p. 443-6.

14. Landsman, L. and S. Jung, *Lung macrophages serve as obligatory intermediate between blood monocytes and alveolar macrophages.* J Immunol, 2007. **179**(6): p. 3488-94.

15. Hashimoto, D., A. Chow, C. Noizat, P. Teo, M.B. Beasley, M. Leboeuf, C.D. Becker, P. See, J. Price, D. Lucas, M. Greter, A. Mortha, S.W. Boyer, E.C. Forsberg, M. Tanaka, N. van Rooijen, A. Garcia-Sastre, E.R. Stanley, F. Ginhoux, P.S. Frenette, and M. Merad, *Tissue-resident macrophages self-maintain locally throughout adult life with minimal contribution from circulating monocytes.* Immunity, 2013. **38**(4): p. 792-804.

16. Maus, U.A., S. Janzen, G. Wall, M. Srivastava, T.S. Blackwell, J.W. Christman, W. Seeger, T. Welte, and J. Lohmeyer, *Resident alveolar macrophages are replaced by recruited monocytes in response to endotoxin-induced lung inflammation.* Am J Respir Cell Mol Biol, 2006. **35**(2): p. 227-35.

17. Metchnikoff, E., *Leçons Sur La Pathologie Comparée De L' inflammation.* Paris: Masson, 1892.

18. Myrvik, Q., E.S. Leake, and B. Fariss, *Studies on pulmonary alveolar macrophages from the normal rabbit: a technique to procure them in a high state of purity.* J Immunol, 1961. **86**: p. 128-32.

19. Hussell, T. and T.J. Bell, *Alveolar macrophages: plasticity in a tissue-specific context.* Nat Rev Immunol, 2014. **14**(2): p. 81-93.

20. Guth, A.M., W.J. Janssen, C.M. Bosio, E.C. Crouch, P.M. Henson, and S.W. Dow, *Lung environment determines unique phenotype of alveolar macrophages.* Am J Physiol Lung Cell Mol Physiol, 2009. **296**(6): p. L936-46.

21. Misharin, A.V., L. Morales-Nebreda, G.M. Mutlu, G.R. Budinger, and H. Perlman, *Flow cytometric analysis of macrophages and dendritic cell subsets in the mouse lung.* Am J Respir Cell Mol Biol, 2013. **49**(4): p. 503-10.

22. Zaynagetdinov, R., T.P. Sherrill, P.L. Kendall, B.H. Segal, K.P. Weller, R.M. Tighe, and T.S. Blackwell, *Identification of myeloid cell subsets in murine lungs using flow cytometry.* Am J Respir Cell Mol Biol, 2013. **49**(2): p. 180-9.

23. Wright, J.R., *Immunoregulatory functions of surfactant proteins.* Nat Rev Immunol, 2005. **5**(1): p. 58-68.

24. Janssen, W.J., K.A. McPhillips, M.G. Dickinson, D.J. Linderman, K. Morimoto, Y.Q. Xiao, K.M. Oldham, R.W. Vandivier, P.M. Henson, and S.J. Gardai, *Surfactant proteins A and D suppress alveolar macrophage phagocytosis via interaction with SIRP alpha.* Am J Respir Crit Care Med, 2008. **178**(2): p. 158-67.

25. Gardai, S.J., Y.Q. Xiao, M. Dickinson, J.A. Nick, D.R. Voelker, K.E. Greene, and P.M. Henson, *By binding SIRPalpha or calreticulin/CD91, lung collectins act as dual function surveillance molecules to suppress or enhance inflammation.* Cell, 2003. **115**(1): p. 13-23.

26. Chitu, V. and E.R. Stanley, *Colony-stimulating factor-1 in immunity and inflammation.* Curr Opin Immunol, 2006. **18**(1): p. 39-48.

27. Sallusto, F., M. Cella, C. Danieli, and A. Lanzavecchia, *Dendritic cells use macropinocytosis and the mannose receptor to concentrate macromolecules in the major histocompatibility complex class II compartment: downregulation by cytokines and bacterial products.* J Exp Med, 1995. **182**(2): p. 389-400.

28. Brinker, K.G., E. Martin, P. Borron, E. Mostaghel, C. Doyle, C.V. Harding, and J.R. Wright, *Surfactant protein D enhances bacterial antigen presentation by bone marrow-derived dendritic cells.* Am J Physiol Lung Cell Mol Physiol, 2001. **281**(6): p. L1453-63.

29. Jones, C.V., T.M. Williams, K.A. Walker, H. Dickinson, S. Sakkal, B.A. Rumballe, M.H. Little, G. Jenkin, and S.D. Ricardo, *M2 macrophage polarisation is associated with alveolar formation during postnatal lung development.* Respir Res, 2013. **14**: p. 41.

30. Charlson, E.S., K. Bittinger, A.R. Haas, A.S. Fitzgerald, I. Frank, A. Yadav, F.D. Bushman, and R.G. Collman, *Topographical continuity of bacterial populations in the healthy human respiratory tract.* Am J Respir Crit Care Med, 2011. **184**(8): p. 957-63.

31. Zhang, J., S.D. Tachado, N. Patel, J. Zhu, A. Imrich, P. Manfruelli, M. Cushion, T.B. Kinane, and H. Koziel, *Negative regulatory role of mannose receptors on human alveolar macrophage proinflammatory cytokine release in vitro.* J Leukoc Biol, 2005. **78**(3): p. 665-74.

32. Palecanda, A., J. Paulauskis, E. Al-Mutairi, A. Imrich, G. Qin, H. Suzuki, T. Kodama, K. Tryggvason, H. Koziel, and L. Kobzik, *Role of the scavenger receptor MARCO in alveolar macrophage binding of unopsonized environmental particles.* J Exp Med, 1999. **189**(9): p. 1497-506.

33. Curtale, G., M. Mirolo, T.A. Renzi, M. Rossato, F. Bazzoni, and M. Locati, *Negative regulation of Toll-like receptor 4 signaling by IL-10-dependent microRNA-146b.* Proc Natl Acad Sci U S A, 2013. **110**(28): p. 11499-504.

34. Murray, P.J., J.E. Allen, S.K. Biswas, E.A. Fisher, D.W. Gilroy, S. Goerdt, S. Gordon, J.A. Hamilton, L.B. Ivashkiv, T. Lawrence, M. Locati, A. Mantovani, F.O. Martinez, J.L. Mege, D.M. Mosser, G. Natoli, J.P. Saeij, J.L. Schultze, K.A. Shirey, A. Sica, J. Suttles, I. Udalova, J.A. van Ginderachter, S.N. Vogel, and T.A. Wynn, *Macrophage activation and polarization: nomenclature and experimental guidelines.* Immunity, 2014. **41**(1): p. 14-20.

35. Sica, A. and A. Mantovani, *Macrophage plasticity and polarization: in vivo veritas.* J Clin Invest, 2012. **122**(3): p. 787-95.

36. Kelley, J., *Cytokines of the lung.* Am Rev Respir Dis, 1990. **141**(3): p. 765-88.

37. Monton, C. and A. Torres, *Lung inflammatory response in pneumonia.* Monaldi Arch Chest Dis, 1998. **53**(1): p. 56-63.

38. Cakarova, L., L.M. Marsh, J. Wilhelm, K. Mayer, F. Grimminger, W. Seeger, J. Lohmeyer, and S. Herold, *Macrophage tumor necrosis factor-alpha induces epithelial expression of granulocyte-macrophage colony-stimulating factor: impact on alveolar epithelial repair.* Am J Respir Crit Care Med, 2009. **180**(6): p. 521-32.

39. Herold, S., W. von Wulffen, M. Steinmueller, S. Pleschka, W.A. Kuziel, M. Mack, M. Srivastava, W. Seeger, U.A. Maus, and J. Lohmeyer, *Alveolar epithelial cells direct monocyte transepithelial migration upon influenza virus infection: impact of chemokines and adhesion molecules.* J Immunol, 2006. **177**(3): p. 1817-24.

40. Marriott, H.M., K.A. Gascoyne, R. Gowda, I. Geary, M.J. Nicklin, F. Iannelli, G. Pozzi, T.J. Mitchell, M.K. Whyte, I. Sabroe, and D.H. Dockrell, *Interleukin-1beta*

regulates CXCL8 release and influences disease outcome in response to Streptococcus pneumoniae, defining intercellular cooperation between pulmonary epithelial cells and macrophages. Infect Immun, 2012. **80**(3): p. 1140-9.

41.   Sindrilaru, A., T. Peters, S. Wieschalka, C. Baican, A. Baican, H. Peter, A. Hainzl, S. Schatz, Y. Qi, A. Schlecht, J.M. Weiss, M. Wlaschek, C. Sunderkotter, and K. Scharffetter-Kochanek, *An unrestrained proinflammatory M1 macrophage population induced by iron impairs wound healing in humans and mice.* J Clin Invest, 2011. **121**(3): p. 985-97.

42.   Korns, D., S.C. Frasch, R. Fernandez-Boyanapalli, P.M. Henson, and D.L. Bratton, *Modulation of macrophage efferocytosis in inflammation.* Front Immunol, 2011. **2**: p. 57.

43.   Voll, R.E., M. Herrmann, E.A. Roth, C. Stach, J.R. Kalden, and I. Girkontaite, *Immunosuppressive effects of apoptotic cells.* Nature, 1997. **390**(6658): p. 350-1.

44.   Kim, S., K.B. Elkon, and X. Ma, *Transcriptional suppression of interleukin-12 gene expression following phagocytosis of apoptotic cells.* Immunity, 2004. **21**(5): p. 643-53.

45.   Ariel, A. and C.N. Serhan, *New Lives Given by Cell Death: Macrophage Differentiation Following Their Encounter with Apoptotic Leukocytes during the Resolution of Inflammation.* Front Immunol, 2012. **3**: p. 4.

46.   Freire-de-Lima, C.G., Y.Q. Xiao, S.J. Gardai, D.L. Bratton, W.P. Schiemann, and P.M. Henson, *Apoptotic cells, through transforming growth factor-beta, coordinately induce anti-inflammatory and suppress pro-inflammatory eicosanoid and NO synthesis in murine macrophages.* J Biol Chem, 2006. **281**(50): p. 38376-84.

47.   Morimoto, K., H. Amano, F. Sonoda, M. Baba, M. Senba, H. Yoshimine, H. Yamamoto, T. Ii, K. Oishi, and T. Nagatake, *Alveolar macrophages that phagocytose apoptotic neutrophils produce hepatocyte growth factor during bacterial pneumonia in mice.* Am J Respir Cell Mol Biol, 2001. **24**(5): p. 608-15.

48.   Granata, F., A. Frattini, S. Loffredo, R.I. Staiano, A. Petraroli, D. Ribatti, R. Oslund, M.H. Gelb, G. Lambeau, G. Marone, and M. Triggiani, *Production of vascular endothelial growth factors from human lung macrophages induced by group IIA and group X secreted phospholipases A2.* J Immunol, 2010. **184**(9): p. 5232-41.

49.	Brecht, K., A. Weigert, J. Hu, R. Popp, B. Fisslthaler, T. Korff, I. Fleming, G. Geisslinger, and B. Brune, *Macrophages programmed by apoptotic cells promote angiogenesis via prostaglandin E2.* FASEB J, 2011. **25**(7): p. 2408-17.

50.	Kirby, A.C., M.C. Coles, and P.M. Kaye, *Alveolar macrophages transport pathogens to lung draining lymph nodes.* J Immunol, 2009. **183**(3): p. 1983-9.

51.	Janssen, W.J., L. Barthel, A. Muldrow, R.E. Oberley-Deegan, M.T. Kearns, C. Jakubzick, and P.M. Henson, *Fas determines differential fates of resident and recruited macrophages during resolution of acute lung injury.* Am J Respir Crit Care Med, 2011. **184**(5): p. 547-60.

52.	Medeiros, A.I., C.H. Serezani, S.P. Lee, and M. Peters-Golden, *Efferocytosis impairs pulmonary macrophage and lung antibacterial function via PGE2/EP2 signaling.* J Exp Med, 2009. **206**(1): p. 61-8.

53.	McGovern, P.E., A. Mirzoian, and G.R. Hall, *Ancient Egyptian herbal wines.* Proc Natl Acad Sci U S A, 2009. **106**(18): p. 7361-6.

54.	Legras, J.L., D. Merdinoglu, J.M. Cornuet, and F. Karst, *Bread, beer and wine: Saccharomyces cerevisiae diversity reflects human history.* Mol Ecol, 2007. **16**(10): p. 2091-102.

55.	McGovern, P.E., J. Zhang, J. Tang, Z. Zhang, G.R. Hall, R.A. Moreau, A. Nunez, E.D. Butrym, M.P. Richards, C.S. Wang, G. Cheng, Z. Zhao, and C. Wang, *Fermented beverages of pre- and proto-historic China.* Proc Natl Acad Sci U S A, 2004. **101**(51): p. 17593-8.

56.	McGovern, P.E., *The beginnings of wine making and viniculture in the ancient Near East and Egypt.* Expedition, 1997. **39**: p. 3-21.

57.	Cavalieri, D., P.E. McGovern, D.L. Hartl, R. Mortimer, and M. Polsinelli, *Evidence for S. cerevisiae fermentation in ancient wine.* J Mol Evol, 2003. **57 Suppl 1**: p. S226-32.

58.	Jernigan, D.H., *Applying commodity chain analysis to changing modes of alcohol supply in a developing country.* Addiction, 2000. **95 Suppl 4**: p. S465-75.

59.	Howland, J. and R. Hingson, *Alcohol as a risk factor for injuries or death due to fires and burns: review of the literature.* Public Health Rep, 1987. **102**(5): p. 475-83.

60.   Dufour, M.C., *What is moderate drinking? Defining "drinks" and drinking levels.* Alcohol Res Health, 1999. **23**(1): p. 5-14.

61.   Naimi, T.S., R.D. Brewer, A. Mokdad, C. Denny, M.K. Serdula, and J.S. Marks, *Binge drinking among US adults.* JAMA, 2003. **289**(1): p. 70-5.

62.   NIAAA, *NIAAA council approves definition of binge drinking.* NIAAA Newletter 2004.

63.   Mokdad, A.H., J.S. Marks, D.F. Stroup, and J.L. Gerberding, *Correction: actual causes of death in the United States, 2000.* JAMA, 2005. **293**(3): p. 293-4.

64.   Stahre, M., J. Roeber, D. Kanny, R.D. Brewer, and X. Zhang, *Contribution of excessive alcohol consumption to deaths and years of potential life lost in the United States.* Prev Chronic Dis, 2014. **11**: p. E109.

65.   Organization, W.H., *Global status report on alcohol and health* 2014.

66.   Savola, O., O. Niemela, and M. Hillbom, *Alcohol intake and the pattern of trauma in young adults and working aged people admitted after trauma.* Alcohol Alcohol, 2005. **40**(4): p. 269-73.

67.   Szabo, G. and P. Mandrekar, *A recent perspective on alcohol, immunity, and host defense.* Alcohol Clin Exp Res, 2009. **33**(2): p. 220-32.

68.   Winkler, C., B. Wirleitner, K. Schroecksnadel, H. Schennach, and D. Fuchs, *Beer down-regulates activated peripheral blood mononuclear cells in vitro.* Int Immunopharmacol, 2006. **6**(3): p. 390-5.

69.   Mandrekar, P., D. Catalano, B. White, and G. Szabo, *Moderate alcohol intake in humans attenuates monocyte inflammatory responses: inhibition of nuclear regulatory factor kappa B and induction of interleukin 10.* Alcohol Clin Exp Res, 2006. **30**(1): p. 135-9.

70.   Patra, M., E. Salonen, E. Terama, I. Vattulainen, R. Faller, B.W. Lee, J. Holopainen, and M. Karttunen, *Under the influence of alcohol: the effect of ethanol and methanol on lipid bilayers.* Biophys J, 2006. **90**(4): p. 1121-35.

71.   Ingolfsson, H.I. and O.S. Andersen, *Alcohol's effects on lipid bilayer properties.* Biophys J, 2011. **101**(4): p. 847-55.

72.   Dolganiuc, A., G. Bakis, K. Kodys, P. Mandrekar, and G. Szabo, *Acute ethanol treatment modulates Toll-like receptor-4 association with lipid rafts.* Alcohol Clin Exp Res, 2006. **30**(1): p. 76-85.

73.   Szabo, G., D. Catalano, B. White, and P. Mandrekar, *Acute alcohol consumption inhibits accessory cell function of monocytes and dendritic cells.* Alcohol Clin Exp Res, 2004. **28**(5): p. 824-8.

74.   Mandrekar, P., D. Catalano, A. Dolganiuc, K. Kodys, and G. Szabo, *Inhibition of myeloid dendritic cell accessory cell function and induction of T cell anergy by alcohol correlates with decreased IL-12 production.* J Immunol, 2004. **173**(5): p. 3398-407.

75.   Goral, J., M.A. Choudhry, and E.J. Kovacs, *Acute ethanol exposure inhibits macrophage IL-6 production: role of p38 and ERK1/2 MAPK.* J Leukoc Biol, 2004. **75**(3): p. 553-9.

76.   Karavitis, J., E.L. Murdoch, C.R. Gomez, L. Ramirez, and E.J. Kovacs, *Acute ethanol exposure attenuates pattern recognition receptor activated macrophage functions.* J Interferon Cytokine Res, 2008. **28**(7): p. 413-22.

77.   Boe, D.M., R.W. Vandivier, E.L. Burnham, and M. Moss, *Alcohol abuse and pulmonary disease.* J Leukoc Biol, 2009. **86**(5): p. 1097-104.

78.   Brown, L.A., F.L. Harris, X.D. Ping, and T.W. Gauthier, *Chronic ethanol ingestion and the risk of acute lung injury: a role for glutathione availability?* Alcohol, 2004. **33**(3): p. 191-7.

79.   Nelson, S., G. Bagby, and W.R. Summer, *Alcohol suppresses lipopolysaccharide-induced tumor necrosis factor activity in serum and lung.* Life Sci, 1989. **44**(10): p. 673-6.

80.   Moss, M., B. Bucher, F.A. Moore, E.E. Moore, and P.E. Parsons, *The role of chronic alcohol abuse in the development of acute respiratory distress syndrome in adults.* JAMA, 1996. **275**(1): p. 50-4.

81.   Boe, D.M., T.R. Richens, S.A. Horstmann, E.L. Burnham, W.J. Janssen, P.M. Henson, M. Moss, and R.W. Vandivier, *Acute and chronic alcohol exposure impair the phagocytosis of apoptotic cells and enhance the pulmonary inflammatory response.* Alcohol Clin Exp Res, 2010. **34**(10): p. 1723-32.

82.   ABA, *American Burn Association National Burn Repository: 2014 Report. Chicago, IL.* 2014.

83. Liffner, G., Z. Bak, A. Reske, and F. Sjoberg, *Inhalation injury assessed by score does not contribute to the development of acute respiratory distress syndrome in burn victims.* Burns, 2005. **31**(3): p. 263-8.

84. Turnage, R.H., F. Nwariaku, J. Murphy, C. Schulman, K. Wright, and H. Yin, *Mechanisms of pulmonary microvascular dysfunction during severe burn injury.* World J Surg, 2002. **26**(7): p. 848-53.

85. Phillips, A.W. and O. Cope, *Burn therapy. II. The revelation of respiratory tract damage as a principal killer of the burned patient.* Ann Surg, 1962. **155**: p. 1-19.

86. Achauer, B.M., P.A. Allyn, D.W. Furnas, and R.H. Bartlett, *Pulmonary complications of burns: the major threat to the burn patient.* Ann Surg, 1973. **177**(3): p. 311-9.

87. Brezel, B.S., J.M. Kassenbrock, and J.M. Stein, *Burns in substance abusers and in neurologically and mentally impaired patients.* J Burn Care Rehabil, 1988. **9**(2): p. 169-71.

88. Grobmyer, S.R., S.P. Maniscalco, G.F. Purdue, and J.L. Hunt, *Alcohol, drug intoxication, or both at the time of burn injury as a predictor of complications and mortality in hospitalized patients with burns.* J Burn Care Rehabil, 1996. **17**(6 Pt 1): p. 532-9.

89. Silver, G.M., J.M. Albright, C.R. Schermer, M. Halerz, P. Conrad, P.D. Ackerman, L. Lau, M.A. Emanuele, E.J. Kovacs, and R.L. Gamelli, *Adverse clinical outcomes associated with elevated blood alcohol levels at the time of burn injury.* J Burn Care Res, 2008. **29**(5): p. 784-9.

90. Ciesla, D.J., E.E. Moore, J.L. Johnson, J.M. Burch, C.C. Cothren, and A. Sauaia, *The role of the lung in postinjury multiple organ failure.* Surgery, 2005. **138**(4): p. 749-57; discussion 757-8.

91. Hollingsed, T.C., J.R. Saffle, R.G. Barton, W.B. Craft, and S.E. Morris, *Etiology and consequences of respiratory failure in thermally injured patients.* Am J Surg, 1993. **166**(6): p. 592-6; discussion 596-7.

92. Davis, C.S., T.J. Esposito, A.G. Palladino-Davis, K. Rychlik, C.R. Schermer, R.L. Gamelli, and E.J. Kovacs, *Implications of alcohol intoxication at the time of burn and smoke inhalation injury: an epidemiologic and clinical analysis.* J Burn Care Res, 2013. **34**(1): p. 120-6.

93.   Baron, P., L.D. Traber, D.L. Traber, T. Nguyen, M. Hollyoak, J.P. Heggers, and D.N. Herndon, *Gut failure and translocation following burn and sepsis.* J Surg Res, 1994. **57**(1): p. 197-204.

94.   Deitch, E.A., *The role of intestinal barrier failure and bacterial translocation in the development of systemic infection and multiple organ failure.* Arch Surg, 1990. **125**(3): p. 403-4.

95.   Choudhry, M.A., S.N. Rana, M.J. Kavanaugh, E.J. Kovacs, R.L. Gamelli, and M.M. Sayeed, *Impaired intestinal immunity and barrier function: a cause for enhanced bacterial translocation in alcohol intoxication and burn injury.* Alcohol, 2004. **33**(3): p. 199-208.

96.   Kavanaugh, M.J., C. Clark, M. Goto, E.J. Kovacs, R.L. Gamelli, M.M. Sayeed, and M.A. Choudhry, *Effect of acute alcohol ingestion prior to burn injury on intestinal bacterial growth and barrier function.* Burns, 2005. **31**(3): p. 290-6.

97.   Zahs, A., M.D. Bird, L. Ramirez, M.A. Choudhry, and E.J. Kovacs, *Anti-IL-6 antibody treatment but not IL-6 knockout improves intestinal barrier function and reduces inflammation after binge ethanol exposure and burn injury.* Shock, 2013. **39**(4): p. 373-9.

98.   Zahs, A., M.D. Bird, L. Ramirez, J.R. Turner, M.A. Choudhry, and E.J. Kovacs, *Inhibition of long myosin light-chain kinase activation alleviates intestinal damage after binge ethanol exposure and burn injury.* Am J Physiol Gastrointest Liver Physiol, 2012. **303**(6): p. G705-12.

99.   Chen, M.M., A. Zahs, M.M. Brown, L. Ramirez, J.R. Turner, M.A. Choudhry, and E.J. Kovacs, *An alteration of the gut-liver axis drives pulmonary inflammation after intoxication and burn injury in mice.* Am J Physiol Gastrointest Liver Physiol, 2014. **307**(7): p. G711-8.

100.   Emanuele, N.V., M.A. Emanuele, M.O. Morgan, D. Sulo, S. Yong, E.J. Kovacs, R.D. Himes, and J.J. Callaci, *Ethanol potentiates the acute fatty infiltration of liver caused by burn injury: prevention by insulin treatment.* J Burn Care Res, 2009. **30**(3): p. 482-8.

101.   Meduri, G.U., S. Headley, G. Kohler, F. Stentz, E. Tolley, R. Umberger, and K. Leeper, *Persistent elevation of inflammatory cytokines predicts a poor outcome in ARDS. Plasma IL-1 beta and IL-6 levels are consistent and efficient predictors of outcome over time.* Chest, 1995. **107**(4): p. 1062-73.

102. Dancey, D.R., J. Hayes, M. Gomez, D. Schouten, J. Fish, W. Peters, A.S. Slutsky, and T.E. Stewart, *ARDS in patients with thermal injury.* Intensive Care Med, 1999. **25**(11): p. 1231-6.

103. Steinvall, I., Z. Bak, and F. Sjoberg, *Acute respiratory distress syndrome is as important as inhalation injury for the development of respiratory dysfunction in major burns.* Burns, 2008. **34**(4): p. 441-51.

104. Patel, P.J., D.E. Faunce, M.S. Gregory, L.A. Duffner, and E.J. Kovacs, *Elevation in pulmonary neutrophils and prolonged production of pulmonary macrophage inflammatory protein-2 after burn injury with prior alcohol exposure.* Am J Respir Cell Mol Biol, 1999. **20**(6): p. 1229-37.

105. Bird, M.D., M.O. Morgan, L. Ramirez, S. Yong, and E.J. Kovacs, *Decreased pulmonary inflammation after ethanol exposure and burn injury in intercellular adhesion molecule-1 knockout mice.* J Burn Care Res, 2010. **31**(4): p. 652-60.

106. Bird, M.D., A. Zahs, C. Deburghgraeve, L. Ramirez, M.A. Choudhry, and E.J. Kovacs, *Decreased pulmonary inflammation following ethanol and burn injury in mice deficient in TLR4 but not TLR2 signaling.* Alcohol Clin Exp Res, 2010. **34**(10): p. 1733-41.

107. Chen, M.M., M.D. Bird, A. Zahs, C. Deburghgraeve, B. Posnik, C.S. Davis, and E.J. Kovacs, *Pulmonary inflammation after ethanol exposure and burn injury is attenuated in the absence of IL-6.* Alcohol, 2013. **47**(3): p. 223-9.

108. Dobke, M.K., J. Simoni, J.L. Ninnemann, J. Garrett, and T.J. Harnar, *Endotoxemia after burn injury: effect of early excision on circulating endotoxin levels.* J Burn Care Rehabil, 1989. **10**(2): p. 107-11.

109. Yao, Y.M., Z.Y. Sheng, H.M. Tian, Y. Yu, Y.P. Wang, H.M. Yang, Z.R. Guo, and W.Y. Gao, *The association of circulating endotoxaemia with the development of multiple organ failure in burned patients.* Burns, 1995. **21**(4): p. 255-8.

110. Bardales, R.H., S.S. Xie, R.F. Schaefer, and S.M. Hsu, *Apoptosis is a major pathway responsible for the resolution of type II pneumocytes in acute lung injury.* Am J Pathol, 1996. **149**(3): p. 845-52.

111. Guinee, D., Jr., E. Brambilla, M. Fleming, T. Hayashi, M. Rahn, M. Koss, V. Ferrans, and W. Travis, *The potential role of BAX and BCL-2 expression in diffuse alveolar damage.* Am J Pathol, 1997. **151**(4): p. 999-1007.

112. Kitamura, Y., S. Hashimoto, N. Mizuta, A. Kobayashi, K. Kooguchi, I. Fujiwara, and H. Nakajima, *Fas/FasL-dependent apoptosis of alveolar cells after lipopolysaccharide-induced lung injury in mice.* Am J Respir Crit Care Med, 2001. **163**(3 Pt 1): p. 762-9.

113. Fukuzuka, K., C.K. Edwards, 3rd, M. Clare-Salzler, E.M. Copeland, 3rd, L.L. Moldawer, and D.W. Mozingo, *Glucocorticoid-induced, caspase-dependent organ apoptosis early after burn injury.* Am J Physiol Regul Integr Comp Physiol, 2000. **278**(4): p. R1005-18.

114. Fukuzuka, K., J.J. Rosenberg, G.C. Gaines, C.K. Edwards, 3rd, M. Clare-Salzler, S.L. MacKay, L.L. Moldawer, E.M. Copeland, 3rd, and D.W. Mozingo, *Caspase-3-dependent organ apoptosis early after burn injury.* Ann Surg, 1999. **229**(6): p. 851-8; discussion 858-9.

115. Magnotti, L.J., J.S. Upperman, D.Z. Xu, Q. Lu, and E.A. Deitch, *Gut-derived mesenteric lymph but not portal blood increases endothelial cell permeability and promotes lung injury after hemorrhagic shock.* Ann Surg, 1998. **228**(4): p. 518-27.

116. Magnotti, L.J., D.Z. Xu, Q. Lu, and E.A. Deitch, *Gut-derived mesenteric lymph: a link between burn and lung injury.* Arch Surg, 1999. **134**(12): p. 1333-40; discussion 1340-1.

117. Lutmer, J., D. Watkins, C.L. Chen, M. Velten, and G. Besner, *Heparin-binding epidermal growth factor-like growth factor attenuates acute lung injury and multiorgan dysfunction after scald burn.* J Surg Res, 2013. **185**(1): p. 329-37.

118. Ma, S., N. Xie, W. Li, B. Yuan, Y. Shi, and Y. Wang, *Immunobiology of mesenchymal stem cells.* Cell Death Differ, 2014. **21**(2): p. 216-25.

119. Kim, J. and P. Hematti, *Mesenchymal stem cell-educated macrophages: a novel type of alternatively activated macrophages.* Exp Hematol, 2009. **37**(12): p. 1445-53.

120. Maggini, J., G. Mirkin, I. Bognanni, J. Holmberg, I.M. Piazzon, I. Nepomnaschy, H. Costa, C. Canones, S. Raiden, M. Vermeulen, and J.R. Geffner, *Mouse bone marrow-derived mesenchymal stromal cells turn activated macrophages into a regulatory-like profile.* PLoS One, 2010. **5**(2): p. e9252.

121. Nemeth, K., A. Leelahavanichkul, P.S. Yuen, B. Mayer, A. Parmelee, K. Doi, P.G. Robey, K. Leelahavanichkul, B.H. Koller, J.M. Brown, X. Hu, I. Jelinek, R.A. Star, and E. Mezey, *Bone marrow stromal cells attenuate sepsis via*

prostaglandin E(2)-dependent reprogramming of host macrophages to increase their interleukin-10 production. Nat Med, 2009. **15**(1): p. 42-9.

122.   Dayan, V., G. Yannarelli, F. Billia, P. Filomeno, X.H. Wang, J.E. Davies, and A. Keating, *Mesenchymal stromal cells mediate a switch to alternatively activated monocytes/macrophages after acute myocardial infarction.* Basic Res Cardiol, 2011. **106**(6): p. 1299-310.

123.   Aggarwal, S. and M.F. Pittenger, *Human mesenchymal stem cells modulate allogeneic immune cell responses.* Blood, 2005. **105**(4): p. 1815-22.

124.   Eggenhofer, E., V. Benseler, A. Kroemer, F.C. Popp, E.K. Geissler, H.J. Schlitt, C.C. Baan, M.H. Dahlke, and M.J. Hoogduijn, *Mesenchymal stem cells are short-lived and do not migrate beyond the lungs after intravenous infusion.* Front Immunol, 2012. **3**: p. 297.

125.   Fischer, U.M., M.T. Harting, F. Jimenez, W.O. Monzon-Posadas, H. Xue, S.I. Savitz, G.A. Laine, and C.S. Cox, Jr., *Pulmonary passage is a major obstacle for intravenous stem cell delivery: the pulmonary first-pass effect.* Stem Cells Dev, 2009. **18**(5): p. 683-92.

126.   Schrepfer, S., T. Deuse, H. Reichenspurner, M.P. Fischbein, R.C. Robbins, and M.P. Pelletier, *Stem cell transplantation: the lung barrier.* Transplant Proc, 2007. **39**(2): p. 573-6.

127.   Yagi, H., A. Soto-Gutierrez, Y. Kitagawa, A.W. Tilles, R.G. Tompkins, and M.L. Yarmush, *Bone marrow mesenchymal stromal cells attenuate organ injury induced by LPS and burn.* Cell Transplant, 2010. **19**(6): p. 823-30.

128.   Xue, L., Y.B. Xu, J.L. Xie, J.M. Tang, B. Shu, L. Chen, S.H. Qi, and X.S. Liu, *Effects of human bone marrow mesenchymal stem cells on burn injury healing in a mouse model.* Int J Clin Exp Pathol, 2013. **6**(7): p. 1327-36.

129.   Huang, L. and A. Burd, *An update review of stem cell applications in burns and wound care.* Indian J Plast Surg, 2012. **45**(2): p. 229-36.

130.   Rasulov, M.F., A.V. Vasilchenkov, N.A. Onishchenko, M.E. Krasheninnikov, V.I. Kravchenko, T.L. Gorshenin, R.E. Pidtsan, and I.V. Potapov, *First experience of the use bone marrow mesenchymal stem cells for the treatment of a patient with deep skin burns.* Bull Exp Biol Med, 2005. **139**(1): p. 141-4.

131. Rasulov, M.F., V.T. Vasilenko, V.A. Zaidenov, and N.A. Onishchenko, *Cell transplantation inhibits inflammatory reaction and stimulates repair processes in burn wound.* Bull Exp Biol Med, 2006. **142**(1): p. 112-5.

132. Ashbaugh, D.G., D.B. Bigelow, T.L. Petty, and B.E. Levine, *Acute respiratory distress in adults.* Lancet, 1967. **2**(7511): p. 319-23.

133. CDC, *Vital Signs: Binge Drinking Prevalence, Frequency, and Intensity Among Adults.* Morbidity and Mortality Weekly Report, 2012. **61**(1): p. 14-19.

134. Hadjizacharia, P., T. O'Keeffe, D.S. Plurad, D.J. Green, C.V. Brown, L.S. Chan, D. Demetriades, and P. Rhee, *Alcohol exposure and outcomes in trauma patients.* Eur J Trauma Emerg Surg, 2011. **37**(2): p. 169-175.

135. Smith, G.S. and J.F. Kraus, *Alcohol and residential, recreational, and occupational injuries: a review of the epidemiologic evidence.* Annu Rev Public Health, 1988. **9**: p. 99-121.

136. Schermer, C.R., *Alcohol and injury prevention.* J Trauma, 2006. **60**(2): p. 447-51.

137. Kawakami, M., B.R. Switzer, S.R. Herzog, and A.A. Meyer, *Immune suppression after acute ethanol ingestion and thermal injury.* J Surg Res, 1991. **51**(3): p. 210-5.

138. Faunce, D.E., M.S. Gregory, and E.J. Kovacs, *Effects of acute ethanol exposure on cellular immune responses in a murine model of thermal injury.* J Leukoc Biol, 1997. **62**(6): p. 733-40.

139. Faunce, D.E., M.S. Gregory, and E.J. Kovacs, *Acute ethanol exposure prior to thermal injury results in decreased T-cell responses mediated in part by increased production of IL-6.* Shock, 1998. **10**(2): p. 135-40.

140. Messingham, K.A., D.E. Faunce, and E.J. Kovacs, *Alcohol, injury, and cellular immunity.* Alcohol, 2002. **28**(3): p. 137-49.

141. Choudhry, M.A., K.A. Messingham, S. Namak, A. Colantoni, C.V. Fontanilla, L.A. Duffner, M.M. Sayeed, and E.J. Kovacs, *Ethanol exacerbates T cell dysfunction after thermal injury.* Alcohol, 2000. **21**(3): p. 239-43.

142. Murdoch, E.L., H.G. Brown, R.L. Gamelli, and E.J. Kovacs, *Effects of ethanol on pulmonary inflammation in postburn intratracheal infection.* J Burn Care Res, 2008. **29**(2): p. 323-30.

143. Murdoch, E.L., J. Karavitis, C. Deburghgraeve, L. Ramirez, and E.J. Kovacs, *Prolonged chemokine expression and excessive neutrophil infiltration in the lungs of burn-injured mice exposed to ethanol and pulmonary infection.* Shock, 2011. **35**(4): p. 403-10.

144. Irvin, C.G. and J.H. Bates, *Measuring the lung function in the mouse: the challenge of size.* Respir Res, 2003. **4**: p. 4.

145. Lundqvist, C., C. Alling, R. Knoth, and B. Volk, *Intermittent ethanol exposure of adult rats: hippocampal cell loss after one month of treatment.* Alcohol Alcohol, 1995. **30**(6): p. 737-48.

146. Callaci, J.J., D. Juknelis, A. Patwardhan, M. Sartori, N. Frost, and F.H. Wezeman, *The effects of binge alcohol exposure on bone resorption and biomechanical and structural properties are offset by concurrent bisphosphonate treatment.* Alcohol Clin Exp Res, 2004. **28**(1): p. 182-91.

147. Przybycien-Szymanska, M.M., Y.S. Rao, and T.R. Pak, *Binge-pattern alcohol exposure during puberty induces sexually dimorphic changes in genes regulating the HPA axis.* Am J Physiol Endocrinol Metab, 2010. **298**(2): p. E320-8.

148. Przybycien-Szymanska, M.M., N.N. Mott, and T.R. Pak, *Alcohol dysregulates corticotropin-releasing-hormone (CRH) promoter activity by interfering with the negative glucocorticoid response element (nGRE).* PLoS One, 2011. **6**(10): p. e26647.

149. Vaagenes, I.C., S.Y. Tsai, S.T. Ton, V.A. Husak, S.O. McGuire, T.E. O'Brien, and G.L. Kartje, *Binge ethanol prior to traumatic brain injury worsens sensorimotor functional recovery in rats.* PLoS One, 2015. **10**(3): p. e0120356.

150. Qin, Y., J.L. Hamilton, M.D. Bird, M.M. Chen, L. Ramirez, A. Zahs, E.J. Kovacs, and L. Makowski, *Adipose inflammation and macrophage infiltration after binge ethanol and burn injury.* Alcohol Clin Exp Res, 2014. **38**(1): p. 204-13.

151. Messingham, K.A., C.V. Fontanilla, A. Colantoni, L.A. Duffner, and E.J. Kovacs, *Cellular immunity after ethanol exposure and burn injury: dose and time dependence.* Alcohol, 2000. **22**(1): p. 35-44.

152. Faunce, D.E., J.N. Llanas, P.J. Patel, M.S. Gregory, L.A. Duffner, and E.J. Kovacs, *Neutrophil chemokine production in the skin following scald injury.* Burns, 1999. **25**(5): p. 403-10.

153. Boehmer, E.D., J. Goral, D.E. Faunce, and E.J. Kovacs, *Age-dependent decrease in Toll-like receptor 4-mediated proinflammatory cytokine production and mitogen-activated protein kinase expression.* J Leukoc Biol, 2004. **75**(2): p. 342-9.

154. Happel, K.I. and S. Nelson, *Alcohol, immunosuppression, and the lung.* Proc Am Thorac Soc, 2005. **2**(5): p. 428-32.

155. Gamble, L., C.M. Mason, and S. Nelson, *The effects of alcohol on immunity and bacterial infection in the lung.* Med Mal Infect, 2006. **36**(2): p. 72-7.

156. Shults, J.A., Curtis, B.J., Chen, M.C., O'Halloran, E.B., Ramirez, L., and Kovacs, E.J., *Impaired Respiratory Function and Heightened Pulmonary Inflammation in Episodic Binge Ethanol Intoxication and Burn Injury.* Alcohol, 2015. **In Press**.

157. Herold, S., K. Mayer, and J. Lohmeyer, *Acute lung injury: how macrophages orchestrate resolution of inflammation and tissue repair.* Front Immunol, 2011. **2**: p. 65.

158. von Garnier, C., L. Filgueira, M. Wikstrom, M. Smith, J.A. Thomas, D.H. Strickland, P.G. Holt, and P.A. Stumbles, *Anatomical location determines the distribution and function of dendritic cells and other APCs in the respiratory tract.* J Immunol, 2005. **175**(3): p. 1609-18.

159. deCathelineau, A.M. and P.M. Henson, *The final step in programmed cell death: phagocytes carry apoptotic cells to the grave.* Essays Biochem, 2003. **39**: p. 105-17.

160. Rogers, N.J., M.J. Lees, L. Gabriel, E. Maniati, S.J. Rose, P.K. Potter, and B.J. Morley, *A defect in Marco expression contributes to systemic lupus erythematosus development via failure to clear apoptotic cells.* J Immunol, 2009. **182**(4): p. 1982-90.

161. Chen, J., S. Namiki, M. Toma-Hirano, S. Miyatake, K. Ishida, Y. Shibata, N. Arai, K. Arai, and Y. Kamogawa-Schifter, *The role of CD11b in phagocytosis and dendritic cell development.* Immunol Lett, 2008. **120**(1-2): p. 42-8.

162. Porcheray, F., S. Viaud, A.C. Rimaniol, C. Leone, B. Samah, N. Dereuddre-Bosquet, D. Dormont, and G. Gras, *Macrophage activation switching: an asset for the resolution of inflammation.* Clin Exp Immunol, 2005. **142**(3): p. 481-9.

163. Roszer, T., *Understanding the Mysterious M2 Macrophage through Activation Markers and Effector Mechanisms.* Mediators Inflamm, 2015. **2015**: p. 816460.

164.   Stein, M., S. Keshav, N. Harris, and S. Gordon, *Interleukin 4 potently enhances murine macrophage mannose receptor activity: a marker of alternative immunologic macrophage activation.* J Exp Med, 1992. **176**(1): p. 287-92.

165.   Ariel, A., I. Maridonneau-Parini, P. Rovere-Querini, J.S. Levine, and H. Muhl, *Macrophages in inflammation and its resolution.* Front Immunol, 2012. **3**: p. 324.

166.   Chakravortty, D. and M. Hensel, *Inducible nitric oxide synthase and control of intracellular bacterial pathogens.* Microbes Infect, 2003. **5**(7): p. 621-7.

167.   Henson, P.M. and R.M. Tuder, *Apoptosis in the lung: induction, clearance and detection.* Am J Physiol Lung Cell Mol Physiol, 2008. **294**(4): p. L601-11.

168.   Raff, T., G. Germann, and U. Barthold, *Factors influencing the early prediction of outcome from burns.* Acta Chir Plast, 1996. **38**(4): p. 122-7.

169.   Aggarwal, N.R., L.S. King, and F.R. D'Alessio, *Diverse macrophage populations mediate acute lung inflammation and resolution.* Am J Physiol Lung Cell Mol Physiol, 2014. **306**(8): p. L709-25.

170.   Fadok, V.A., D.L. Bratton, A. Konowal, P.W. Freed, J.Y. Westcott, and P.M. Henson, *Macrophages that have ingested apoptotic cells in vitro inhibit proinflammatory cytokine production through autocrine/paracrine mechanisms involving TGF-beta, PGE2, and PAF.* J Clin Invest, 1998. **101**(4): p. 890-8.

171.   Taylor, P.R., L. Martinez-Pomares, M. Stacey, H.H. Lin, G.D. Brown, and S. Gordon, *Macrophage receptors and immune recognition.* Annu Rev Immunol, 2005. **23**: p. 901-44.

172.   Mathias, L.J., S.M. Khong, L. Spyroglou, N.L. Payne, C. Siatskas, A.N. Thorburn, R.L. Boyd, and T.S. Heng, *Alveolar macrophages are critical for the inhibition of allergic asthma by mesenchymal stromal cells.* J Immunol, 2013. **191**(12): p. 5914-24.

173.   Song, X., S. Xie, K. Lu, and C. Wang, *Mesenchymal stem cells alleviate experimental asthma by inducing polarization of alveolar macrophages.* Inflammation, 2015. **38**(2): p. 485-92.

174.   Gao, S., F. Mao, B. Zhang, L. Zhang, X. Zhang, M. Wang, Y. Yan, T. Yang, J. Zhang, W. Zhu, H. Qian, and W. Xu, *Mouse bone marrow-derived mesenchymal stem cells induce macrophage M2 polarization through the nuclear factor-kappaB and signal transducer and activator of transcription 3 pathways.* Exp Biol Med (Maywood), 2014. **239**(3): p. 366-75.

175. Lee, R.H., A.A. Pulin, M.J. Seo, D.J. Kota, J. Ylostalo, B.L. Larson, L. Semprun-Prieto, P. Delafontaine, and D.J. Prockop, *Intravenous hMSCs improve myocardial infarction in mice because cells embolized in lung are activated to secrete the anti-inflammatory protein TSG-6.* Cell Stem Cell, 2009. **5**(1): p. 54-63.

176. Weir, C., M.C. Morel-Kopp, A. Gill, K. Tinworth, L. Ladd, S.N. Hunyor, and C. Ward, *Mesenchymal stem cells: isolation, characterisation and in vivo fluorescent dye tracking.* Heart Lung Circ, 2008. **17**(5): p. 395-403.

177. Chen, M.M., J.L. Palmer, J.A. Ippolito, B.J. Curtis, M.A. Choudhry, and E.J. Kovacs, *Intoxication by intraperitoneal injection or oral gavage equally potentiates postburn organ damage and inflammation.* Mediators Inflamm, 2013. **2013**: p. 971481.

178. Glaab, T., C. Taube, A. Braun, and W. Mitzner, *Invasive and noninvasive methods for studying pulmonary function in mice.* Respir Res, 2007. **8**: p. 63.

179. Bates, J.H. and C.G. Irvin, *Measuring lung function in mice: the phenotyping uncertainty principle.* J Appl Physiol (1985), 2003. **94**(4): p. 1297-306.

180. Milton, P.L., H. Dickinson, G. Jenkin, and R. Lim, *Assessment of respiratory physiology of C57BL/6 mice following bleomycin administration using barometric plethysmography.* Respiration, 2012. **83**(3): p. 253-66.

181. Adler, A., G. Cieslewicz, and C.G. Irvin, *Unrestrained plethysmography is an unreliable measure of airway responsiveness in BALB/c and C57BL/6 mice.* J Appl Physiol (1985), 2004. **97**(1): p. 286-92.

182. Hoymann, H.G., *Invasive and noninvasive lung function measurements in rodents.* J Pharmacol Toxicol Methods, 2007. **55**(1): p. 16-26.

183. Verheijden, K.A., P.A. Henricks, F.A. Redegeld, J. Garssen, and G. Folkerts, *Measurement of airway function using invasive and non-invasive methods in mild and severe models for allergic airway inflammation in mice.* Front Pharmacol, 2014. **5**: p. 190.

184. Bates, J., C. Irvin, V. Brusasco, J. Drazen, J. Fredberg, S. Loring, D. Eidelman, M. Ludwig, P. Macklem, J. Martin, J. Milic-Emili, Z. Hantos, R. Hyatt, S. Lai-Fook, A. Leff, J. Solway, K. Lutchen, B. Suki, W. Mitzner, P. Pare, N. Pride, and P. Sly, *The use and misuse of Penh in animal models of lung disease.* Am J Respir Cell Mol Biol, 2004. **31**(3): p. 373-4.

185. Guntheroth, W.G. and I. Kawabori, *Hypoxic apnea and gasping.* J Clin Invest, 1975. **56**(6): p. 1371-7.

186. McCutcheon, F.H., *Atmospheric respiration and the complex cycles in mammalian breathing mechanisms.* J Cell Physiol, 1953. **41**(2): p. 291-303.

187. Galani, V., E. Tatsaki, M. Bai, P. Kitsoulis, M. Lekka, G. Nakos, and P. Kanavaros, *The role of apoptosis in the pathophysiology of Acute Respiratory Distress Syndrome (ARDS): an up-to-date cell-specific review.* Pathol Res Pract, 2010. **206**(3): p. 145-50.

188. Hengartner, M.O., *The biochemistry of apoptosis.* Nature, 2000. **407**(6805): p. 770-6.

189. Dauphinee, S.M. and A. Karsan, *Lipopolysaccharide signaling in endothelial cells.* Lab Invest, 2006. **86**(1): p. 9-22.

190. Pober, J.S. and R.S. Cotran, *Cytokines and endothelial cell biology.* Physiol Rev, 1990. **70**(2): p. 427-51.

191. Collins, T., *Endothelial nuclear factor-kappa B and the initiation of the atherosclerotic lesion.* Lab Invest, 1993. **68**(5): p. 499-508.

192. Huber, A.R., S.L. Kunkel, R.F. Todd, 3rd, and S.J. Weiss, *Regulation of transendothelial neutrophil migration by endogenous interleukin-8.* Science, 1991. **254**(5028): p. 99-102.

193. Bingisser, R., C. Stey, M. Weller, P. Groscurth, E. Russi, and K. Frei, *Apoptosis in human alveolar macrophages is induced by endotoxin and is modulated by cytokines.* Am J Respir Cell Mol Biol, 1996. **15**(1): p. 64-70.

194. Z'Graggen B, R., J. Tornic, B. Muller-Edenborn, L. Reyes, C. Booy, and B. Beck-Schimmer, *Acute lung injury: apoptosis in effector and target cells of the upper and lower airway compartment.* Clin Exp Immunol, 2010. **161**(2): p. 324-31.

195. Smith, W.B., L. Noack, Y. Khew-Goodall, S. Isenmann, M.A. Vadas, and J.R. Gamble, *Transforming growth factor-beta 1 inhibits the production of IL-8 and the transmigration of neutrophils through activated endothelium.* J Immunol, 1996. **157**(1): p. 360-8.

196. Lee, A., M.K. Whyte, and C. Haslett, *Inhibition of apoptosis and prolongation of neutrophil functional longevity by inflammatory mediators.* J Leukoc Biol, 1993. **54**(4): p. 283-8.

197.   Granero-Molto, F., J.A. Weis, M.I. Miga, B. Landis, T.J. Myers, L. O'Rear, L. Longobardi, E.D. Jansen, D.P. Mortlock, and A. Spagnoli, *Regenerative effects of transplanted mesenchymal stem cells in fracture healing.* Stem Cells, 2009. **27**(8): p. 1887-98.

198.   Kang, J.W., K.D. Park, Y. Choi, D.H. Baek, W.S. Cho, M. Choi, J.H. Park, K.S. Choi, H.S. Kim, and T.M. Yoo, *Biodistribution and in vivo efficacy of genetically modified human mesenchymal stem cells systemically transplanted into a mouse bone fracture model.* Arch Pharm Res, 2013. **36**(8): p. 1013-22.

199.   Lee, S.W., P. Padmanabhan, P. Ray, S.S. Gambhir, T. Doyle, C. Contag, S.B. Goodman, and S. Biswal, *Stem cell-mediated accelerated bone healing observed with in vivo molecular and small animal imaging technologies in a model of skeletal injury.* J Orthop Res, 2009. **27**(3): p. 295-302.

200.   Obermeyer, T.S., D. Yonick, K. Lauing, S.R. Stock, R. Nauer, P. Strotman, R. Shankar, R. Gamelli, M. Stover, and J.J. Callaci, *Mesenchymal stem cells facilitate fracture repair in an alcohol-induced impaired healing model.* J Orthop Trauma, 2012. **26**(12): p. 712-8.

201.   Demling, R.H., *The burn edema process: current concepts.* J Burn Care Rehabil, 2005. **26**(3): p. 207-27.

202.   Chen, M.M., E.B. O'Halloran, J.A. Ippolito, M.A. Choudhry, and E.J. Kovacs, *Alcohol potentiates postburn remote organ damage through shifts in fluid compartments mediated by bradykinin.* Shock, 2015. **43**(1): p. 80-4.

203.   Djouad, F., P. Plence, C. Bony, P. Tropel, F. Apparailly, J. Sany, D. Noel, and C. Jorgensen, *Immunosuppressive effect of mesenchymal stem cells favors tumor growth in allogeneic animals.* Blood, 2003. **102**(10): p. 3837-44.

204.   Duan, M., W.C. Li, R. Vlahos, M.J. Maxwell, G.P. Anderson, and M.L. Hibbs, *Distinct macrophage subpopulations characterize acute infection and chronic inflammatory lung disease.* J Immunol, 2012. **189**(2): p. 946-55.

VITA

Jill Ann (Ippolito) Shults was born in Chicago, IL on August 10, 1984 to James and Diane Ippolito. In June of 2006, she received a Bachelor of Science in Biology from DePaul University (Chicago, IL). At DePaul, Jill was awarded an undergraduate research assistant grant and her first laboratory research experience was under the guidance of Dr. Phillip E. Funk. After graduation, Jill spent four years working in the laboratory of Dr. Pamela L. Witte as a research specialist at Loyola University Chicago.

In August of 2010, Jill joined the Integrative Cell Biology Program at Loyola University Chicago (Maywood, IL). Shortly thereafter, she joined the laboratory of Dr. Elizabeth J. Kovacs where she studied the effect of alcohol on post-burn pulmonary inflammation. While at Loyola, Jill received a pre-doctoral fellowship from a National Institutes of Health Institutional Training Grant and a pre-doctoral Ruth L. Kirchstein National Research Service Award from the National Institutes of Health.

In June 2014, Jill married fellow graduate student, Cody Lee Shults, who completed his Ph.D. in the laboratory of Dr. Toni R. Pak. Jill plans to continue with immunology research and is currently in the process of applying for post-doctoral positions.